



NATIONAL INSTITUTE OF TECHNOLOGY  
ROURKELA

2011

PREDICTION OF FLOW AND ITS  
RESISTANCE IN COMPOUND OPEN  
CHANNEL



MRUTYUNJAYA SAHU

DEPARTMENT OF CIVIL ENGINEERING

NATIONAL INSTITUTE OF TECHNOLOGY, ROURKELA

2011

---

# PREDICTION OF FLOW AND ITS RESISTANCE IN COMPOUND OPEN CHANNEL

---

*A Thesis Submitted in Partial Fulfillment of the Requirements for the  
Degree of*

**Master of Technology  
in  
Civil Engineering**



**MRUTYUNJAYA SAHU**

**DEPARTMENT OF CIVIL ENGINEERING  
NATIONAL INSTITUTE OF TECHNOLOGY, ROURKELA  
2011**

---

# PREDICTION OF FLOW AND ITS RESISTANCE IN COMPOUND OPEN CHANNEL

---

*A Thesis Submitted in Partial Fulfillment of the Requirements for the  
Degree of*

Master of Technology  
in  
Civil Engineering

Under the guidance and supervision of  
Prof. K.K.KHATUA  
&  
Prof. K.C.BISWAL

*Submitted By:*

**MRUTYUNJAYA SAHU**

**ROLL.NO: 609CE103**



**DEPARTMENT OF CIVIL ENGINEERING  
NATIONAL INSTITUTE OF TECHNOLOGY, ROURKELA**

2011



National Institute of Technology Rourkela

---

## CERTIFICATE

This is to certify that the thesis entitled “**Prediction of flow and its resistance in compound open channel**” being submitted by **Mrutyunjaya Sahu** in partial fulfillment of the requirements for the award of **Master of Technology** in **Civil Engineering** at National Institute of Technology Rourkela, is a bonafide research carried out by him under our guidance and supervision.

The work incorporated in this thesis has not been, to the best of our knowledge, submitted to any other University or Institute for the award of any degree or diploma.

Prof. K. K. Khatua  
(Supervisor)

Prof. K.C. Biswal  
(Co-Supervisor)



## National Institute of Technology Rourkela

---

### DECLARATION

I hereby, declare that this submission is my own work and that, to the best of my knowledge and belief, it contains no material previously published or written by another person nor material which to a substantial extent has been accepted for the award of any other degree or diploma of the university or other institute of higher learning, except where due acknowledgement has been made in the text.

**MRUTYUNJAYA SAHU**

### CONTENTS

	Page No:
Abstracts	i
Acknowledgement	ii
List of Figures	iii

List of Tables	vi
List of Abbreviations	vii
List of Symbols	vii
Chapter 1: Introduction and Literature Review	
1.1 Introduction.	2
1.2 Aim and Objective of Thesis.	3
1.3 Organization of the thesis	4
Chapter 2: Literature Review	5
2.1 Literature Review	6
Chapter 3: Numerical modeling of turbulent flow structures in open channel flow.	
3.1. Introduction	12
3.2. Geometry Setup and Discretization of domain	13
3.3. Turbulence modeling	14
3.4. Boundary Conditions	18
3.5. Solver: Analysis of Turbulence Modeling	20
3.6. Post Processing: Analysis of Turbulence models	20
Chapter 4: Analysis of flow and its resistance in open channel flow	
4.1. Introduction	29
4.2. Modeling of discharge using Back Propagation Neural Network (BPNN)	30
4.2.1. Analysis and prediction of discharge in compound open channel	29
4.2.2. Single Channel Method	29
4.2.3. Divided Channel Method	31
4.2.4. Coherence Method	32
4.2.5. Exchange Discharge Method	34
4.2.6. Experimental set-up and procedure	35
4.2.7. Development of back propagation neural network (BPNN)	37
4.2.8. Source of data	39
4.2.9. Selection of hydraulic parameter	40
4.2.10. Results	40
4.2.11. Discussion	47

4.3. Modeling of Composite Friction Factor Using Artificial Neuro Fuzzy Inference System	
4.3.1. Introduction	49
4.3.2. Modeling of Adaptive-Neuro Fuzzy Inference System (ANFIS)	53
4.3.3. Selection of Hydraulic parameters	54
4.3.4. Fuzzy Logic and Fuzzy Inference Systems	54
4.3.5. Architecture and Basic Learning Rules	55
4.3.6. Hybrid learning algorithm	57
4.3.7. Training And Testing of ANFIS Network	58
4.3.8. Comparison of different methods with true value for prediction of composite friction factor	61
4.3.9. Results of Artificial Nuro-Fuzzy Inference System	65
4.3.10. Coefficient of determination	69
4.3.11. Discussion	73
Chapter 5: Conclusion	
5.1. Conclusion	76
5.2. Scope for future study	76
5.3. Relevant Publications	77
Chapter 6: Reference	79
Rebuttall and Errata	87

# ABSTRACT

---

Flooding situation in rivers is a complex phenomenon and affects the livelihood and economic condition of the region. This complex condition has long been identified and intensive research work has been carried out to find out its remedial solution. During flood, river overtops its banks and spreads to its flood plains, called compound channel. It has been observed that the flow velocity in flood plain subsection is slower than the velocity of its course. Due to this difference in velocities between main channel and flood plain, a large shear layer produces. This large shear layer retains complex turbulent structures of different scales within it. These turbulent structures produce extra resistance to flow, which induces uncertainty in predictions of flow and its resistance. It has been also observed that, numerical turbulence models can be used to find the point to point information. Hence the analysis of turbulent structures is prevalent in this situation. Earlier, researchers have adopted various numerical, analytical and empirical models to analyze turbulent flow in compound channels, generally for low development length. Therefore, in this study an effort is made to analyze the turbulent structure by Large Eddy Simulation method (LES) to predict the flow and its resistance involved in it. The LES is carried out by taking sufficient development length so that uniform turbulent flow is developed. The development length is incorporated in the computational domain. However, it is a fact that numerical simulation of compound channels with different hydraulic conditions are computationally very expensive and arduous. Therefore, this analysis is further done by using adaptive approaches such as Artificial Neural Network (ANN) and Artificial Neuro Fuzzy Inference System (ANFIS). These models are used to predict flow and its resistance of a compound channel for different hydraulic conditions. All the proposed models are compared well with the standard modes previously developed. The proposed models are found to give better results compared to other models when applied to global data sets.

**Keywords:**

*Turbulent structure, Large eddy simulation, Composite friction factor, Discharge, ANFIS, BPNN, compound channel.*

## ACKNOWLEDGEMENTS

---

I sincerely express my deep sense of indebtedness and gratitude to Prof. K.K.Khatua and Prof. K.C. Biswal for providing me an opportunity to work under their supervision and guidance. Their continuous encouragement, invaluable guidance and immense help have inspired me for the successful completion of the thesis work. I sincerely thank them for their intellectual support and creative criticism, which led me to generate my own ideas and made my work interesting as far as possible.

I would also like to express my sincere thanks to, Prof. N. Wright (University of Leeds), Prof. T. Stoesser (Georgia Institute of Technology), Prof. N. Roy (Head of Department, Civil Engineering), Prof. S.S.Mahapatra (Department of Mechanical Engineering, NIT Rourkela) , Prof. K.C.Patra, Prof. A.K.Pradhan, Prof. M. Panda, and Prof. R. Jha in providing me with all sorts of help and paving me with their precious comments and ideas. I am indebted to all of them. I am also thankful to staff members and students associated with the Fluid Mechanics and Hydraulics Laboratory of Civil Engineering Department, especially Mr. Prabir Kumar Mohanty, Mr. Gouri Shankar Beriha, Mrs. Nirjharini Sahoo, Mr. P. Rout and Mr. K. M. Patra for their useful assistance and cooperation during the entire course of the my study and helping me in all possible ways.

Friendly environment and cooperative company I have during my stay at NIT Rourkela are memorable and pleasant. The affection received from my batch mates and juniors will always remind me of my days as a student here. I wish to thank all of them heartily. Their support and suggestions are indeed of great help.

I am thankful to my parents and my sisters for their emotional support and being patient during the completion of my dissertation. Last but not the least; I thank the ALMIGHTY for blessing me and supporting me throughout.

**MRUTYUNJAYA SAHU**

## List of Figures

	Pg.no
Figure 1.1 Hydraulic parameters associated with overbank flow (after Knight & Shiono 1991) .....	2
Figure 3.1 Schematic diagram of hybrid mesh.....	14
Figure 3.2 Energy cascade process with length scale.....	15
Figure 3.3 The subdivisions of the near-wall region.....	18
Figure 3.4 Wall functions used to resolve boundary layer.....	18
Figure 3.5 Schematic presentation of geometric alignment and boundary conditions of the channel .....	20
Figure 3.6 Mean Velocity distribution of LES Simulation.....	21
Figure 3.7 Mean Velocity distribution of experiment. (Tominaga and Nezu 1991).....	22
Figure 3.8 The distribution of depth averaged velocity head.....	23
Figure 3.9 The distribution of non-dimensional bed shear stress.....	24
Figure 3.10 Experimental velocity vectors from experimentation (Tominaga and Nezu 1991) .....	24
Figure 3.11 Stream-wise non-dimensional averaged secondary velocity vectors	25
Figure 3.12 Lateral distribution of turbulent transport and secondary circulation component.....	27
Figure 3.13 Lateral distribution of secondary circulation component (T).....	27
Figure 4.1 The diagonal division of the compound channel cross-sectional view.....	32
Figure 4.2 The plan form of the channel.....	35
Figure 4.3 Geometrical parameters of Type-I channel.....	36
Figure 4.4 Experimental compound channel (Type-I) in Fluid mechanics and hydraulics engineering Laboratory at NIT Rourkela with measurement equipments at upstream.....	36
Figure 4.5 Architecture of ANN for discharge estimation in straight compound channel...	38

Figure 4.6	Convergence plot.....	41
Figure 4.7	Residual distribution of training data.....	42
Figure 4.8	Correlation of actual discharge and predicted discharge (training data).....	42
Figure 4.9	Comparison of actual and predicted discharge (training data).....	44
Figure 4.10	Comparison of actual and predicted discharge (testing data).....	45
Figure 4.11	Correlation plot of actual discharge and Discharge predicted by VDCM (Testing data).....	45
Figure 4.12	Correlation plot of actual discharge and Discharge predicted by COHM.....	46
Figure 4.13	Correlation plot of actual discharge and Discharge predicted by EDM.....	46
Figure 4.14	Correlation Testing regression plot of actual discharge and Discharge predicted by ANN (Testing data).....	47
Figure 4.15	Schematic diagram of fuzzy based inference system.....	55
Figure 4.16	A typical architecture of ANFIS system.....	57
Figure 4.17	Procedure for developing the ANFIS model.....	59
Figure 4.18	Architecture of five layered ANFIS model.....	60
Figure 4.19	membership-function is used for output during generating FIS.....	60
Figure 4.20	Comparison of methods in Atabay (2004) experimental flow conditions.....	61
Figure 4.21	Comparison of methods in Soong and DePue (1996) experimental flow conditions.....	62
Figure 4.22	Comparison of methods in Tang (2001) experimental flow conditions.....	62
Figure 4.23	Comparison of methods for prediction in Tang (2001) experimental flow conditions.....	63
Figure 4.24	Comparison of methods in Tominaga and Nezu (1991) experimental flow conditions.....	63
Figure 4.25	Comparison of methods in FCF- Series A experimental flow conditions.....	64
Figure 4.26	Comparison of methods in Khatua et al. (2011) experimental flow conditions.....	64
Figure 4.27	Predicted data points through ANFIS model (training).....	65
Figure 4.28	Predicted data points through ANFIS model (testing).....	66

Figure 4.29 surface plot.....	66
Figure 4.30 Rule base generated for prediction of Composite Friction Factor.....	67
Figure 4.31 Distribution of Composite Friction Factor over all collected data for training data set data set.....	67
Figure 4.32 Distribution of Composite Friction Factor over all collected data for training data set data set.....	68
Figure 4.33 Residual distribution of training data set.....	68
Figure 4.34 Correlation plot for training set of data points. ....	69
Figure 4.35 Correlation plot for testing set of data points. ....	70
Figure 4.36 Correlation plot for Cox Method for data points. ....	70
Figure 4.37 Correlation plot for Eienstein and Banks Method for data points.....	71
Figure 4.38 Correlation plot for Krishnamurthy and Christensen Method for data points. .	71
Figure 4.39 Correlation plot for Lotter Method for data points. ....	72
Figure 4.40 Correlation plot for Dracos and Haddger Method for data points.....	72

## List of Tables

Table 3.1 Summary of Mesh and Simulation details Using ANSYS-CFX.	20
Table 3.2 Comparison of the experiment and simulation results.....	21
Table 4.1 Geometrical parameters of experimental data.....	36
Table 4.2 The details of experimental parameters for Type-I Compound Channel.....	40
Table 4.3 Network learning parameters.....	41
Table 4.4 The average absolute percentage error.....	43
Table 4.5 Different Models for Composite Friction Factor (after Yen 2003).....	50
Table 4.6 Geometrical parameters of experimental data.....	52
Table 4.7 Summarizes the activities in each pass.....	58
Table 4.8 Absolute relative error of different methods for different hydraulic conditions.....	65

## List of Abbreviations

CFD	Computational Fluid Dynamics
N-S	Navier-Stokes equation
LES	Large Eddy Simulation
DNS	Direct Numerical Simulation
SGS	Subgrid scale
BPNN	Back-Propagation Artificial Neural Network
ANFIS	Artificial-Neuro-Fuzzy Inference System
SCM	Single Channel Method
VDM	Vertical Division Method
COHM	Coherence Method
EDM	Exchange Discharge Method
DISDEF	Discharge Deficit Factor
DISDAF	Discharge Adjustment Factor
FCF	Flood Channel Facility
ADV	Acoustic Doppler Velocimeter
FIS	Fuzzy inference system

## List of Symbols

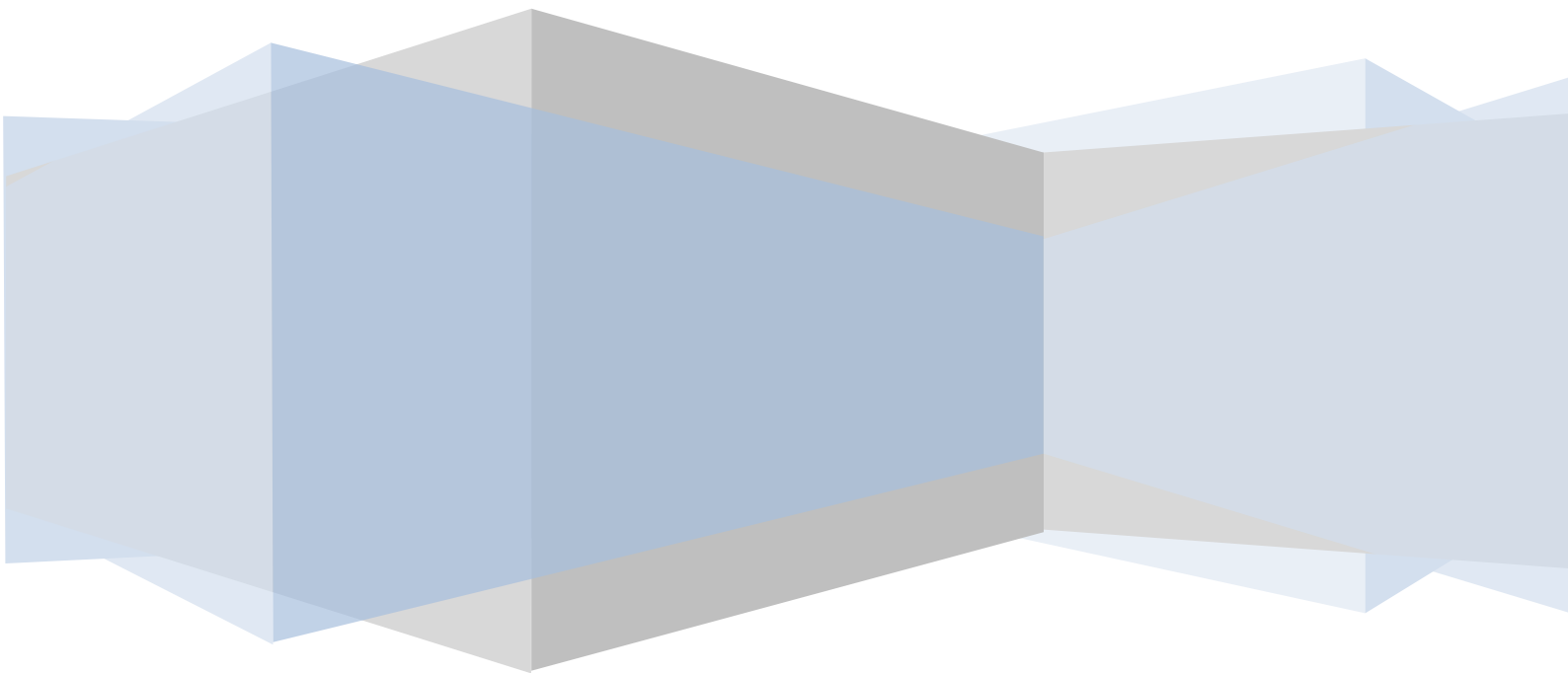
A	cross-sectional area
$A_r$	aspect ratio
B	In-bank channel width/over-bank channel half width
c	log-law constant
$C_r$	Courant number
$C_s$	Smagorinsky constant
$D_r$	depth ratio
E	location of secondary flow cell centre
f	Darcy-Weisbach friction coefficient
$f_{fp}$	floodplain friction factor
$f_{mc}$	main channel friction factor
f	overall friction factor
g	gravitational acceleration
h	floodplain height
H	channel height
Q	discharge
P	pressure
P	wetted perimeter
R	cross section hydraulic radius
$R_e$	Reynolds number
s	channel side slope ( $s = 0$ for vertical side walls)
S	longitudinal channel bed slope
$S_{ij}$	Resolved strain rate tensor
T	Shear stress due to spanwise Reynolds number,
J	Spanwise advection due to secondary current in W
t	time
T	turbulent diffusive transport
$U_{avg}$	average cross-sectional velocity
$W_d$	depth averaged velocity
$W_{max}$	maximum cross-sectional velocity
$u_*$	friction velocity
$u_+$	near wall velocity

$U, V, W$	Velocities along Z, Y and X-axis
$v$	instantaneous velocity component in the y -direction
$v'$	turbulence intensity in the y -direction
$w$	instantaneous velocity component in the x –direction
$w'$	turbulence intensity in the x -direction
$x$	Streamwise direction
$y$	lateral direction
$y_+$	dimensionless distance from the wall
$z$	vertical direction
$\Delta l$	largest mesh spacing
$\Delta t$	time step
$\Delta x$	mesh spacing in the streamwise direction
$\Delta y$	mesh spacing in the lateral direction
$\Delta z$	mesh spacing in the vertical direction
$\delta$	boundary layer width
$\kappa$	von Kármán's constant
$\eta$	Kolmogorov scale
$\mu$	dynamic viscosity
$\nu$	kinematic viscosity
$\nu_t$	eddy viscosity
$\Omega$	vorticity
$\rho$	fluid density
$\tau$	apparent shear stress
$\tau_{ave}$	average boundary shear stress
$\tau(z), \tau_b, \tau_{bed}$	bed shear stress
$\tau_{wall}$	shear stress
$\tau_{mean}$	shear stress
$\tau_{ij}$	Reynolds stresses
$\tau_{ij}$	SGS stress tensor
$\theta$	angle between channel bed and horizontal
ave	average
$b_b$	bed bed
d	depth-averaged
fp	floodplain
$i, j, k$	directions respectively
l	local

max	maximum
mc	main channel
$P_{mc}$	main channel perimeters,
$P_{fp}$	flood plain perimeters,
$A_{mc}$	main channel area,
$A_{fp}$	flood plain areas,
$n_{mc}$	main channel Manning's coefficient,
$n_{fp}$	flood plain Manning's coefficient.
$Q_{basic}$	basic total discharge calculated using zones
$\psi^g$	exchange correction factor
$\psi^t$	turbulent exchange model co-efficient
$K_i$	conveyance factor for each subsection;
$S_f$	friction slope;
$S_e$	Energy slope;
$A_i$	area of each subsections;
$R_i$	hydraulic radius of each subsections.
$w_{ij}$	interconnection weight
$f$	sigmoid transfer function
$E_p$	Mean square error,
$D_{pi}$	target output,
$O_{pi}$	computed output for the $i^{th}$ pattern
$\eta$	Learning rate
$\alpha$	Momentum coefficient
n	Manning's coefficient
C	Chezy's coefficient
f	Darcy-Weisbach Coefficient
$n_c$	Composite friction factor
$n_i$	sub-sectional Manning's roughness,
$w_i$	weighted function of subsections

# CHAPTER 1

## INTRODUCTION



## SECTION 1.1: INTRODUCTION

---

Rivers are always things of beauty and the historic livelihood of a settlement. People have been living near the banks of rivers for centuries for the sake of food, water, and transport. However, flooding in rivers has always been threat for mankind as this causes a huge loss of property and lives. Furthermore, the frequency of occurrence of floods has increased recently due to consequences of climate change, excessive human intervention, growing population on the banks of rivers and industrialization. Therefore, it is essential to take measures to understand flooding situations by analyzing the physics behind it.

Rivers are capable of conveying moderate flow until the flow is confined to its main course. But when flow gradually increases, the water rises above bank and overflows to the flood plains. As long as the flow depth of the flood plain is small and not comparable to depth of main channel, the mean velocity of main channel is larger than the flood plain and carries more discharge than flood plains. The difference of these flow velocities in both these subsections creates vertical vortices (as shown in Figure 1.1) along the vertical interface of main channel and flood plain. These vortices are created due to momentum and mass exchange between flood plain and main channel, which generates shear force and extra resistance consuming extra energy. Due to the consumption of this extra energy the prediction of stage discharge curve becomes difficult to obtain.

It is essential to investigate the flow structures that exist in compound open channels to understand the distribution of flow and its variables. The interaction between the primary longitudinal velocity and the secondary flow velocities are responsible for non-uniform distribution of flow variables in a compound open channel flow. This non-uniform distribution of flow variables, change resistance to flow across the wetted perimeter of compound open channel flow. In such situations the change in resistance to flow is composite and marks difference in individual main channel and flood plain resistance. From early 18th century many empirical models are modeled to encounter the discrepancies in predicting composite friction factor and discharge in compound open channel. But the anomaly behind the inaccuracy of these models are that, either these models are developed for a particular hydraulic conditions or these models neglect three dimensional flow phenomenon or convective momentum transfer due to secondary current, turbulent transport etc .

Turbulent flow structures are creating complexities in predicting discharge and composite friction factor in compound open channel. Therefore, computational modeling is inevitable to analyze

nature of flow structures and to extract point to point information of this critical condition. Hence, this present study is focused on the investigation of turbulence in compound channel by computational turbulence modeling, to analyze the complexity involved in it. Further, this analysis will carry forward to predict discharge and composite friction factor in compound open channel flow.

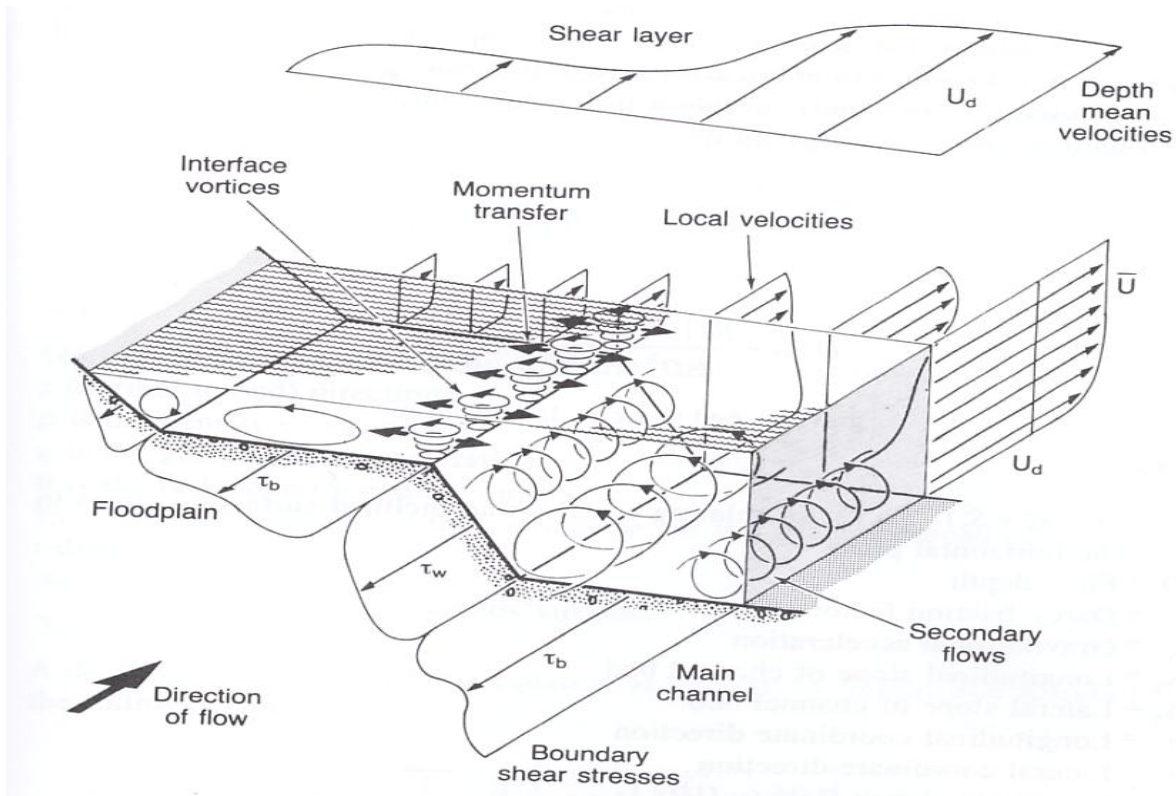


**Figure 1.1 Hydraulic parameters associated with overbank flow (after Knight & Shiono 1991)**

### 1.1 AIM AND OBJECTIVE

Flow in a compound open channel is generally turbulent in nature. The turbulent nature of flow in such channels is three dimensional due to strong secondary lateral flow. Furthermore, it has been observed from earlier studies that turbulence flow structure has direct impact in predicting the discharge and resistance in compound channel. To calculate discharge, the conventional models such as Single channel method, Divided Channel method etc. give higher error in prediction of discharge and similarly for composite friction factor, because the models are improperly accounting the turbulent structure such as lateral momentum transfer. Thus, it is essential to acquire the knowledge of turbulent flow structures to analyze the affect of lateral secondary flow in open channel flows. Therefore, in this present study, secondary current, lateral momentum transfers etc. of a compound channel has been analyzed by Large Eddy Simulation (LES) turbulent method. This

method is capable of giving in-detail information of this flow condition and also can predict discharge and resistance.

Although, LES successfully predicts the discharge and resistance of compound channel for a given flow depth by analyzing its flow structure, But for compound channels with different types of geometrical and hydraulic conditions, this method is cumbersome and time consuming. Therefore, adaptive methods are applied to establish the nonlinear correlation between the dependent and independent variables. Hence, the present study follows an analysis of resistance in compound channel flow and development of suitable adaptive methods for predicting composite friction factor and discharge in compound open channel. Further the developed models has been compared well with other defined models. The present study focuses on the following aspects:

- To study the turbulent flow structures of a compound open channel flow using Large Eddy Simulation turbulent method.
- Validation and verification of the turbulent flow structure such as secondary current, turbulent transport and flow variables such as velocity distribution, boundary shear stress etc. with that of the experimental results available in the literature.
- Development of two adaptive approaches to predict discharge and composite friction factor respectively in a compound channel.
- Validation of both the developed models with the models of different investigators applied to different compound channels with different hydraulic conditions.

## **1.2 ORGANIZATION OF THE THESIS**

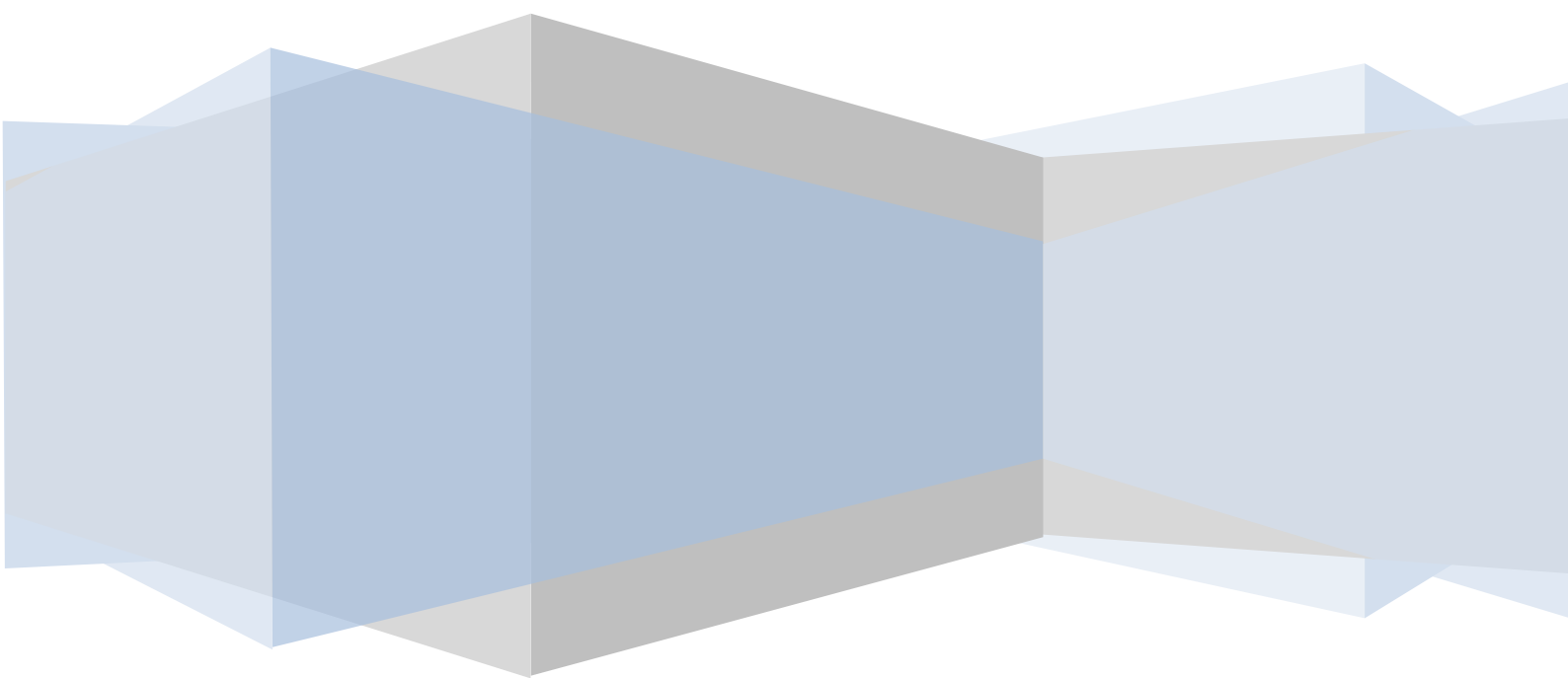
The thesis has been arranged in five chapters as discussed below:

- Chapter 1: A brief introduction to the problem is presented
- Chapter 2: A detailed literature review is described.
- Chapter 3: Numerical analysis of turbulent flow structure of compound open channel.
- Chapter 4: This chapter includes
  - ✓ Analysis of discharge prediction models with the development of a BPNN approach to predict discharge in a compound channel.

- ✓ Analysis of composite friction factor prediction models with the development of a ANFIS approach to predict composite friction factor in a compound channel.
- Chapter 5: The conclusions and scope for the future study are presented.

# CHAPTER 2

## LITERATURE REVIEW



## SECTION 2.1: LITERATURE REVIEW

---

Floods occur when main channel inundates and severe discharge follows the flood plains. The channels formed so are known as compound channels. Many practical problems in river engineering require accurate prediction of flow in compound channels. For example, the hydraulic response to flood prevention measures, such as dredging in the main channel and lowering or smoothing in the floodplains, depends on flow velocities in these compartments. Likewise, local flow conditions determine the erosion and deposition rates of sediment in the main channel and floodplains. Therefore, accurate prediction of discharge capacity of compound channels is extremely essential to imply in flood mitigation schemes. When flood occurs, the difference in flow velocity between the main channel and the floodplain generates mixing patterns and secondary currents, as noticed by Sellin (1964), Zheleznyakov (1965), Van Prooijen (2005). Experimental studies indicate that lateral momentum transfer occurs between main channel and floodplain and generally slows down the flow in the main channel while accelerating the flow into the flood plain Sellin (1964), Zheleznyakov (1965). Prinos and Townsend (1984) have described the lateral momentum transfer by introducing an interface shear stress between adjacent compartments parameterized in terms of the velocity difference between main channel and floodplains and the channel dimensions. Ackers (1992, 1993) has proposed a set of empirical equations based on coherence concept for assessing discharge in straight compound channels considering momentum transfer between main channels and flood plains. Ackers Coherence method is recommended by UK Environmental Agency in Bristol. Shiono and Knight (1999) have proposed a continuum model that resolves the depth-averaged flow velocity  $U(y)$ , as a function of the cross-channel coordinate, to improve the prediction capability. Bousmar and Zech (1999) have proposed exchange discharge method for estimating discharge in compound channels. They accounted momentum transfer proportional to the product of velocity gradient at the interface and the mass discharge exchanged through the interface between the flood plain and main channels due to turbulence and the resulting averaged flow velocities are determined from a rather complicated set of analytical equations. Solution techniques proposed by Van Prooijen et al. (2005) are relatively cumbersome and, in addition, transverse numerical integration of  $U(y)$  is required to obtain stage-discharge relationships. A new method to calculate flow in compound channels is proposed by Huttoff et al. (2008). The proposed method is based on a new parameterization of the interface stress

between adjacent flow compartments, typically between the main channel and floodplain of a two-stage channel. A modified expression to predict the boundary shear stress distribution and stage-discharge in compound channels is derived by Khatua et al. (2011). The practical method is taking due care of the momentum transfer.

During flood it is very difficult to do field investigations, so investigators generally choose experimental approaches in laboratories to understand the complex phenomenon with ease. This approach also carries some drawbacks such as, the data can only be collected at a limited number of points; the full-scale modeling and detailed measurements of turbulence usually can't be taken. Thus, a computational approach can be handy to overcome some of these issues and provide a complementary tool. In particular, a computational approach is readily repeatable, can simulate at full-scale and provide a spatially dense field of data points. In recent years numerical modeling of open channel flows has successfully reproduced experimental results. Computational Fluid Dynamics (CFD) has been used to model open channel flows ranging from main channels to full-scale modeling of flood plain. Simulations have been performed by Krishnappan and Lau (1986), Larson(1988), Kawahara and Tamai(1988) and Cokljat (1993). More detailed numerical modeling has been undertaken by Thomas and Williams (1995a; 1995b; 1999) and Shi et al. (2001) to examine the detailed time dependant three dimensional nature of the flow in compound channels. CFD has also been used to model flow features in natural rivers by Sinha et al. (1998), Hodskinson and Ferguson (1998), Lane et al. (1999) and Morvan (2001). Thomas and Williams (1995a; 1995b; 1999), Shi et al. (1999) have adopted LES method to investigate over-bank channel flow. Salvetti et al. (1997) has conducted LES simulation at a relatively large Reynolds number for producing results of bed shear, secondary motion and vorticity well comparable to experimental results. Pan and Banerjee (1995), Hodges and Street (1999), Nakayama and Yokojima (2002) have recently studied free surface fluctuations of open channel flow by employing LES method where the free surface was filtered along with the flow field itself, which introduced extra SGS terms. Kim et al. (2008) analyses three-dimensional flow and transport characteristics in two representative multi-chamber ozone contactor models with different chamber width using LES. Beaman (2010) studied the conveyance estimation using LES method.

The resistance factors such as resistance coefficient, drag, boundary shear stress, channel roughness, shear stress due to secondary flow directly influences the conveyance capacity and play

an important role in predicting conveyance in compound channels. Research concerning resistance to flow in compound open channel has been studied by many scholars, such as Lotter (1933), Pavlovskii (1932), Einstein and Banks (1950), Krishnamurthy and Christensen (1972), Myers and Elsayy (1975) developed models for composite friction factor. These models provided scope for further modeling on composite roughness and discharge estimation. Rajaratnam and Ahmadi (1979) studied the flow interaction between straight main channel and symmetrical floodplain with smooth boundaries. The results demonstrated the transport of longitudinal momentum from main channel to flood plain. Posey (1967), Wormleation (1982) have done experimentations and observed that the Manning's equation and the Darcy-Weisbach equation are not suitable for compound channels. Knight and Demetriou (1983) conducted experiments in straight symmetrical compound channels to understand the discharge characteristics, boundary shear stress and boundary shear force distributions in the section. Knight and Hamed (1984) extended the work of Knight and Demetriou (1983) to rough floodplains. Dracos and Hardegger (1987) proposed a model to predict composite friction factor in compound open channel flow by considering momentum transfer in to account and also mentioned that composite friction factor is depending on main channel and flood plain width and the ratio between hydraulic radius to the depth of the main channel. Pang (1998) conducted experiments on compound channel in straight reaches under isolated and interacting conditions. It was found that the distribution of discharge between the main channel and floodplain was in accordance with the flow energy loss, which can be expressed in the form of flow resistance coefficient. Christodoulou and Myers (2004) quantified the apparent shear on the vertical interface between main channel and flood plain in symmetrical compound sections. The apparent shear stress is expressed in terms of an apparent friction factor and the square of the velocity difference between subsections. Yang et al. (2005) presented the study of Manning's and Darcy's Weisbach equation and through vast number of collected experimental data indicated that Darcy's Weisbach resistance factor is a function of Reynolds number but the functional relationship is different from single channel. Cao et al. (2006) developed new formulations to present the flow resistance and momentum flux in compound open channels. As implemented in the St.Venant equations, these formulations facilitate a physically enhanced approach for evaluating conveyance, roughness, stage-discharge relationship. Experimental data, analysis, and formula recommendations are presented in Yang et al.(2007). Through series of experimentation analyzed Manning's, Darcy's Weisbach, Chezy's resistance factor

as well as the Nikuradse roughness height and compared the conventional methods for determination of composite friction factor. They comprehended that conventional methods are not suitable for the prediction of composite resistance in compound channel flow. Hin et al. (2008) developed method to predict discharge by means of composite friction factor. Here they observed that composite friction factor depends upon apparent friction factor, which increases rapidly with increase in flow depth. Zeng et al. (2010) predicted, lateral depth varying open channel flow using an analytical model, which can be affected by the friction factor and the dimensionless eddy viscosity. This approach is found to be effective once the roughness coefficients and hydraulic radius in different sub-regions have been determined.

The reason behind the inadequacy in prediction of composite friction factor and discharge in compound channels may be the improper accounting of momentum transfer between main channel and flood plain. In addition to it, the environmental condition, impact of thermodynamic parameters, physical parameters and hydraulic parameters holds strong non-linear relation. Presently rapid development in intelligence computing not only lessening the cumbersome effort of experimentation but also it eliminates cumbersome computations. Walid and Shyam (1998) adopted back propagation (BP) algorithm of artificial neural network (ANN) for the prediction of discharge in a compound open channel flow. Notable past studies in this direction are Neuro-fuzzy model to simulate Coolbrook-White equation for prediction of friction factor in smooth open channel flow (Bigil and Altun 2008; Yuhong and Wenxin 2009) and prediction of friction factor in pipe flow problems (Fadare and Ofidhe 2009). Esen et al. (2009) have demonstrated the use of adaptive-neuro fuzzy inference system (ANFIS) for modeling of ground-coupled heat pump system. The model based on fuzzy systems uses hybrid learning algorithm proposed by Das and Kishor (2009) for the prediction of heat transfer in pool boiling of distilled water.

# CHAPTER 3

## NUMERICAL ANALYSIS OF TURBULENT FLOW STRUCTURES

# NUMERICAL ANALYSIS OF TURBULENT FLOW STRUCTURES

---

## 3.1 INTRODUCTION

Computational Fluid Dynamics (CFD) is a computer based mathematical tool. The growing interest on the use of CFD based simulation by researchers has long been identified in various fields of engineering. It has started around 1960 and with the process of improvement in hardware of computers, CFD simulation is now showing astounding accuracy. The basic principle in the application of CFD is to analyze fluid flow in-detail by solving a system of non-linear governing equations over the region of interest, after applying specified boundary conditions. The CFD based simulation relies on combined numerical accuracy, modeling precision and computational cost.

Application of CFD in open channel flow needs solving Navier-Stokes equation (N-S). These are the non-linear partial differential equations, which provide the fundamental basis for single phase fluid flow. There is no direct solution of the equation for the flow. The N-S in vector form for single phase incompressible fluid flow can be expressed as:

$$\frac{\partial}{\partial t}(\rho \bar{u}_i) + \frac{\partial(\rho \bar{u}_i \bar{u}_j)}{\partial z_j} = \frac{\partial}{\partial z_j} \left( \mu \frac{\partial \sigma_{ij}}{\partial z_j} \right) - \frac{\partial \bar{p}}{\partial z_i} - \frac{\partial \tau_{ij}}{\partial z_j} \quad (3.1)$$

where  $\sigma_{ij}$  and  $\tau_{ij}$  are normal and shear stress component on any assumed plane normal to  $i$  along  $j$  direction.  $\bar{u}_i, \bar{u}_j$  are time averaged instantaneous velocity component along  $i, j$  directions.  $p$  = pressure,  $\mu$  = co-efficient of viscosity,  $\rho$  = density. The process of the numerical simulation of fluid flow using the above equation generally involves three steps (a) Pre-Processing (b) solver and (c) post processing, the details are:

- Pre-Processing
  - Geometry set-up and Discretization of domain
  - Defining the condition of flow (e.g turbulent, laminar etc.)
  - Specification of appropriate boundary condition and temporal condition.
- Solver
  - The equation iterates over and over till desirable level of accuracy is achieved.

- Post-Processing
  - Results are analyzed and visualized.

### 3.2 GEOMETRY SET UP AND DISCRETIZATION OF DOMAIN

The fluid flow governing equations (momentum equation, continuity equation) are solved based on the discretization of domain using the Cartesian co-ordinate system. This procedure involves dividing the continuum into finite number of nodes. The CFD computations need a spatial discretization scheme and time marching scheme. Mainly the domain discretization is based on *Finite element, Finite Volume and Finite Difference Method*. Finite Element method is based on dividing the domain into elements. The numerical solution can be obtained in this method by integrating the shape function and weighted factor in an appropriate domain. This method is suitable with respect to both structured and unstructured mesh. The application of Finite Volume method needs dividing the domain into finite number of volumes. Here the specified variables are calculated by solving the discretized equation in the center of the cell. This method is developed by taking conservation law in to account. Finite Volume method is suitable for applying in unstructured domain. Finite Difference method is based on Taylor's series approximation. This method is more suitable for regular domain.

The discretization of complex computational domain is critical. These kinds of domain don't coincide with the co-ordinate lines with that of a structured grid, which leads to approximation of the geometry. The only procedure to represent complex computational domain is to use a stepwise approximation. But such an approximation is also arduous and quite time consuming. Further, the stepwise approximation introduces truncation error and that can be overcome by providing very fine Cartesian mesh. Thus, structure of grid lines causes further wastage of computer storage due to unnecessary refinement. Hence in this study, the geometry of experimental channel (S-1 case) adopted by Tominaga and Nezu (1991) is discretized with hybrid unstructured meshes as shown in Figure 3.1. These meshes are mixture of triangular and quadrilateral elements used to construct the grid. The most efficient feature of unstructured mesh generation is that, it allows the calculation of flows in or around geometrical features of arbitrary complexity such as change of geometry from main channel to flood plain, without spending more time on mesh generation and mapping. The channel flume had the configuration of 8 m length and  $0.4 \times 0.4 \text{ m}^2$  cross-section as shown in Figure 3.5. Geometry of the compound channel is created using ANSYS 13 design modeler and shown in Figure 3.1. For this

case of experimentation, the depth of flow in main channel is 0.803 m. and flood plain is 0.603 m. , B/H ratio is 4.981. The channel slope is 0.00064 m/m.

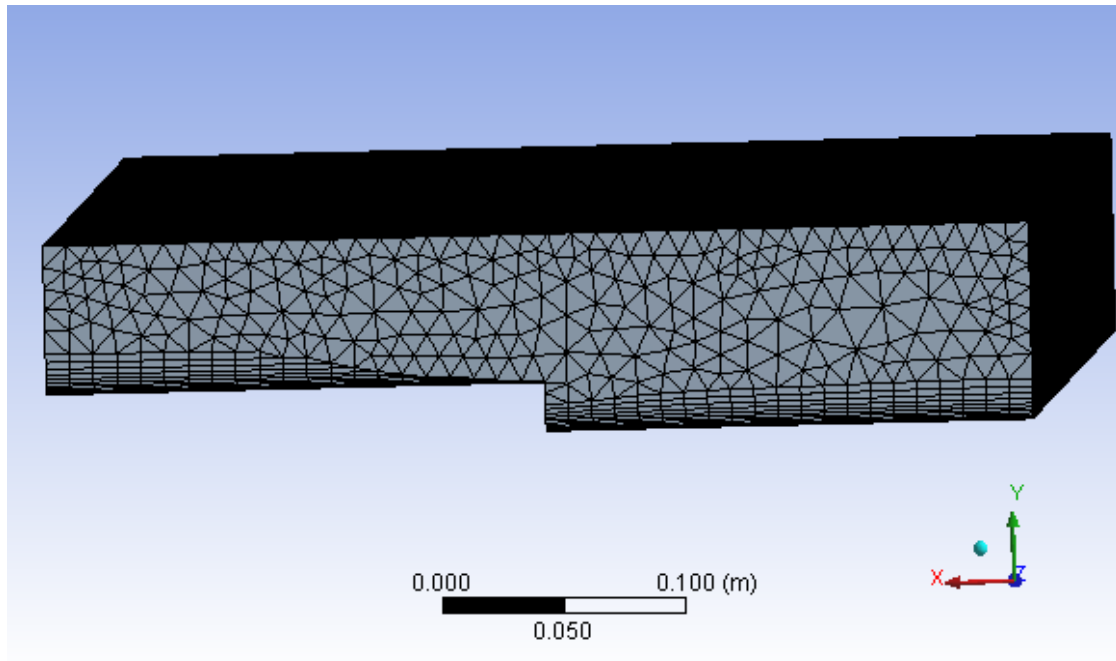


**Figure.3.1. Schematic diagram of hybrid mesh**

### 3.3 TURBULENCE MODELING

The nature of flow in compound open channel is turbulent. Gravity, channel geometry are mainly responsible for turbulent flow for this particular condition. Turbulence in nature is a random three dimensional time-dependent eddying motion with many length scales . This is also efficient transporter and mixture of momentum, energy constituents. The three dimensional nature of turbulent flow can be decomposed into mean part and fluctuation part, which is called Reynolds decomposition. The spatial character of turbulence reveals the eddies with wide range of length scales. In turbulence, particles of fluid which are widely separated, are brought close together by eddying motion. This makes the effective exchange of heat, mass and momentum. Figure 3.2 shows the energy cascade process, where the larger eddies are converted to smaller eddies and are finally dissipated. In this figure  $L$  = larger turbulent length scale,  $Re$  = Reynolds number,  $l_\epsilon$  = length scale at any stage for a particular Reynolds number.

The turbulence in open channel is quite complex and the flow structure involved in it creates uncertainty in prediction of flow variables. Particularly in straight compound channel, turbulent structures are characterized by large shear layers generated by difference of velocity between main channel and flood plain flow. This large shear layer region creates vortices both longitudinally as well

as vertically. Further, turbulent structure such as secondary current (which is generally driven by the anisotropy and in-homogeneity of turbulence) creates velocity dip and affects the flow. Although, the influence of secondary flows for river processes has long been recognized, but their origin, mechanics, effects and co-relations with primary mean flow and turbulence are still a matter of debate. Hence in this study an effort has made to recognize the affect of the turbulence in compound open channel.

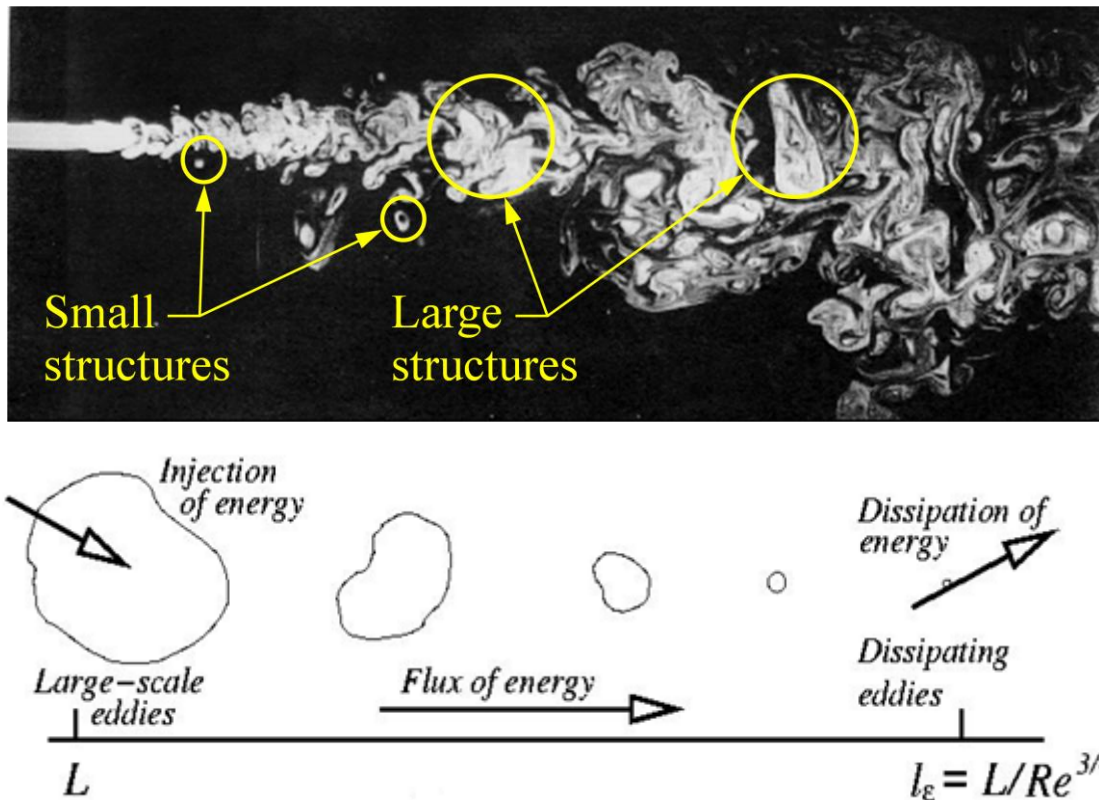


**Figure.3.2. Energy cascade process with length scale.**

### 3.3.1. LARGE EDDY SIMULATION

Turbulent flow has wide range of length and time scales. The larger scale motions are generally energetic than the small ones and their size makes them the most effective transporters, also larger eddies depend highly on boundary conditions and hence determine the basic feature of flow. Large scale eddy helps in transfer of momentum and heat. This accounts for 0.8 times of the total turbulent energy. Further, small scale eddies are isotropic and universal in nature. So a simulation study which can treat these larger eddies and take account the effect of smaller makes sense.

To get in-detail flow feature in turbulent flow requires proper analysis of the larger and smaller eddies. The larger eddies account for 80% of the turbulent flow energy and hence need to be computed. Presently for simulating fully fledged flow of practical open channels, computational

turbulent models are used. It has been observed that, DNS method can simulate almost all ranges of scales of this flow condition. However, it requires very finer meshes equivalent to Kolmogorov Length and time scale. Hence to simulate DNS, higher processing system is inevitable. Subsequently it is found that, LES method simulates large scale turbulent motions directly, while the unresolved small scale motions are modeled through the use of a Smagorinsky model. This model captures larger scale motion such as DNS, as well as it covers the effects of small scales of eddies by using sub-grid scale (SGS) model. Therefore to ease the difficulties somewhat, LES method can be adopted.

The governing equations employed for LES are obtained by filtering the time-dependent Navier-Stokes equations in either Fourier (wave-number) space or configuration (physical) space.

$$\frac{\partial \rho}{\partial t} + \frac{\partial(\rho \bar{u}_i)}{\partial z_i} = 0 \quad (3.2)$$

$$\frac{\partial}{\partial t}(\rho \bar{u}_i) + \frac{\partial(\rho \bar{u}_i \bar{u}_j)}{\partial z_j} = \frac{\partial}{\partial z_j} \left( \mu \frac{\partial \sigma_{ij}}{\partial z_j} \right) - \frac{\partial \bar{p}}{\partial z_i} - \frac{\partial \tau_{ij}}{\partial z_j} \quad (3.3)$$

The eqn. (3.2) is the continuity equation. This equation is linear and does not change due to filtering. The filtering process filters out the eddies whose scales are smaller than the filter width or grid spacing used for the computations. The resulting equations thus govern the dynamics of large eddies. A filtered variable is defined by:

$$\bar{\phi}(x) = \int_D \phi(z') G(z, z') dx' \quad (3.4)$$

Where G is the characteristics of the filter used. z = stream-wise direction, z' = instantaneous length, This function is associated with the cutoff scale with space and time. The cutoff scale is associated with cutoff wave number and cutoff time scale is associated with cutoff frequency. The unresolved part of  $\phi$  denoted as  $\phi'$  can be defined operationally as:  $\phi' = \phi - \bar{\phi}$ ,

where,  $\phi$  = spectral space,.

**3.3.2. SUB-GRID SCALE MODEL:** From the equation (3.2) the non-linear transport term  $\overline{u_i u_j}$  can represent as :

$$\begin{aligned} \overline{u_i u_j} &= \overline{(U_i + u_i')(U_j + u_j')} \\ &= \overline{U_i U_j} + \overline{U_i u_j'} + \overline{U_j u_i'} + \overline{u_i' u_j'} \\ &\quad \text{I} \quad \text{II} \quad \text{III} \quad \text{IV} \end{aligned}$$

Here,  $u_i$  and  $u_j$  are velocity along  $x_i$  and  $x_j$  directions.  $u'_j$  and  $u'_i$  are fluctuation velocities,  $\overline{u}$ ,  $\overline{v}$ ,  $\overline{w}$  are time averaged instantaneous velocity component along X, Y, Z directions.

During time averaging, term II and term III vanishes but not in volume averaging. This time averaging introduces Sub-grid scale stress  $\tau_{ij}$  (SGS) as:  $u_i u_j = \overline{u'_i u'_j} - \overline{U_i U_j}$

The non-linear transport of energy generates smaller scales of eddies as shown in cascade process in Figure 3.2. The essential measure LES method takes in to account the affect of resolved large scale to unresolved sub-grid smaller scales. The SGS method plays this role. In this study Smagorinsky model is used to carry out the analysis. For the present study, the commonly used Smagorinsky model is utilized in which the sub-grid stress tensor  $(u_i u_j)_{av}$ , which is related to eddy viscosity as:  $(u_i u_j)_{av} = 2\nu_s S_{ij}$

(3.5)

$$S_{ij} = \frac{1}{2} \left( \frac{\partial u_j}{\partial z_i} + \frac{\partial u_i}{\partial z_j} \right)$$

(3.6)

Where  $u_i$  and  $u_j$  are the unresolved velocity components in the  $x_i$  and  $x_j$  directions, respectively.  $S_{ij}$  is the rate-of-strain tensor and  $\nu_s$  is an estimate of the eddy viscosity given by:

$$\nu_s = L^2 (2S_{ij} S_{ji})^{1/2},$$

(3.7)

Where,  $L$  is a length scale.

**3.3.3. NEAR WALL MODELING:** Rapid variation of flow variables generally occurs at the boundary layer regions i.e. in viscous layer. Viscous effects on the transport processes are also large in the boundary layer. As viscous is a very thin layer and further transition from viscous to buffer layer produces large variation within the flow features. Therefore, it is essential to reflect these changes in the discretization process to carry out simulation successfully. Hence, near wall modeling is done to incorporate these changes in flow features for this study.

It has been observed from experiments and mathematical analysis that, the near-wall region can be subdivided into two layers. The innermost layer, so-called “viscous sublayer”, where the flow is almost laminar and the (molecular) viscosity plays a dominant role in momentum and energy transfer. Further away from the wall is the “logarithmic layer”, where turbulence dominates and the mixing process takes place. Finally, there exists a region between the viscous sublayer and the logarithmic layer called the “buffer layer”, where the effects of molecular viscosity and turbulence are of equally

importance. The Figure 3.3 illustrates these subdivisions of velocity profile as the near-wall region, buffer and outer region of the flow.

The logarithmic nature of the velocity profile in open channels gives rise to the well known 'log law of the wall'. Assuming that the logarithmic profile reasonably approximates the velocity distribution near the wall, it provides basic means to numerically compute the fluid shear stress as a function of the velocity at a given distance from the wall. This is known as 'wall function'. Consequently, the near wall behavior is generally taken into account during discretization of the continuum by using wall function. The Figure 3.4 illustrates wall functions.

However, to perform LES, requires an extremely fine grid, which resolves the viscous sub-layer down to a wall-normal distance  $y^+$ , where  $y^+ = \frac{u_* y}{\nu}$ ,  $y$  = depth at a point. LES directly computes the variables down to the wall without implementing a wall function. Even though, LES does not replace the N-S equations with a wall-function near the wall, it uses a wall-function approximation to make an estimate of  $u_*$  (shear velocity) at the wall. This has proven to be accurate for numerically simulating open channel flows. It involves fitting the log-law to the mean velocity profile of the flow to calculate shear velocity from simulation. Thomas and Williams (1994) has adopted this method and drew comparison between  $u^+$  and  $y^+$  for experiment and LES.

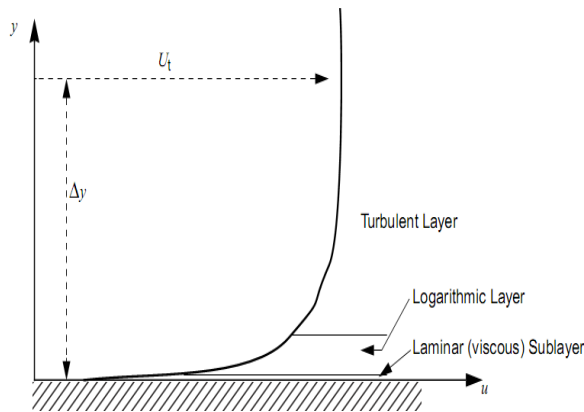


**Figure.3.3.** The subdivisions of the near-wall region.

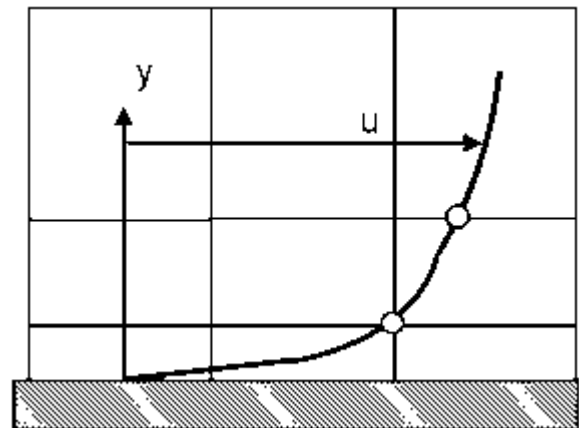


**Figure.3.4.** Wall functions used to resolve boundary layer.

### 3.4 BOUNDARY CONDITIONS

For a given computational domain, boundary conditions are imposed which can sometimes over-specify or under-specify the problem. Usually, after imposing boundary conditions in non-physical domain may lead to failure of the solution to converge. It is therefore important, to understand the meaning of well-posed boundary conditions. The boundary conditions implemented for this study are shown in Figure 3.5. Subsequently, these conditions are discussed in detail below:

#### 3.6.1 INLET AND OUTLET BOUNDARY CONDITION

The channel reported here allows the values on the inlet and outlet boundaries to coincide, and a pressure gradient was further specified across the domain to drive the flow. To initialize the flow a mean velocity was specified over the whole inlet plane upon which velocity fluctuations were imposed. The inlet mean velocities were derived where possible from the experimental average values.

In order to specify the pressure gradient the channel geometries were all created flat and the effects of gravity and channel slope implemented via a resolved gravity vector. It represents the angle between the channel slope and the horizontal, the gravity vector is resolved in x, y and z components

$$\text{as } (0, -\rho g \sin \theta, \rho g \cos \theta) \quad (3.8)$$

Where  $\theta$  = angle between bed surface to horizontal axis. Here, the z component denotes the direction responsible for flow of water along the channel and the y component is responsible for creating the hydrostatic pressure. From the simulation, y component of the gravity vector ( $-\rho g \sin \theta$ ) is found to be responsible for the convergence problem of the solver.

#### 3.6.2 FREE-SURFACE

Here, Symmetry Boundary condition is used for the free-surface. This condition follows that, no flow of scalar flux occurs across the boundary. In implementing this condition normal velocities are set to zero and values of all other properties outside the domain are equated to their values at the nearest node just inside the domain. Here the experimental bulk velocity of the flow is initially approximated as

$$W = 0.368 \text{ m/s}, V = 0, U = 0 \text{ and } \frac{\partial W}{\partial z} = 0$$

#### 3.6.3 WALL

A no-slip boundary condition is the most common boundary condition implemented at the wall and prescribes that the fluid next to the wall assumes the velocity at the wall, which is zero.

$$U = V = W = 0$$

**Table 3.1 Summary of Mesh and Simulation details Using ANSYS-CFX.**

Case	Mesh spacing (m)	$y_+$ range	$H/u_*$ (sec.)	Time step (sec)	LETOT	
					Initial	Trial
S-1	0.005	9.23 -110.87	5	0.001	70	10

**3.5 SOLVER**

ANSYS-CFX solver manager is used to carry out the simulation process. Here the Advection term is discretized with bounded central difference scheme and transient terms are discretized with Second order scheme. Courant number ( $C_r$ ) is controlled between 0 - 0.5. After that, the equation is iterated over and over till desirable level of accuracy of  $10^{-6}$  of residual value is achieved.

**3.6 POST PROCESSING : ANALYSIS OF TURBULENCE MODEL**

**3.6.1. FLOW PARAMETERS**

Tominaga and Nezu (1991) has carried out experimentation by using fibre-optic Laser-Doppler Anemometer to measure three directional components of turbulent velocity. Their data is comprehensively available for comparison and simulation. They noticed that, the flow is considered to be uniform incompressible turbulent flow at the test section of 7.5 m. So, to incorporate this the length of channel is taken as 8 m, because the uniform flow is developed after this length approximately. The hydraulic radius (R) of the channel is 0.043m. The Reynolds number (Re) of the flow for the case S-1 is  $6.72 \times 10^4$ .

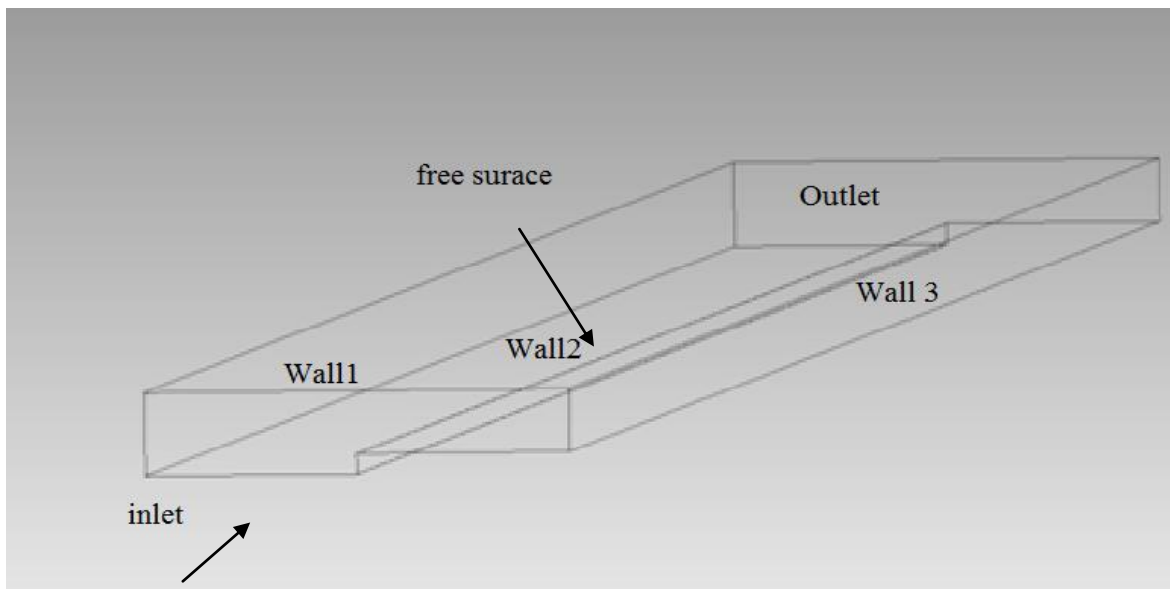


**Figure.3.5. Schematic presentation of geometric alignment and boundary conditions of the channel.**

### 3.6.2. RESULTS

The numerical simulation are carried out by using ANSYS-CFX solver and the numerical results are compared with the experimental results. The results are tabulated in Table 3.2. Here mean bulk velocity is calculated using the formulation:

$$W_b = \frac{\int w dA}{A} \quad (3.9)$$

.Where,  $W_b$  = Bulk Velocity along Stream-line of flow.  $w$  = streamline velocity at any point,  $A$  = Cross-section area of the channel. The composite Manning's friction factor is calculated from Manning's equation.

**Table 3.2 Comparison of the experiment and simulation results**

Case	Maximum Velocity $W_{max}$ (m/s)	Mean Bulk Velocity $W_b$ (m/s)	Discharge ( $m^3/s$ )	Composite manning's 'n'	Shear Velocity $u^*$ (m/s)
S-1 (Tominaga and Nezu 1991)	0.409	0.368	0.00738	0.011383	0.0161
Present LES simulation	0.4049	0.367	0.00736	0.011380	0.01606

The table shows that, the results obtained from LES simulation are in good agreement with case S-1 of Tominaga and Nezu (1991).

### 3.6.3. VELOCITY DISTRIBUTION

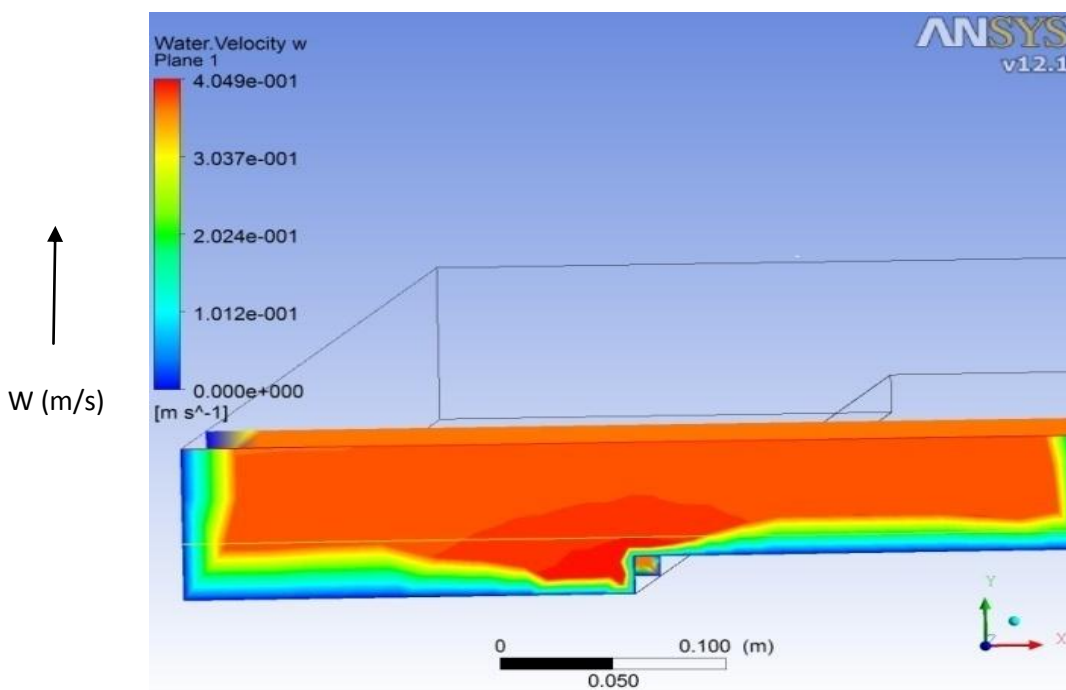


**Figure.3.6. Mean Velocity distribution of LES Simulation**

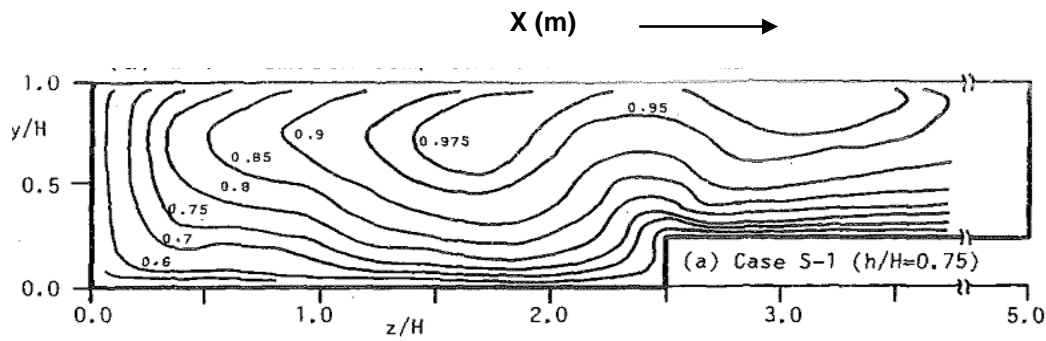


**Figure.3.7. Mean Velocity distribution of experiment. (Tominaga and Nezu 1991)**

The isovel-lines of the non-dimensional stream-wise velocity  $W(z)$  are computed by LES method as shown in Figure 3.6. It shows from simulation that maximum velocity is 0.4049 m/s and can be observed near centerline of channel at approximately 0.057m from centerline of the channel. The bulk velocity is 0.367 m/s. Isovel lines bulge significantly upward in the vicinity of the junction edge along the flow. The patterns of the isovel lines are convincingly followed by LES simulation results with the experimental results of Tominaga and Nezu (1991) as shown in Figure 3.8. The reason of this bulge is the decelerated region on the both side of the junction region of main channel. The decelerated region is created because of low-momentum transport due to secondary current away from the wall. This causes the bulge in the main channel and flood plain interface due to high momentum transport by secondary current. Consequently, primary velocity is directly affected by momentum transport due to secondary current. Figure 3.8 shows the distribution of non- dimensional depth averaged velocity head. It shows that velocity head peaks in the center of main channel and slightly in the floodplain. Depth averaged velocity is calculated from eqn. (3.10):

$$W_d = \frac{1}{H} \int_0^H w dy \quad (3.10)$$

where  $W_d$  = depth averaged velocity along streamline,  $H$  = depth of flow.

The peak value of the depth averaged velocity head lies at the main channel just before the junction of main channel and flood plain. Also a subsequent small peak can be observed on the flood plain. It shows the maximum depth averaged velocity lies velocity at main channel with and subsequently at the flood plain which is on line with Cater and Williams (2008).

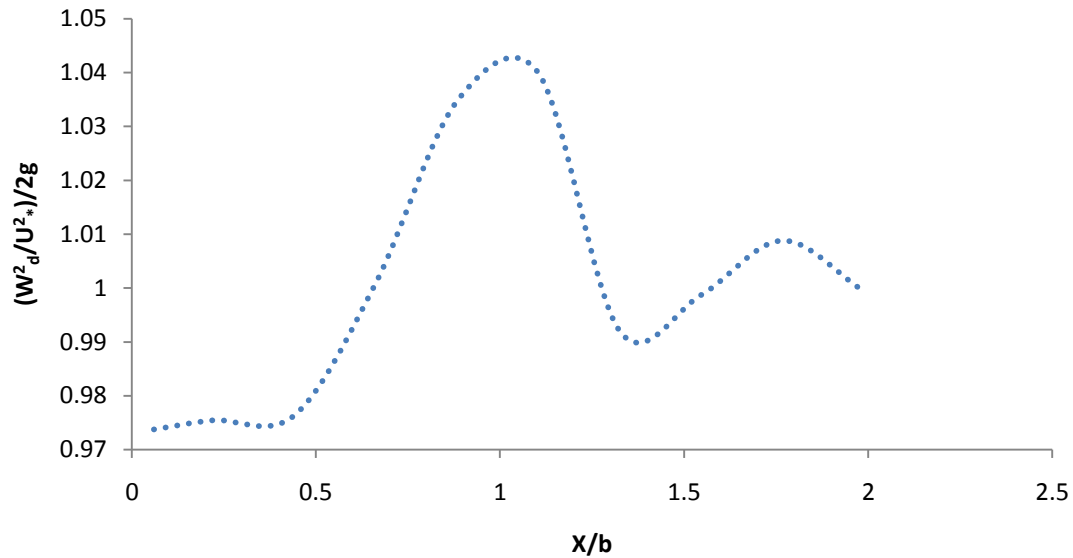


**Figure.3.8. The distribution of depth averaged velocity head.**

#### **3.6.4. BED SHEAR STRESS**

The distribution of the non-dimensional bed shear stress ( $\tau/\tau_{avg}$ ) obtained after simulation is presented in Figure 3.9. The pattern of distribution is found to be distributed evenly with the experimental results. The actual distribution of bed shear stress in experimental results attains two peak one at flood plain and other at the main channel. The simulation result has also attained the same pattern and which show high degree of accuracy of simulation. The distribution shows that the peaks can be observed both side of the junction of the main channel and flood plain. The average bed shear distribution in main channel is found to be lesser than the flood plain.

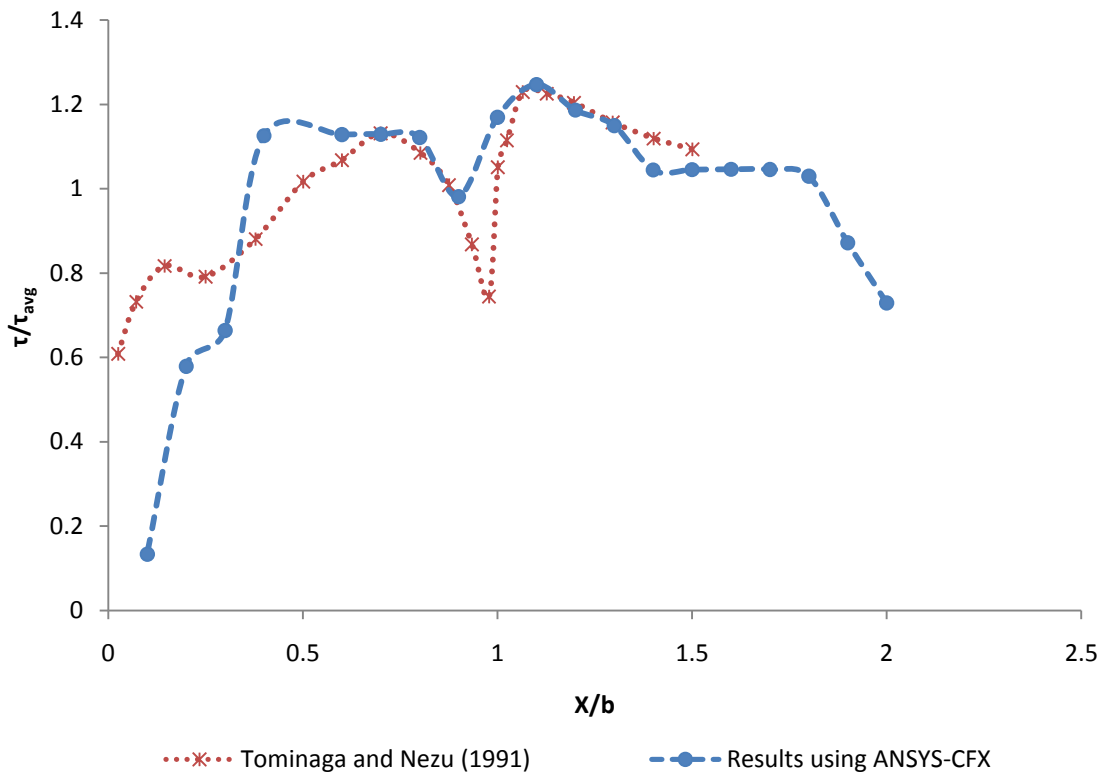


Figure.3.9. The distribution of non-dimensional bed shear stress

3.6.5. SECONDARY CURRENT

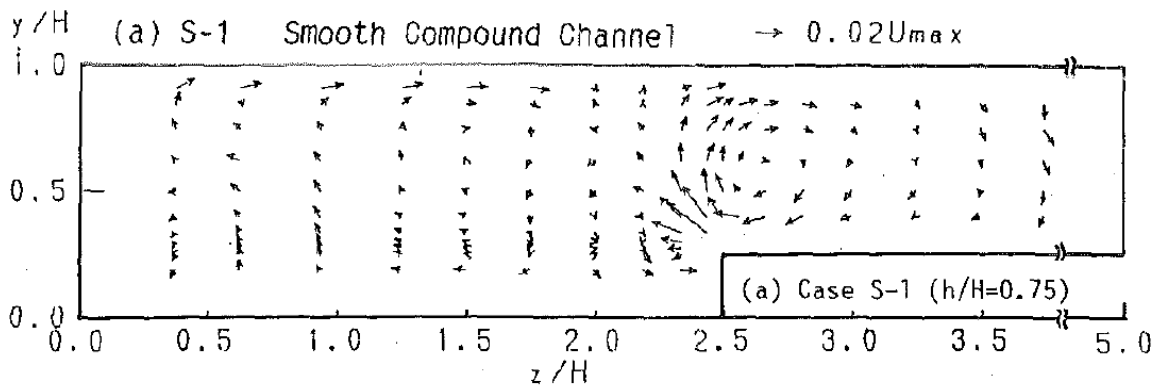
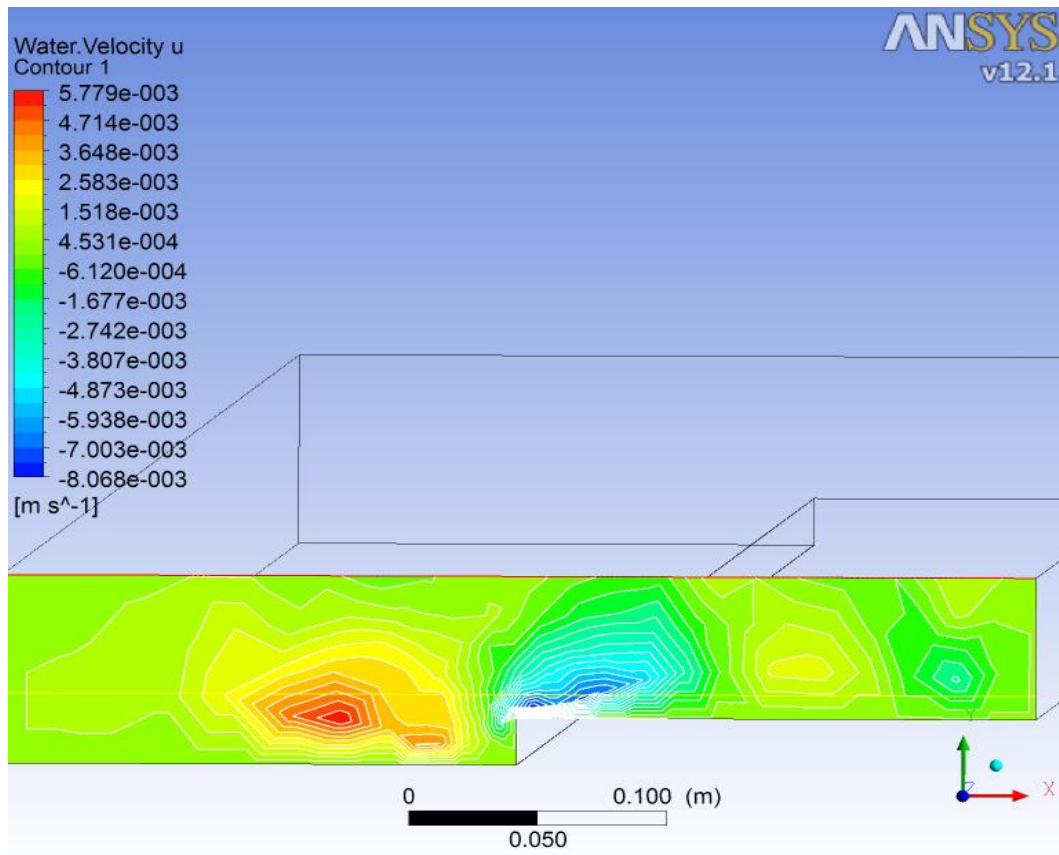


Figure.3.10. Experimental velocity vectors from experimentation (Tominaga and Nezu1991).



**Figure.3.11. Stream-wise non-dimensional averaged secondary velocity contours**

From Figure 3.10 and Figure 3.11, it can be observed a pair of secondary currents on the both side of the junction of the main channel and flood plain. These currents can be regarded as longitudinal vortex as mentioned by Tominaga and Nezu (1991). The vortex in flood plain reaches the free surface. The mean secondary velocity contours show circulation at the main channel corner, main channel flood plain interface, at the corner of flood plain as shown in Figure 3.11. Which are quiet convincing with experimental secondary current vectors as shown in the Figure 3.10. These resemblances of result have significant contribution on the distribution of average velocity. The large counter rotating secondary structure produces usual velocity dip and has maximum impact on stream wise velocity. These counter rotating flow structure creates resistance and reduce the average velocity, thus discharge. Because of this structure, it is difficult construct a one dimensional model.

### 3.6.6. LATERAL MOMENTUM TRANSFER

The presence of secondary current can be observed from Figure 3.11. It can be seen that these turbulence driven flow structure affects the velocity, wall shear stress etc. Tominaga and Nezu (1991) investigated the contribution of secondary current to lateral momentum transfer on the basis of

Reynolds equation. The equation of the stream-wise component for fully developed turbulent open channel flow is:

$$V \frac{\partial W}{\partial y} + U \frac{\partial W}{\partial z} = gl_e + \frac{\partial(-\overline{uv'})}{\partial y} + \frac{\partial(-\overline{uw'})}{\partial z} + \nu \left( \frac{\partial^2 W}{\partial y^2} + \frac{\partial^2 W}{\partial z^2} \right) \quad (3.11)$$

Where,  $U, V, W$  are velocities along  $X, Y$  and  $Z$ -axis,  $\overline{u'}$ ,  $\overline{v'}$ ,  $\overline{w'}$  are time averaged instantaneous velocity component along  $X, Y, Z$  directions.

To examine the effect of secondary current on span-wise momentum transport Tominaga and Nezu (1991) integrated eqn.(3.11) over the full depth separately for main channel and flood plain, Which transforms this equation to the depth averaged momentum equation for fully developed turbulent open channel flow as :

$$\frac{\tau(z)}{\rho} = gh_l e + \frac{d}{dz}(h \cdot T) - \frac{d}{dz}(h \cdot J) \quad (3.12)$$

Where  $h$  = depth of flow,  $\tau(z)$  = bed shear stress component,  $T$  = shear stress due to span-wise Reynolds number,  $J$  = Spanwise advection due to secondary current in  $W$ .

$$T = \frac{1}{h_0} \int (-\overline{u'w'}) dy \quad (3.13)$$

$$J = \frac{1}{h_0} \int (-UW) dy \quad (3.14)$$

Here,  $T$  and  $J$  are derived by integrating the depth averaged momentum equation (3.12). These values further helps to get the boundary shear stress and apparent shear stress at a point. The Figure 3.12 shows the variation of  $T$  and  $J$ . It can be observed that the variation of  $J$  is always less than that of  $T$ .  $(T - J)$  explains the apparent shear stress on the  $YX$  plain. From this it can be inferred that near the junction of main channel and flood plain apparent shear stress is negative. The value of apparent shear stress is positive at the main channel flood plain.  $J$  obtained extreme positive and negative peak at the both side of main channel and flood plain.  $T$  has positive peak at the main channel and highest negative peak at the flood plain and main channel junction.

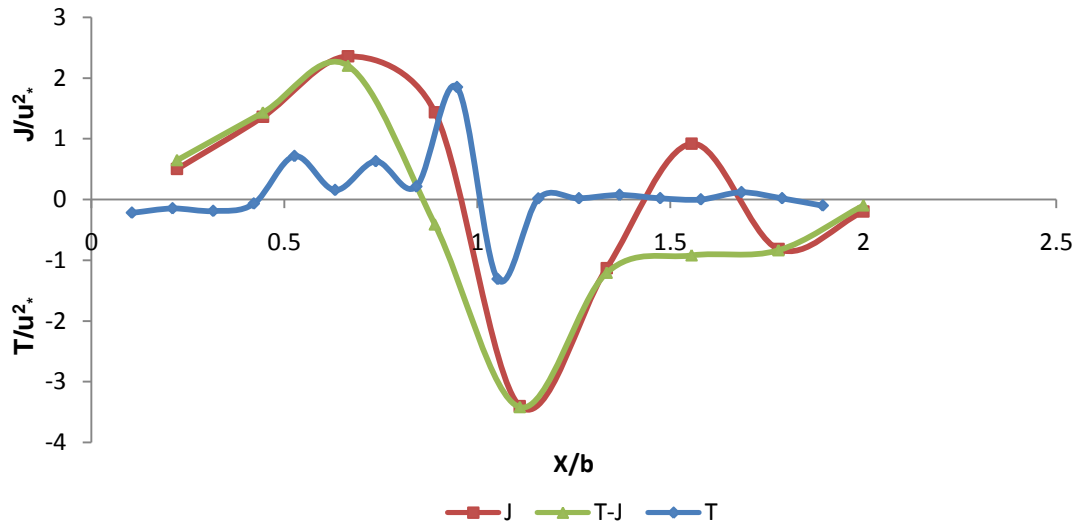


**Figure.3.12. Lateral distribution of turbulent transport and secondary circulation component.**

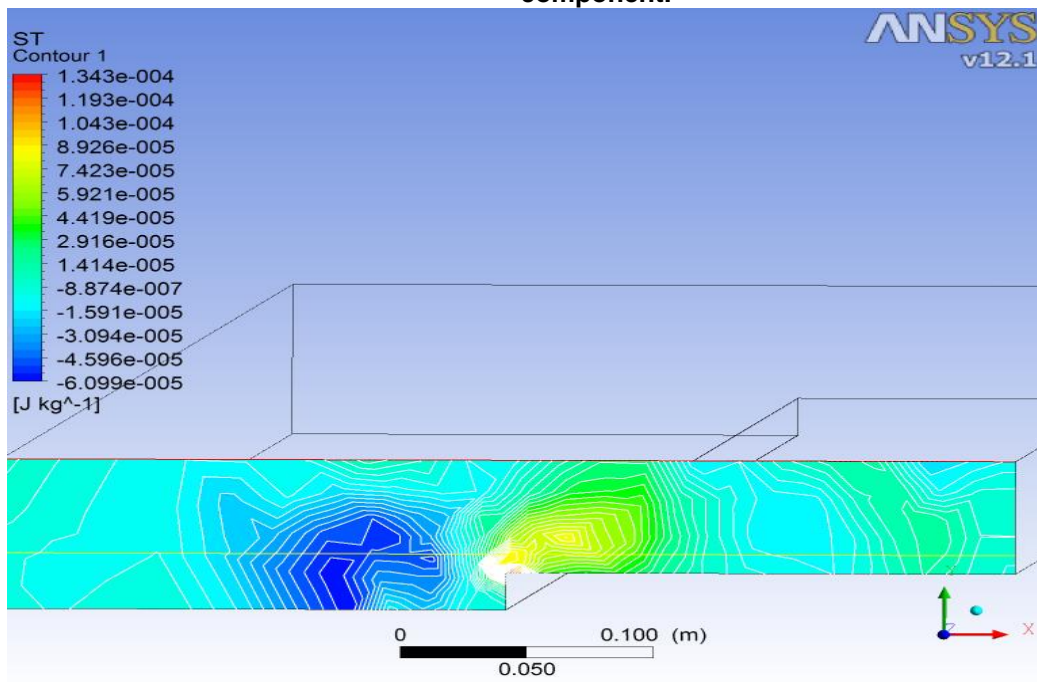
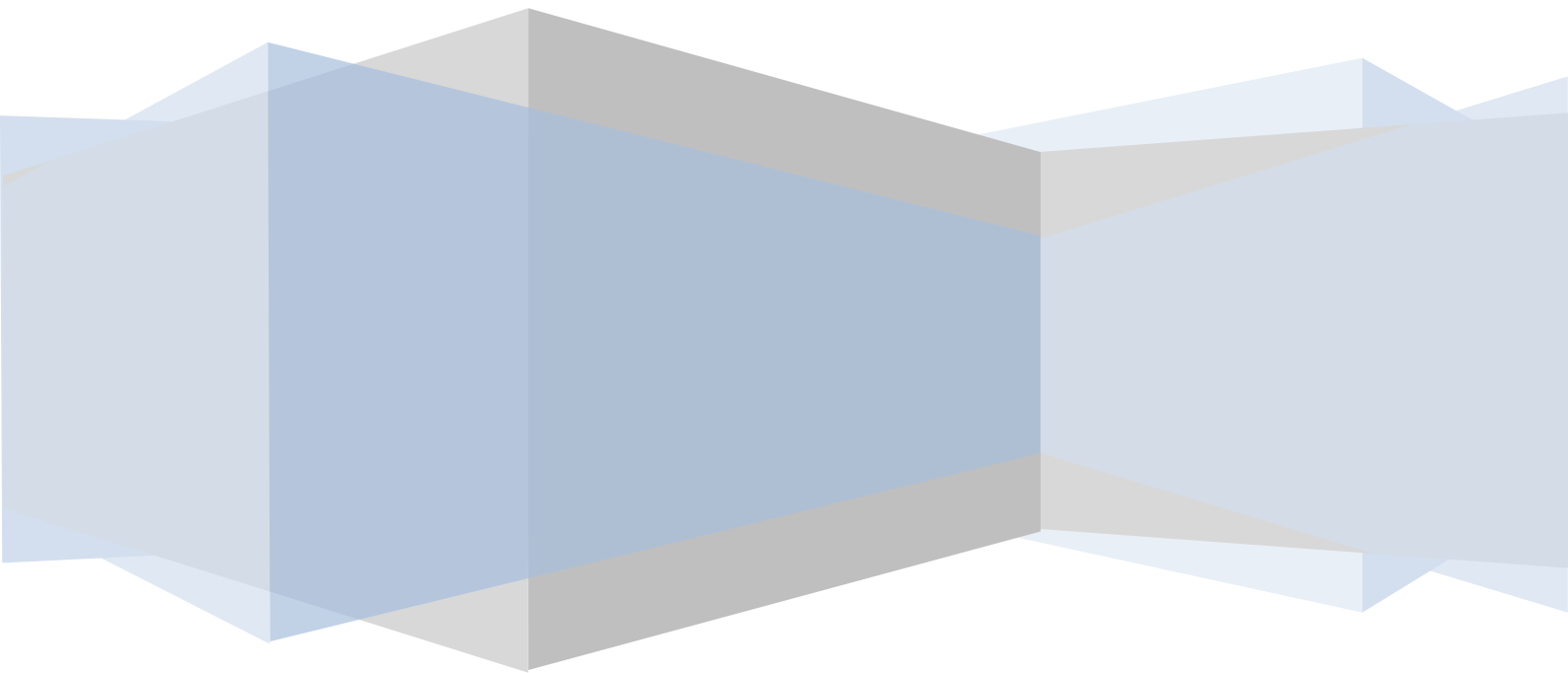


**Figure.3.13. Lateral distribution of secondary circulation component (T)**

The momentum transfer due to secondary circulation component and turbulent transport is shown in Figure 3.13. Apart from momentum transfer phenomenon, the turbulent flow structure also depends upon the corner of the channel and shape of the compound cross-section. The channel corner circulations can be observed from Figure 3.13. This also retards the flow and exerts resistance.

# CHAPTER 4

## ANALYSIS AND PREDICTION OF FLOW AND ITS RESISTANCE FACTOR



## SECTION 4.1: INTRODUCTION

---

Simulation by LES is done for a single flow depth of compound channel as explained in Chapter 3. This helps in predicting the flow variables such as discharge, composite friction factor for a given flow depth with particular flow condition and extracting point to point information from the whole domain of computational space . It is further noticed that, simulating LES for compound channels of different flow depths with different hydraulic condition are arduous and computationally expensive. For this situation a researcher or river engineers dealing in this field need a handy approach, which can easily evaluate the average value of flow variables such as total discharge, total frictional resistance for different hydraulic conditions . Therefore, in this present study artificial intelligence methodologies are taken in to account to eradicate the efficacy involved in prediction of discharge and composite friction factor for wide range of geometric and hydraulics conditions of a compound channel flow. Advantages of Artificial Intelligence techniques are that, these methods are easily implementable to all conditions, as well as it needs less computational facility and time to complete a process. There are many such systems which make the calculation simple and reliable. Among those techniques, currently two advances adaptive approaches such as Back-Propagation Artificial Neural Network (BPNN) and an Artificial-Neuro-Fuzzy Inference System (ANFIS) are chosen for the present study. These approaches have applied to predict the discharge and composite friction factor of compound channel for variable hydraulic flow conditions.

## SECTION 4.2: Modeling of discharge using Back Propagation Neural Network (BPNN)

### 4.2.1 INTRODUCTION

In the present study, four well known methods are studied and compared with developed BPNN model to predict the discharge in compound open channel flow. These are (i) Single Channel Method (Chow 1959) (ii) Vertical Division Method (Lotter 1993, Khatua et al. 2011) (iii) Coherence Method (Ackers' 1999) and (iv) Exchange Discharge Method (Bousmar and Zech 1998). These methods are applied to the compound channels of different hydraulic conditions. The proposed BPNN approach is also applied to the same data sets.

### 4.2.2 SINGLE CHANNEL METHOD

During recent decades, a major area of uncertainty in river channel analysis is that of accurately predicting the discharge capability of compound channel i.e. river channel with flood plains. Cross sections of these compound channels are generally characterized by deep main channel bounded by one or both sides by a relatively shallow flood plain. Chow (1959) suggested that, Manning's, or Chezy or Darcy-Weischbach equations (shown in Eqn. (4.1), (4.2) and (4.3) respectively) are used to predict discharge capacity at low depths when the flow is only in main channel.

$$Q = \frac{1}{n} AR^{2/3} S^{1/2} \quad (4.1)$$

$$Q = CA\sqrt{RS} \quad (4.2)$$

$$Q = \left( \frac{8g}{f} \right)^{1/2} A\sqrt{RS} \quad (4.3)$$

where,  $Q$  = Overall discharge of the compound channel,  $A$  = Area of the compound channel,  $R$  = Aspect ratio of the compound channel,  $S$  = Slope of the main channel,  $f$  = Darcy-Weischbach friction factor of the compound channel, and  $n$  = composite Manning's coefficient of the compound channel.

When over bank flow occurs, these classical formulae either overestimate or underestimate the discharge. Composite roughness methods of Chow (1959) are essentially flawed when applied to compound channels because compound channel is considered as single entity through the process of refined one dimensional methods of analysis. Thus, the carrying capacity is underestimated because

the single channel method suffers from a sudden reduction in hydraulic radius as the main channel discharge inundates to flood plains.

#### 4.2.3 DIVIDED CHANNEL METHOD

The simple sub-division and composite roughness methods given in Chow (1959) are not appropriate to predict discharge and flow resistance in a compound channel. In the light of the knowledge gained about flow structure in compound channels, a number of suggestions have been made to account the interaction process in straight compound channels more accurately. The usual practice of calculating discharge in a compound channel is the use of 'divided channel method'. Assumed vertical, horizontal or diagonal interface planes running from the main channel-floodplain junctions are used to divide the compound section into subsections and the discharge for each subsection is calculated using Manning's or Chezy's or Darcy-Weisbach equation and added up to give the total discharge carried by the compound section. Generally, Manning's formula are used for discharge calculation in compound channels and written as.

$$Q = \sqrt{S} \left( \frac{1}{n_{mc}} A_{mc}^{5/3} P_{mc}^{-2/3} + \frac{1}{n_{fp}} A_{fp}^{5/3} P_{fp}^{-2/3} \right) \quad (4.4)$$

where,  $S$  = longitudinal slope of the channel,  $P_{mc}$  = main channel perimeters,  $P_{fp}$  = flood plain perimeters,  $A_{mc}$  = main channel area,  $A_{fp}$  = flood plain areas,  $n_{mc}$  = main channel Manning's coefficient, and  $n_{fp}$  = flood plain Manning's coefficient.

Mainly, the divided channel method is divided into three methods such as horizontal, vertical and diagonal division methods. Horizontal division method, although a realistic approach, but it neglects the main channel and flood plain interface. In the diagonal division method, division lines for all shapes and flow depths cannot be accurately drawn because uncertainty is gleaned into prediction of zero-shear line due to three dimensional nature of velocity flow field. Therefore, vertical division method is considered to predict discharge in straight compound channel in this study. There are several vertical division methods which are based on altering the wetted perimeter of the sub-area to account for the effect of interaction. Typically, the vertical division lines between the main channel and the flood plain is included in the wetted perimeter for the discharge calculation in the main channel flow. This is intended to have the effect of retarding the flow in main channel and enhancing it in the flood plain. However, simply altering the wetted perimeter by the vertical line does not completely reflect the

interaction effect in a simple function Shiono (1999), Khatua et al. (2011). It is found that this approach generally over predicts flow rate (Wormleaton et al. (1982)) and conceptually, it is flawed since it applies an imbalance of shear forces at the interface. A typical example of vertical division method is shown in Figure 4.1.

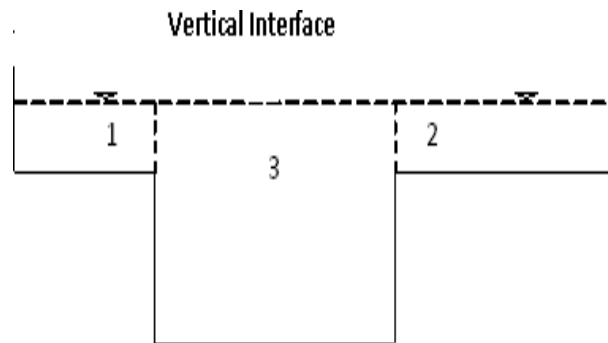


Figure.4.1. Vertical division of the compound channel cross-sectional view.

#### 4.2.4 COHERENCE METHOD (COHM)

It is based on the principle of adjusting the discharges calculated separately for each sub-area by an appropriate method. The coherence method (COHM) of Ackers' (1993,1994) is now well established 1-D approaches for dealing with overbank flow and the related problems of heterogeneous roughness and shape effects. The 'coherence', *COH*, is defined as the ratio of the basic conveyance calculated by treating the channel as a single unit with perimeter weighting of the friction factor to that calculated by summing the basic conveyances of the separate zones.

$$COH = \frac{\sum A_i \sqrt{\sum A_i / \sum (f_i P_i)}}{\sum [A_i \sqrt{A_i / (f_i P_i)}} \quad (4.5)$$

where, *i* identifies each of the *n* flow zones, *A* is the sub-area, *P* is the wetted perimeter and *f* is the Darcy-Weisbach friction factor. As *COH* approaches unit, it is appropriate to treat the channel as a single unit using the overall geometry and discharge is estimated as per single channel method. In extreme cases, *COH* may be as low as 0.5. When coherence is much less than unity then discharge adjustment factors are required in order to correct the individual discharges in each sub-area and calculations are similar to divided channel method. The experimental data of flood channel facility (FCF) is analyzed by Ackers (1994). He has suggested four distinct levels of flow regions above the main channel level existing in straight compound channel flow and different discharge adjustment

factors to be evaluated by methodologies provided by Ackers (1994) for each region to estimate the overall discharge of the compound channel.

**Region 1:**

Here, the depth of flow is low; hence the velocities in flood plain and main channel are very dissimilar.

This region is characterized by the relative depth  $H_r < 0.2$ .

$$H_r = \frac{(H - h)}{H} \tag{4.6}$$

where,  $H$  = water level above channel bottom and  $h$  = bank level above channel bottom.

$$Q = Q_{basic} - DISDEF \tag{4.7}$$

where,  $DISDEF$  = Discharge deficit factor

**Region 2:**

This zone is also of greater depth where interaction effect again disappears and flow computation depends on discharge adjustment factor  $DISADF$  in each part of the channel under consideration.

$$Q = Q_{basic} \times DISADF_2 \tag{4.8}$$

$DISADF_2$  = Discharge adjustment factor for region 2.

**Region 3:**

This zone appears when the relative depth is around 0.5 which again increase the interference effect.

$$Q = Q_{basic} \times DISADF_3 \tag{4.9}$$

$DISADF_3$  = Discharge adjustment factor for region 3.

**Region 4:**

This zone is of greater than relative depth of 0.6 and behaves as single unit due to the coherence character that obeys both the main channel and flood plains.

$$Q = Q_{basic} \times DISADF_4 \tag{4.10}$$

$DISADF_4$ = Discharge adjustment factor for region 4.

where,  $Q_{basic}$  = basic total discharge calculated using zones separated by vertical divisions (omitted from the wetted perimeter). The coherence method is based originally on laboratory data from the FCF. At very shallow depth on flood plain i.e. at depth  $H_f < 0.0625$ , this model disregards. The COHM is more difficult to apply when the roughness of the main channel river bed varies with discharge as is the case in sand bed rivers. Also Ackers (1993) has pointed out that the zonal discharge adjustment factors are not well established because of lack of data when the flow is in region 2, 3, and 4.

#### 4.2.5 EXCHANGE DISCHARGE METHOD (EDM):

This 1-D model of compound channel flows is developed by Bousmar and Zech (1999) and modeled for straight and skew channel with maximum skew angle of  $9^\circ$  by taking the interaction between main channel and flood plain into consideration. EDM also divides the channel as subsections but computes the total discharge by summing up the corrected discharge in each subsection discharge. The EDM requires geometrical exchange correction factor ( $\psi^s$ ) and turbulent exchange model co-efficient ( $\psi^t$ ) for evaluating discharge. Here, momentum transfer is proportional to the product of velocity gradient at the interface with the mass discharge exchanged through this interface due to turbulence. The main channel and each subsection of a compound channel can be considered as a single channel submitted to a lateral flow per unit length  $q_i$ . By assuming the head loss is the same in all subsections and applying the conservation of mass and the momentum equations, the subsection discharge can be evaluated as shown below.

$$Q = \frac{A_i R_i^{2/3}}{n_i} S_f^{1/2} = K_i S_f^{1/2} = K \left( \frac{S_e}{1 + \chi_i} \right)^{1/2} \quad (4.11)$$

where subscript 2 stands for the main channel; subscripts 1 and 3 stands for the floodplains;  $h_1$  and  $h_3$  are main-channel bank level on floodplain 1 and 3 side respectively;  $K_i$  = conveyance factor for each subsection;  $S_f$  = friction slope;  $S_e$  = Energy slope;  $A_i$  = area of each subsections;  $R_i$  = hydraulic radius of each subsections.

The factor  $\chi_i$  calculated by equations provided in Bousmar and Zech (1999) for each subsection of the flow. The system of equations is function of water depth, geometry and roughness. An analytical

solution for straight symmetrical uniform flow is given by them and proposed a numerical solution procedure for the general case. When developing these solutions, it is assumed that the main channel velocity is larger than the floodplain velocity. This hypothesis enables the absolute values to be replaced by the difference without any sign change. After calculating  $\chi_i$  for each subsection by iterative procedure, it can be used in equation (4.11) to obtain overall discharge of the compound channel.

#### 4.2.6 EXPERIMENTAL SETUP AND PROCEDURE

For the purpose of present research, one straight experimental compound channel (*Type-I*) available at Fluid Mechanics and Hydraulics Engineering Laboratory of the Civil Engineering Department at the National Institute of Technology, Rourkela, India is used. The cross-sectional and geometrical parameters are shown in Figure 4.2. The view of *Type-I* experimental compound channels with measuring equipments from the upstream side is shown in Figure 4.3. The plan form of the channel, which is having the straight compound channel (*Type-I*) with equal flood plain at both sides of the main channel as shown in Figure 4.4. The compound channel is laid inside tilting flume. The flume is equipped with hydraulic jack arrangement. Inside each flume, separate meandering/straight channels are cast using 50 mm thick Perspex sheets. To facilitate fabrication, the whole channel length has been made in blocks of 1.20 m length each. The models thus fabricated have details as: The straight compound *Type-I* channel section has the main channel dimension of 120 mm×120 mm and flood plain width,  $B = 440$  mm. The channel is cast inside a tilting flume of 12 m long, 450 mm wide, and 400 mm deep. The bed slope of the channel is kept at 0.0019.

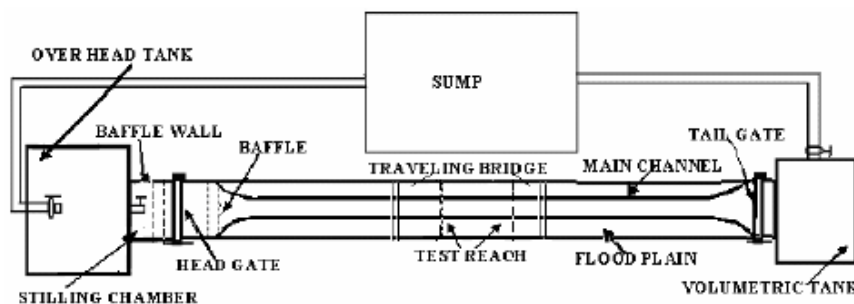


Figure.4.2. The plan form of the channel

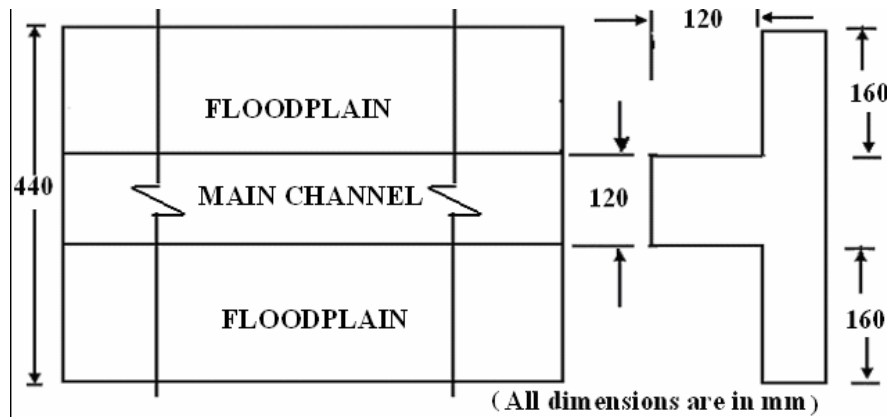


Figure.4.3. Geometrical parameters of Type-I channel



Figure.4.4. Experimental compound channel (Type-I) in Fluid mechanics and hydraulics engineering Laboratory at NIT Rourkela with mesurement equipments at upstream

The measuring devices consists of a point gauge mounted on a traversing mechanism to measure flow depths with least count of 0.1 mm. Point velocities are measured at a number of locations across the channel section using a 16-Mhz Micro ADV (Acoustic Doppler Velocity-meter) having accuracy of 1% of the measured range. A guide rail was provided at the top of the experimental flume on which a traveling bridge is moved in the longitudinal direction of the entire channel. The point gauge and the micro-ADV attached to the traveling bridge can move both longitudinal and the transverse direction at the bridge position. Readings from the micro-ADV are recorded in a computer. As the ADV (down probe) was unable to read the data up to 50 mm from free surface, a micro-Pitot tube of 4 mm external diameter in conjunction with suitable inclined manometer were also used to measure velocity at some other points of the flow-grid. The Pitot tube was physically rotated with respect to the main stream

direction till it recorded the maximum deflection of the manometer reading. A flow direction finder having a least count of 0.1 was used to get the direction of maximum velocity with respect to the longitudinal flow direction. The angle of limb of Pitot tube with longitudinal direction of the channel was noted by the circular scale and pointer arrangement attached to the flow direction meter. The details of experimental parameters for Type-I Compound Channel are shown in Table.4.1.

**Table.4.1. The details of experimental parameters for Type-I Compound Channel**

Sl.No	Item Description	Straight Type-I
1.	Geometry of Main channel section	Rectangular
2.	Main channel width(b)	120 mm
3.	Bank full depth of main channel	120 mm
4.	Top width of compound channel (B)	440 mm
5.	Slope of the channel	0.0019
6.	( $\alpha$ ) =Ratio of top width (B) to channel width(b)	3.667
7.	Sinuosity	1.00
8.	Flume size	0.45mx0.4m x 12m long

#### 4.2.7 DEVELOPMENT OF BACK PROPAGATION NEURAL NETWORK (BPNN)

##### 4.2.9.1 BACK PROPAGATION NEURAL NETWORK ARCHITECTURE

The I-m-n (I input neurons, m hidden neurons, and n output neurons) architecture of a back propagation neural network model is shown in Figure 4.5. Input layer receives information from the external sources and passes this information to the network for processing. Hidden layer receives information from the input layer, and does all the information processing, and output layer receives processed information from the network, and sends the results out to an external receptor. The input signals are modified by interconnection weight, known as weight factor  $w_{ij}$ , which represents the interconnection of  $i^{th}$  node of the first layer to  $j^{th}$  node of the second layer. The sum of modified signals (total activation) is then modified by a sigmoid transfer function ( $f$ ). Similarly, outputs signal of hidden layer are modified by interconnection weight ( $w_{ij}$ ) of  $k^{th}$  node of output layer to  $j^{th}$  node of hidden layer. The sum of the modified signal is then modified by sigmoid transfer ( $f$ ) function and output is collected at output layer.

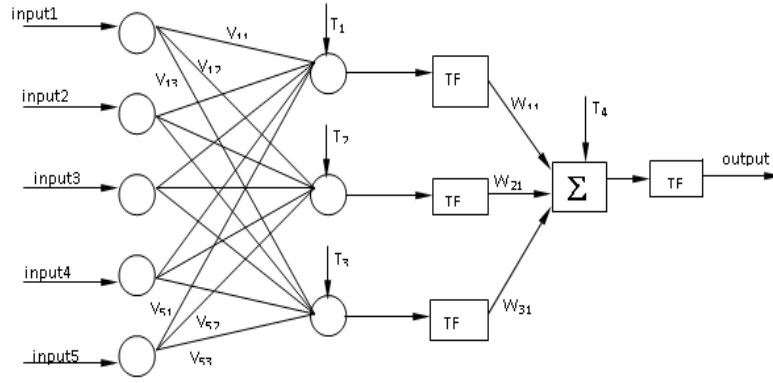


Figure.4.5. **Architecture of ANN for discharge estimation in straight compound channel**

Let  $I_p = (I_{p1}, I_{p2}, \dots, I_{pl})$ ,  $p = 1, 2, \dots, N$  be the  $p^{th}$  pattern among  $N$  input patterns. Where  $W_{ij}$  and  $W_{kj}$  are connection weights between  $i^{th}$  input neuron to  $j^{th}$  hidden neuron, and  $j^{th}$  hidden neuron to  $k^{th}$  output neuron respectively.

Output from a neuron in the input layer is,

$$O_{pi} = I_{pi}, i = 1, 2, \dots, l \quad (4.12)$$

Output from a neuron in the hidden layer is,

$$O_{pj} = f(NE_{pj}) = f\left(\sum_{i=0}^l W_{ji} O_{pi}\right), j = 1, 2, \dots, m \quad (4.13)$$

Output from a neuron in the output layer is,

$$O_{pk} = f(NE_{pk}) = f\left(\sum_{j=0}^m W_{kj} O_{pj}\right), k = 1, 2, \dots, n \quad (4.14)$$

#### 4.2.9.2 SIGMOID TRANSFER FUNCTION ( $f$ )

A bounded, monotonic, non-decreasing, S-shaped function provides a graded nonlinear response. It includes the logistic sigmoid function

$$f(x) = \frac{1}{1 + e^{-x}} \quad (4.15)$$

where  $x$  = input parameters taken as described above.

#### 4.2.9.3 LEARNING OR TRAINING IN BACK PROPAGATION NEURAL NETWORK

Batch mode type of supervised learning has been used in the present case in which interconnection weights are adjusted using delta rule algorithm after sending the entire training sample to the network. During training, the predicted output is compared with the desired output, and the mean square error is calculated. If the mean square error is more than a prescribed limiting value, it is back propagated from output to input, and weights are further modified till the error or number of iterations is within a prescribed limit.

Mean square error,  $E_p$  for pattern  $p$  is defined as

$$E_p = \sum_{i=1}^n \frac{1}{2} (D_{pi} - O_{pi})^2 \quad (4.16)$$

where,  $D_{pi}$  is the target output, and  $O_{pi}$  is the computed output for the  $i^{th}$  pattern.

Weight change at any time  $t$ , is given by

$$\Delta W(t) = -\eta E_p(t) + \alpha \times \Delta W(t-1) \quad (4.17)$$

$\eta$  = learning rate i.e  $0 < \eta < 1$

$\alpha$  = momentum coefficient i.e  $0 < \alpha < 1$

#### 4.2.8 SOURCE OF DATA

The data are collected from research work done in Flood Channel Facility, which is a large scale compound channel facility, available at the laboratory of University of Birmingham, Wallingford. FCF data series A for straight rough and smooth channels, work done by Knight and Demetriou (1983), Atabay (2004) for symmetrical and asymmetrical data series, and Tang (2001) for rough bed and mobile channel data series are used along with experimental work done in Fluid Mechanics Laboratory, NIT Rourkela. The descriptions of geometrical parameters of above experimental data are mentioned in Table.4.2.

**Table.4.2.Geometrical parameters of experimental data**

Source of data	Main side slope	Flood plain type	Roughness type	Cross-sectional geometry
<b>FCF-A</b>				
Series 1	1:1	Symmetric	Smooth	Trapezoidal
Series 2	1:1	Symmetric	Smooth	Trapezoidal
Series 3	1:1	Symmetric	Smooth	Trapezoidal
Series 6	1:1	Asymmetric	Smooth	Trapezoidal
Series 8	0:1	Symmetric	Smooth	Rectangular
Series10	1:2	Symmetric	Smooth	Trapezoidal
<b>Knight And Demotriue (1983)</b>				
Series 1	0:1	Symmetric	Smooth	Rectangular
Series 2	0:1	Symmetric	Smooth	Rectangular
Series 3	0:1	Symmetric	Smooth	Rectangular
<b>NIT Rourkela (Experimental)</b>				
Type I	0:1	Symmetric	Smooth	Rectangular
<b>Tang and Knight (2001)</b>				
ROA	0:1	Symmetric	Smooth	Rectangular
ROS	0:1	Symmetric	Smooth	Rectangular
<b>Tang and Knight (2001) mobile channel</b>				
LOSR	0:1	Symmetric	Rough	Rectangular
ALL	0:1	Symmetric	Rough	Rectangular
<b>Atabay et al. (2004)</b>				
ROA	0:1	Asymmetric	Smooth	Rectangular
ROS	0:1	Symmetric	Smooth	Rectangular

#### 4.2.9 SELECTION OF HYDRAULIC PARAMETERS

Flow hydraulics and momentum exchange in straight channel are significantly influenced by both geometrical and hydraulic variables. Previous study undertaken by Yang et al. (2005) has suggested that resistance of flow is constant for relative depth of 0.1 and varied for all other cases. Also, the computation becomes more complex when the total channel width to the main channel width value decreases. The flow factor like (i) relative depth ( $H_r$ ), i.e. depth of flood plain to total depth, (ii) channel longitudinal slope ( $S_0$ ), (iii) influence of flood plain and main channel roughness ( $f_r$ ) (iv) Ratio of area of flood plain to main channel ( $A_r$ ) and (v) ratio of hydraulic radius of flood plain and main channel ( $R_r$ ) also varies with symmetry are responsible for the estimation of overall discharge in compounds channel as suggested by Yang et al. (2005). Hence, in this study, these five flow variables are chosen as input parameters and discharge as output parameter.

#### 4.2.8 RESULTS

##### 4.2.10.1 TESTING OF BACK PROPAGATION NEURAL NETWORK.

Entire experimental data set is divided into training set and testing set. A total of 129 data sets are used. Among 129 data, 110 are considered as training data and 19 as testing data. The number of

layers and neurons in the hidden layer are fixed through exhaustive experimentation when mean square error is minimized for training data set. Thus, the back propagation neural network (BPNN) used in this work has three-layered feed forward architecture. The three layers are known as input, hidden and output layer. The network was run on MATLAB platform using Pentium IV desktop computer. The different parameters of the network are presented in Table 4.3. Thus, learning parameter is set to 0.07, momentum parameter is 0.5 and the maximum epochs is set to 200,000 epochs as shown in Table 4.3.

**Table.4.3. Neural network learning parameters**

Neural network structure:	5 7 1	5 neurons in input layer 7 neurons in hidden layer 1 neuron in output layer
net.trainParam.show	1000	% display result after 5 batch
net.trainParam.lr	0.07	% learning rate
net.trainParam.mc	0.5	Momentum constant
net.trainParam.epochs	200000	Maximum Epochs
net.trainParam.goal	1e-3	Mean square error

The error on the training set is monitored during the training process. The error during training period normally decreases during the initial phase of training rapidly and slows down. When the error decreases to a threshold value, training is stopped and the weights at the minimum value of the error are stored. The network is converged at 65,000 epochs and means square error (MSE) reaches at 0.001 as shown in Figure 4.6.

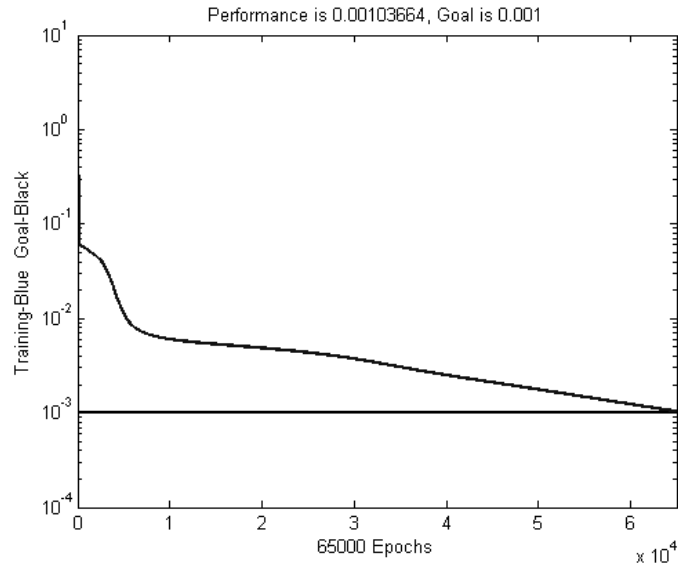


Figure.4.6. Convergence plot

The residual analysis is carried out by calculating the residuals from the actual discharge data and predicted discharge data for training data set. The residuals are plotted with the sample number as shown in Figure 4.7. It shows that the residuals are distributed evenly along the centerline of the plot. From this illustration, it can be said that the data is well trained.

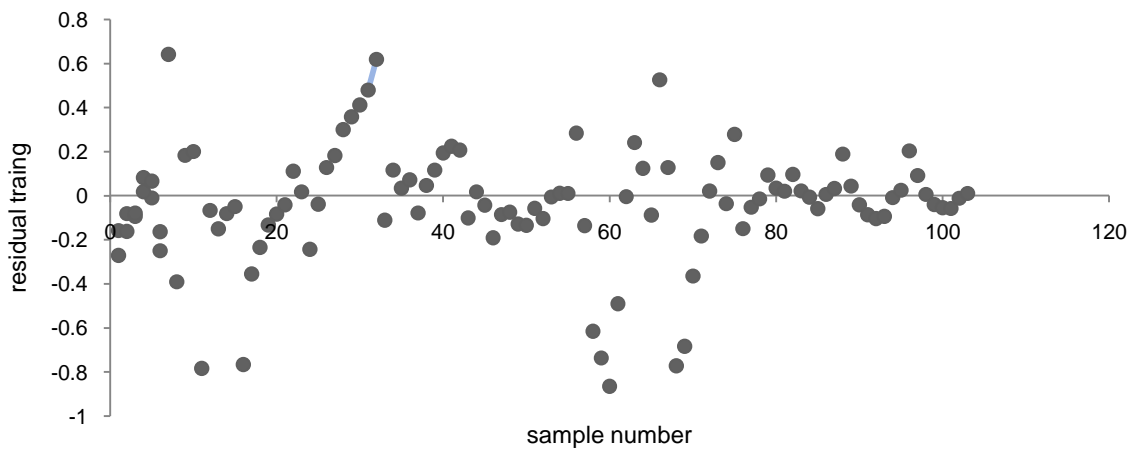


Figure.4.7. Residual distribution of training data

A regression curve is plotted in Figure.4.8 between actual discharge and predicted discharge via ANN model. It can be observed that data are well fitted because a high degree of coefficient of determination ( $R^2$ ) as 0.997 is obtained. The actual data and predicted discharge against the sample number is shown in Figure 4.9. As the predicted data pattern follows actual data with little or no

exception, it demonstrates that the model predicts the pattern of the data distribution with adequate accuracy.

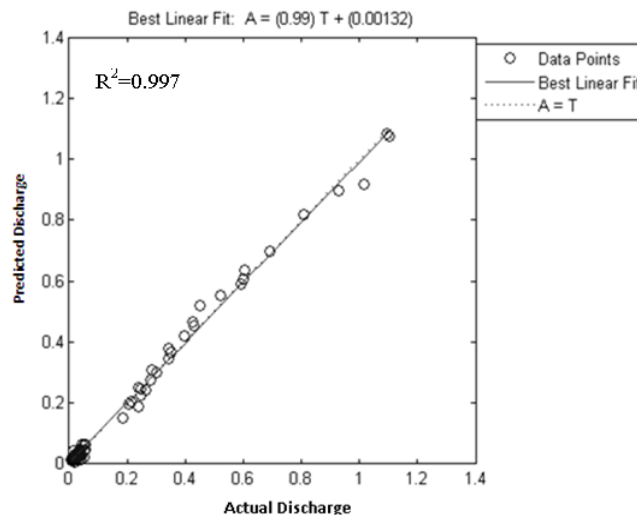


Figure.4.8. **Correlation of actual discharge and predicted discharge (training data)**

Then, testing data is fed to the trained network to check the percentage variation of predicted output in comparison to the actual discharge. It should be noted that output is fed to the network during testing phase. It can be observed from Figure 4.10 that fitting of actual and predicted discharge for testing data is quite good and the pattern or trend is more or less matched.

Comparison of discharge calculated with appropriate hydraulic parameters using conventional models like VDCM, COHM and EDM models with the ANN model is done by plotting the correlation plots. Twenty seven data set is shown in Table 4.4 are used for estimation of discharge using conventional methods and discharge predicted using ANN model. The correlation plot between the actual discharge and discharge predicted by VDCM shows the coefficient of determination of 0.806 (Figure 4.11). Also, it can be observed that VDCM over predicts the discharge as discussed earlier and the average absolute percentage error is found to be 31.2% for this method, which is highest among all. Again the correlation plot of actual discharge with discharge data predicted with COHM method is carried out and it shows coefficient of determination of 0.922 as shown in Figure 4.12. The coefficient of determination for the plot Figure 4.13 between the actual discharge and predicted discharge with EDM method shows 0.982. From Table 4.4, the calculated average absolute percentage error for COHM is 10.8% whereas it is 12.76% for EDM method. The coefficient of determination of the EDM and COHM model from Figure 4.13 and Figure 4.12 respectively shows that the two models are quiet

convincing and close to each other. However, correlation plot of actual discharge and the predicted discharge for testing data using the ANN model shows coefficient of determination 0.9962 as shown in Figure 4.14 and also the average absolute error for the prediction with the ANN model is 6.26%.

**Table.4.4.The average absolute percentage error**

Source of Data	Actual Discharge cm <sup>3</sup> /sec	ANN cm <sup>3</sup> /sec	Error In %	VDCM cm <sup>3</sup> /sec	Error in %	COHM cm <sup>3</sup> /sec	Error	EDM cm <sup>3</sup> /sec	Error In %
<b>Atabay (2001)</b>	0.018	0.018	3.8	0.021	1.23	0.018	2.1	0.015	13.7
	0.021	0.022	7.2	0.023	4.26	0.201	3.0	0.018	15.08
	0.24	0.258	15.8	0.234	13.47	0.230	4.5	0.022	9.14
	0.027	0.029	8.1	0.015	51.72	0.026	3.8	0.03	9.5
<b>FCF phase-A</b>	0.05	0.050	1.2	0.055	9.56	0.048	3.3	0.042	15.85
	0.208	0.226	8.1	0.073	64.8	0.195	6.25	0.203	2.6
	0.234	0.205		0.091	60.9	0.233	0.25	0.222	4.8
	0.605	0.636	5.2	0.702	13.8	0.675	11.67	0.585	3.2
	0.212	0.204	3.39	0.167	21.2	0.240	13.36	0.205	3.6
<b>Illinois</b>	0.480	0.475	1	0.360	25.0	0.527	9.96	0.476	8.2
	0.034	0.037	9.4	0.052	51.22	0.027	21.0	0.031	9.8
	0.042	0.047	9.31	0.027	34.50	0.037	9.9	0.038	8.5
	0.047	0.045	3.8	0.017	62.65	0.038	17.18	0.042	10.2
	0.036	0.037	3.6	0.003	91.44	0.036	1.94	0.032	12.3
<b>Tang (2001) Rigid channel</b>	0.046	0.045	1.73	0.078	68.2	0.039	15.13	0.064	10.6
	0.015	0.016	6.67	0.014	0.2	0.016	7.9	0.014	5.7
	0.018	0.0167	7.2	0.017	3.2	0.019	2.7	0.017	5.2
	0.034	0.0305	11.07	0.033	3.11	0.027	20.37	0.032	6.0
	0.015	0.0143	4.67	0.014	3.11	0.017	15.75	0.015	3.9
<b>Tang (2001) Mobile Channel</b>	0.024	0.0257	5.76	0.024	0.8	0.027	15.4	0.023	4.4
	0.0143	0.01390	2.80	0.017	20	0.011	25.85	0.017	17.65
	0.0306	0.0284	7.1	0.007	77.8	0.024	22.44	0.042	38.4
	0.01023	0.011	7.0	0.011	7.0	0.009	12.47	0.104	2.1
	0.0172	0.0152	11.62	0.019	13.3	0.011	35.08	0.022	28.52
<b>NIT Rourkela (Type-I)</b>	0.01971	0.0214	8.5	0.003	82.14	0.013	31.71	0.023	18.56
	0.019861	0.0205	3.2	0.019	30.9	0.016	20.95	0.015	24.75
	0.0253	0.0248	2.1	0.09	26.67	0.022	10.64	0.023	7.11
<b>Average Absolute error</b>		6.26		31.2		12.76		10.8	

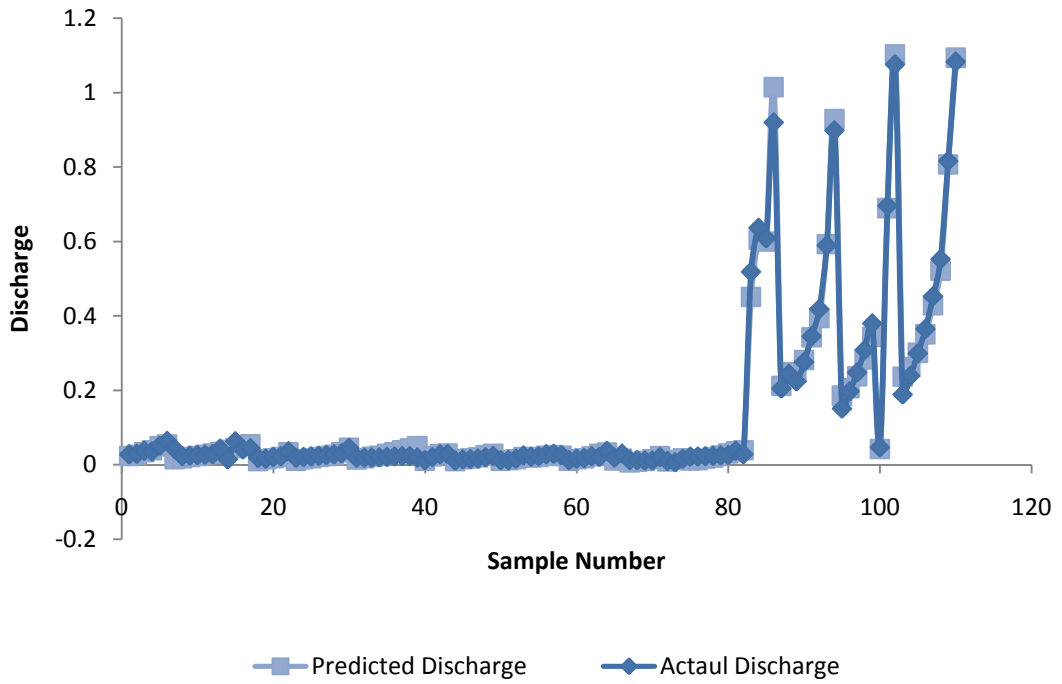


Figure.4.9. Comparison of actual and predicted discharge (training data)

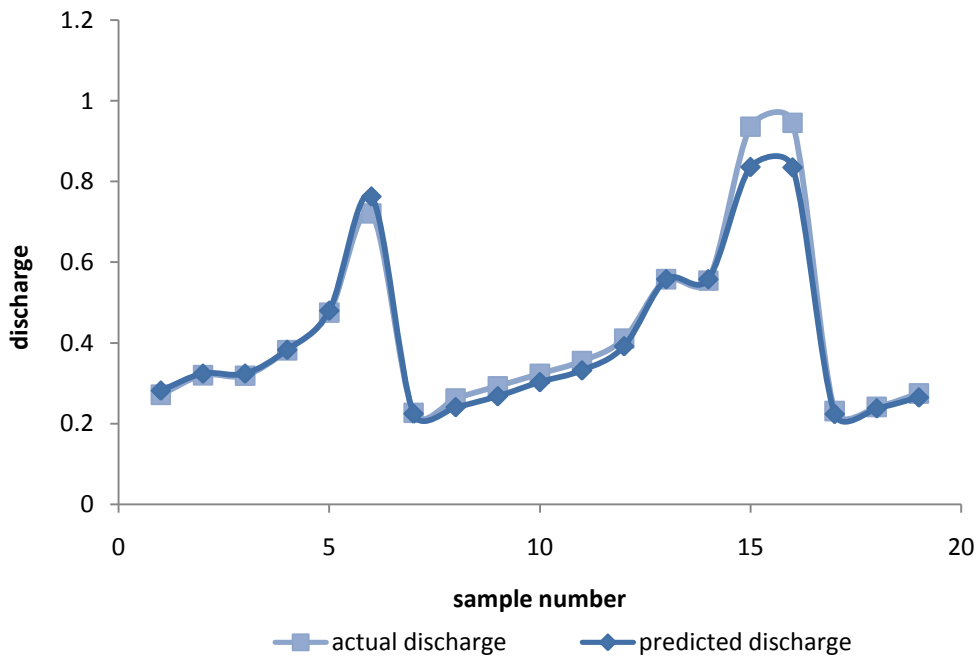


Figure.4.10. Comparison of actual and predicted discharge (testing data)

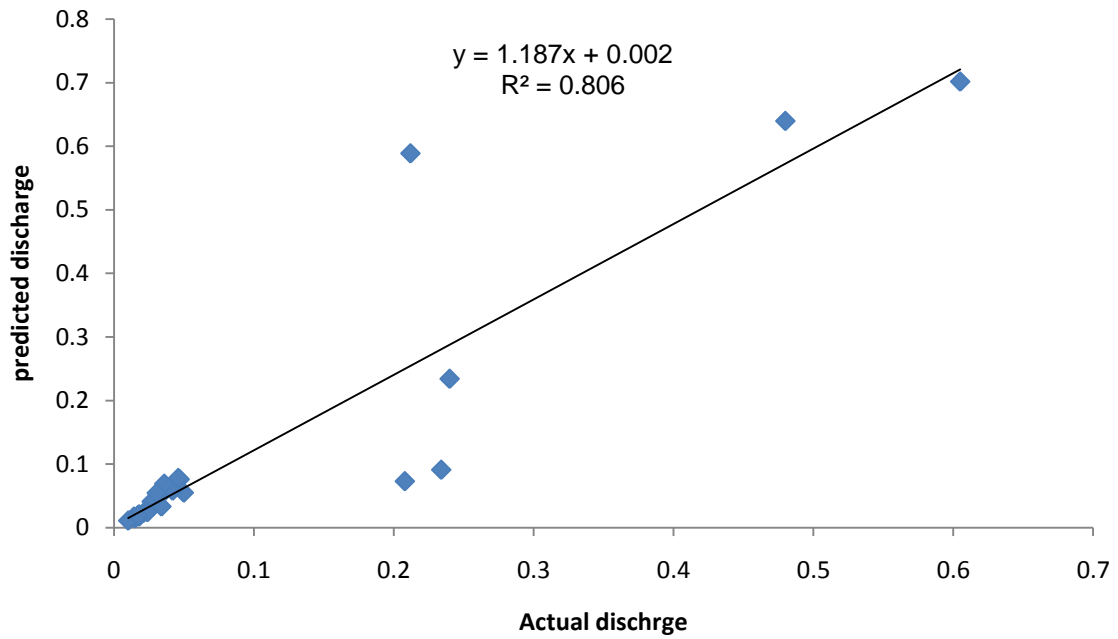


Figure.4.11. Correlation plot of actual discharge and Discharge predicted by VDCM (Testing data)

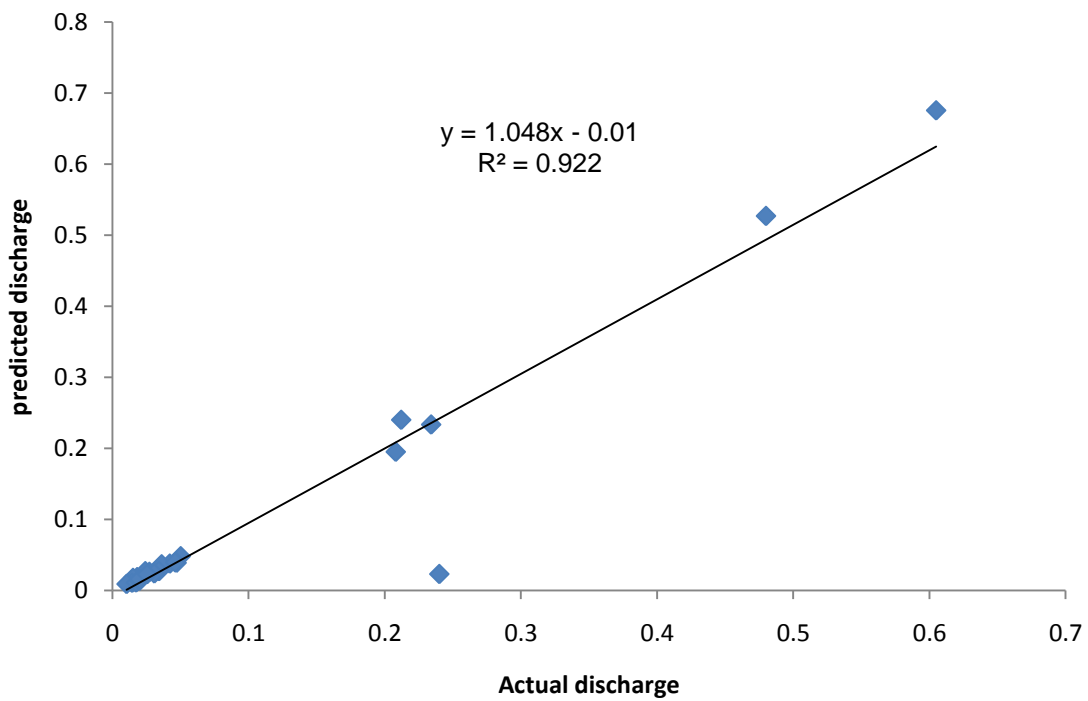


Figure.4.12. Correlation plot of actual discharge and Discharge predicted by COHM

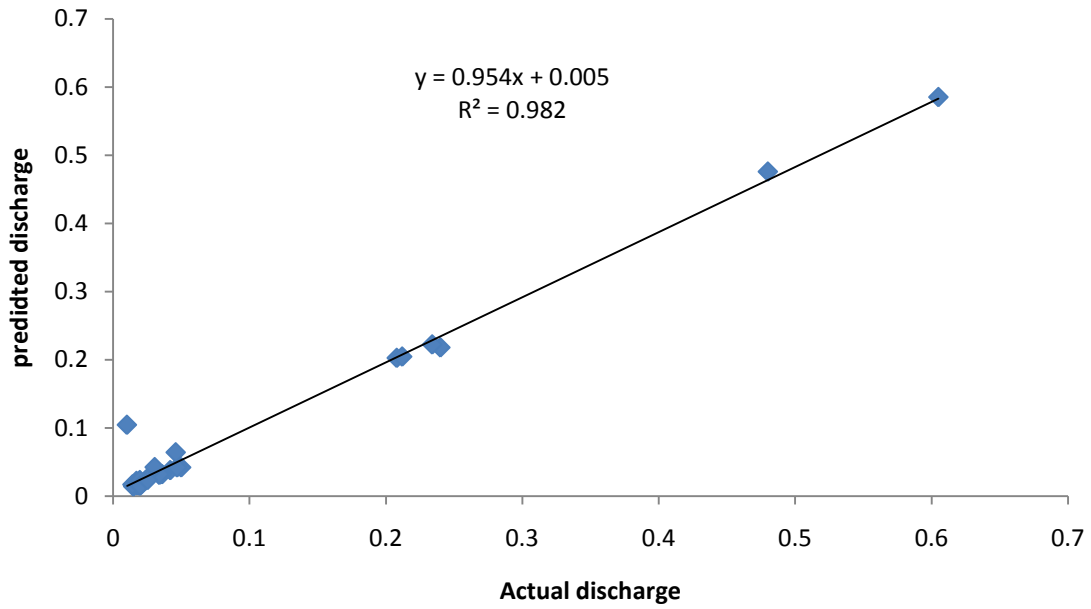


Figure.4.13. Correlation plot of actual discharge and Discharge predicted by EDM

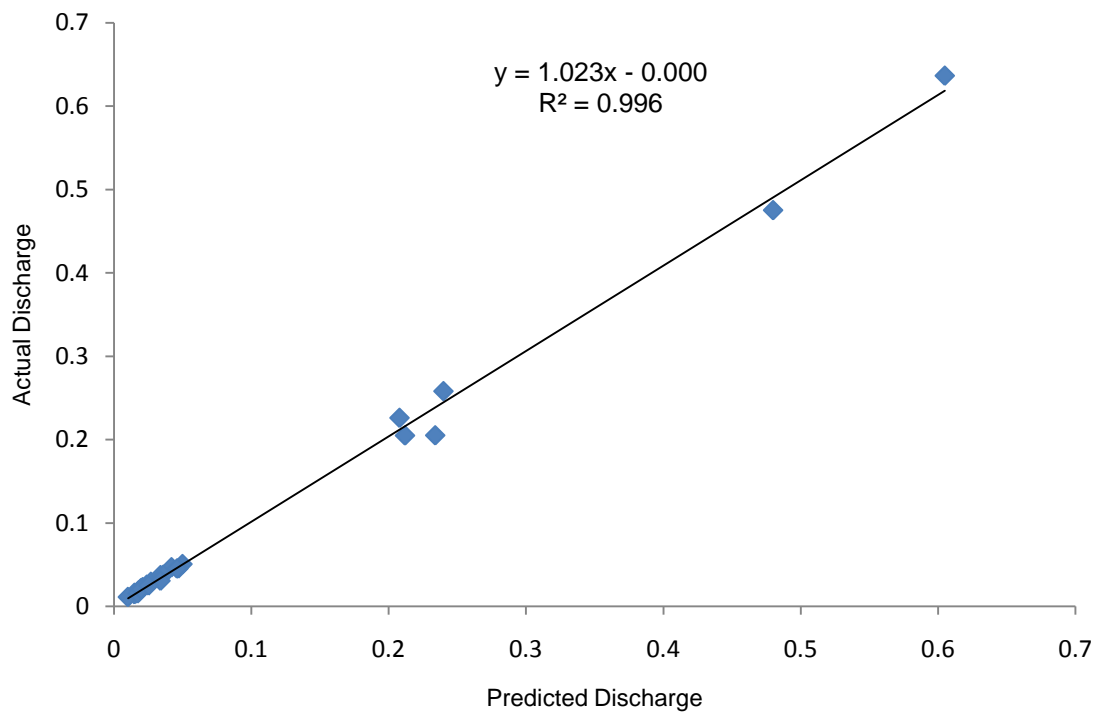


Figure.4.14. Correlation Testing regression plot of actual discharge and Discharge predicted by ANN (Testing data)

#### 4.2.9 DISCUSSION

1. A BPNN model is proposed for accurate estimation of discharge in compound channel flume. The discharge data from experimentation covers a wide range of variety like conditions having both smooth and rough main channel and flood plains as well as mobile and fixed channel boundary. Also data from compound channel having symmetric and asymmetric cross-section have been considered. The trend and pattern of experimental data matches with predicted discharge and superiority of prediction of discharge via ANN has been demonstrated. The basic reason of high degree of prediction accuracy lies in the fact of capability of non-linear mapping of inputs and outputs in ANN. The non-linear relation of geometrical and hydraulic input parameters with discharge is difficult to establish with traditional discharge prediction methodology. In addition, the conventional techniques cannot be taken into account the real life factors operating in the system.
2. The traditional methods for predicting discharge in compound channels are based on Chezy's, Manning's, or Darcy-Weisbach equation. Among these methods, SCM underestimates the discharge while DCM overestimates it. It is a well established fact that flood plain and main channel interaction affects the flow structures in compound channel in both rigid and smooth channels. Traditional methods like SCM and DCM neglect this effect. But COHM and EDM, which is developed by taking momentum transfer into account, are useful approaches for dealing with overbank flow and related problems of composite roughness and shape effect. However, COHM and EDM estimate discharge consistently better than SCM and DCM but ANN supersedes all the methods as far as accuracy is concerned.
3. The study proposed by Seckin (2004) reveals EDM and COHM give accurate results when applied to laboratory data for fixed boundaries. The error estimated by these methods generally lower than 10% for fixed boundaries. But the error increases up to 20 % for the case of mobile boundaries. Table.4.4 shows that EDM and COHM models estimate the discharge with 38% error. But ANN based approach predicts the discharge up to 11.2% error for the case of mobile boundaries.
4. The regression plots for different methods show that the ANN model is fitted with astounding accuracy whereas the coefficient of determination for COHM is obtained as 0.922 and EDM as 0.982. But coefficient of determination for VDCM is 0.806 and happens to be lowest among all

methods. From it can be inferred that ANN model is more adaptive to the prediction of discharge under different conditions.

5. ANN model holds the discharge prediction with minimal error i.e. less than 10 %. Other models are not that efficient to predict the discharge. Although COHM and EDM predicts discharge with desirable accuracy but ANN model is more convincing model than these models.

## SECTION 4.3: MODELING OF COMPOSITE FRICTION FACTOR USING ANFIS

---

### 4.3.1 INTRODUCTION

It is crucial for river engineers, and investigators to evaluate resistance to flow in compound channel as it has direct relation in evaluating bed resistance and discharge. Further, it is customary to evaluate resistance as a form of factor i.e. friction factor or a resistance coefficient for a cross-section or reach in simple open channel flow, which is generally expressed in terms of Manning's coefficient [n] or Chezy's coefficient [C] or Darcy-Weisbach [f] which are related as.

$$\frac{C}{\sqrt{g}} = \frac{R^{1/6}}{\sqrt{g}} \frac{1}{n} = \frac{8}{\sqrt{f}} \quad (4.18)$$

For a particular geometric and hydraulic condition of a compound channel, the Manning's or Chezy's or Darcy-Weisbach equations are used to find the velocities and hence the discharge in an open channel flow. Further the resistance coefficients are helpful to evaluate the boundary shear stress given as:

$$f_b = \frac{\tau_b}{\frac{1}{2}\rho W_b^2} \quad (4.19)$$

Where  $\tau_b$  = local boundary shear stress, and depth averaged velocity  $W_b$  = depth averaged velocity as calculated in eqn. (3.10),  $\rho$  = density of water. For this situation Darcy's Weisbach resistance coefficient follows the relation. But this factor for a subsection of the compound channel can be expressed as :

$$f_i = \frac{8gR_i S_f}{W_i^2} \quad \text{and} \quad n_i = \frac{R_i^{2/3} g^{1/4} S_f^{1/2}}{8W_i} \quad (4.20)$$

Where,  $R_i$  = hydraulic depth of the sub section,  $S_f$  = longitudinal slope of the sub section,  $W_i$  = sub-sectional mean velocity

Primary factors affecting the resistance in compound open channel are the geometric parameter, flow depth 'h' and the wall roughness resistant. In compound channels wall roughness and lateral depth changes along the wetted perimeter of the cross-section. The variation of this flow of both the subsections i.e main channel and flood plain in compound channel makes complexities in

determining its composite resistance factor. Therefore, an equivalent resistance factor is required to calculate flow variables. This equivalent resistance factor for a particular flow is called as composite friction factor.

Traditionally the composite roughness in a compound channel is expressed in Manning's form 'n' as in eqn. (4.21). The composite friction factor  $n_c$  across perimeter can be evaluated as:

$$n_c = \int w_i n_i dp \tag{4.21}$$

where  $n_i$  = sub-sectional Manning's roughness,  $w_i$  = weighted function of subsections, Using this formulation the calculation of open channel flow reduced to 1D formulation.

A number of empirical relations are proposed by investigators to predict composite manning's friction factor in compound open channel flow. These are derived from relationships based on different assumptions based on the within the variables like discharges, velocities, forces, shear stresses etc. between the component subsections. The formulations proposed by different investigators are expressed in Table 4.5 to calculate composite friction factor.

**Table.4.5. Different Models for Composite Friction Factor** (after Yen B.C. 2002)

Composite Friction Factor	Concept	Reference
$= \sqrt{\sum n_i^2 \frac{A_i}{A}}$	Total resistance force is equal to sum of subarea resistance forces; or, $n_i$ weighted by $\sqrt{A_i}$ .	COX (1973)
$= \frac{A}{\sum \left( \frac{A_i}{n_i} \right)}$	Total discharge is sum of subarea discharges.	
$= \left[ \frac{\sum (n_i^{3/2} A_i)}{A} \right]^{2/3}$	Same as Horton and Einstein's	Colebatch (1941)
$= \left[ \frac{\sum (n_i^{3/2} P_i)}{P_t} \right]^{2/3}$	Total cross sectional mean velocity equal to subarea mean velocity.	Einstein (1934)

$= \frac{P_t}{\sum \left( \frac{P_i}{n_i} \right)}$	Total discharge is sum of subarea discharges.	Felkel (1960)
$= \sqrt{\sum n_i^2 \frac{P_i}{P_t}}$	Total resistance force, $F$ , is sum of subarea resistance forces, $\sum F_i$ .	Pavlovskii (1931)
$= \left[ \frac{R^{1/3}}{P_t} \sum \frac{n_i^2 P_i}{R_i^{1/3}} \right]^{1/2}$	Total resistance force, $F$ , is sum of subarea resistance forces, $\sum F_i$ .	
$= \left[ \frac{\sum n_i^2 P_i R_i^{2/3}}{P_t R^{2/3}} \right]^{1/2}$	Total resistance force equal to sum of subarea resistance forces	
$= \frac{P_i R^{7/6}}{\sum \frac{P_i R_i^{7/6}}{n_i}}$	Total discharge is sum of subarea discharges	
$= \frac{P_i R^{5/3}}{\sum \frac{P_i R_i^{5/3}}{n_i}}$	Total discharge is sum of subarea discharges	Lotter (1993)
$= \frac{\sum P_i R_i^{5/3}}{\sum \frac{P_i R_i^{5/3}}{n_i}}$	Same as Lotter (1993) method with modified definition of 'R'	Ida (1960) Engelund (1964)
$= \frac{\sum (n_i P_i R_i^{1/2})}{P_t R^{1/2}}$	Total shear velocity is weighted sum of subarea shear velocity	
$= \frac{\sum (n_i P_i R_i^{1/3})}{P_t R^{1/3}}$	Total shear velocity is weighted sum of subarea shear velocity	Yen (1991)
$= \exp \left[ \frac{\sum P_i h_i^{3/2} \ln n_i}{\sum P_i h_i^{3/2}} \right]$	Logarithmic velocity distribution over depth 'h' for wide channel	Krishnamurthy and Christensen (1972)
$= f \left( \alpha, \frac{R}{H} \right) \times n_{mc}$	The main channel and flood plain width ratio, and the	Dracos T and Hardegger P (1987)

	ratio of the total hydraulic radius to the flow depth in the main channel.	
$f_c = 1.03 \left[ \left[ 0.117 \left( \frac{P_{mc}}{P_t} \right)^{-7.06} f_{mp} + 0.507 \right] \left( \frac{2h}{P_t} \right)^{1.08} f_a \right] - 0.008$	Apparent friction factor between main channel and flood plain	Hin et al. (2008)

Where,  $n$  = Manning's composite friction factor,  $n_{mc}$  = Manning's friction factor for main channel,  $P_{mc}$  = perimeter for main channel,  $P_{fp}$  = perimeter for flood plain,  $P_t$  = perimeter for total cross-section,  $f_{mp}$  = Darcy's friction factor for main channel,  $f_{fp}$  = Darcy's friction factor for flood plain,  $f_c$  = Darcy's composite friction factor,  $A$  = Total area of cross-section,  $A_{mc}$  = Area of Cross section for main channel,  $A_{fp}$  = Area of cross-section for flood plain,  $f_a$  = apparent friction factor,  $R$  = hydraulic radius.

The above described methods possess their own basic assumptions. It is seen that the investigators generally use five categories of assumptions. Therefore, in the present study five standard methods have been used such as: Einstein and Banks (1950), Krishnamurthy and Christensen (1972), Cox (1973), Lotter (1933), Dracos and Hardegger (1987) methods respectively by categorizing according to their assumptions. Among these methods only Dracos T and Hardegger P (1987) considered the effect of momentum transfer in to account. The model proposed by Hin et al. (2008) also uses momentum transfer in to account but is limited to the field observations only. Therefore, this model could not be considered in the present analysis because of non availability of shape factor parameters to calibrate the apparent friction factor. Table 4.6 shows the summary of the data sets used.

**Table.4.6.Geometrical parameters of experimental data.**

Source of data	Main channel side slope	Flood plain type	Roughness type	Main channel Cross-sectional geometry
<b>FCF-Series A</b>				
Series 1	1:1	Symmetric	Smooth	Trapezoidal
Series 2	1:1	Symmetric	Smooth	Trapezoidal
Series 3	0:1	Symmetric	Smooth	Trapezoidal
Series 6	1:1	Asymmetric	Smooth	Trapezoidal
Series 8	0:1	Symmetric	Smooth	Rectangular
Series10	2:1	Symmetric	Smooth	Trapezoidal

<b>Tominaga and Nezu (1991)</b>				
S(1-3)	0:1	Asymmetric	Smooth	Rectangular
<b>Tang and Knight (2001)</b>				
ROA	0:1	Symmetric	Smooth	Rectangular
ROS	0:1	Symmetric	Smooth	Rectangular
<b>Tang and Knight (2001) Mobile</b>				
LOSR	0:1	Symmetric	Rough	Rectangular
ALL	0:1	Symmetric	Rough	Rectangular
<b>Atabay et al.(2004)</b>				
ROA	0:1	Asymmetric	Smooth	Rectangular
ROS	0:1	Symmetric	Smooth	Rectangular
<b>Soong and Depue (1996)</b>				
	1:1	Asymmetric	Rough	Trapezoidal
<b>Khatua et al. (2011)</b>				
Type I	0:1	Symmetric	Smooth	Rectangular

#### 4.3.2 MODELING OF ADAPTIVE-NEURO FUZZY INFERENCE SYSTEM (ANFIS)

Researchers have used various intelligent techniques including neural network, fuzzy logic, neuro-fuzzy, Adaptive-Neuro Fuzzy Inference System (ANFIS) etc. for the prediction of friction factor in simple channel flow to minimize forecasting errors. Therefore, in this study a step has taken to predict the composite friction factor in a compound open channel flow using ANFIS. This technique is coupled between artificial neural network (ANN) and fuzzy inference system (FIS). Neural network and fuzzy logic are two complementary technologies. A neural network can learn from both the data and feedback without understanding the pattern involved in the data. But, the Fuzzy logic models are easy to comprehend the pattern because they use linguistic terms in the form of IF-THEN rules. A neural network with their learning capabilities can be used to learn the fuzzy decision rules, thus creating a hybrid intelligent system. The fuzzy system provides expert knowledge to be used by the neural network. A fuzzy inference system consists of three components. First, a rule base contains a selection of fuzzy rules. Secondly, a database defines the membership functions used in the rules and, finally, a reasoning mechanism to carry out the inference procedure on the rules and given facts. This combination merges the advantages of fuzzy system and a neural network. Jang (Jang 1991<sup>a</sup>) proposed a combination of a neural network and fuzzy logic, called an adaptive neuro-fuzzy inference system. ANFIS is a fuzzy inference system implemented in the framework of neural networks. The combination of both ANN and FIS thus improves system performance without interference of operators. The ANFIS architecture is also used to model nonlinear functions for prediction of desired result logically (Jang 1991<sup>a</sup>; Jang 1991<sup>b</sup>; Jang 1993; Jang 1994). In this present analysis a novel

architecture of ANFIS network is used to predict composite friction factor. The network can be served as basis for creating a set of fuzzy IF-THEN rules and fuzzy inference systems propitiate with membership functions to generate the result adequately.

#### 4.3.3 SELECTION OF HYDRAULIC PARAMETERS

The dimensionless parameters used for the present ANFIS model to estimate the composite friction factor in compounds channel are (i) relative Width ( $B_r$ ), Ratio of width of flood plain ( $B-b$ ) to total width ( $B$ ) where  $B$  = main channel width,  $b$  = flood plain width (ii) The ratio of perimeter of main channel ( $P_{mc}$ ) to flood plain perimeter ( $P_{fp}$ ) denoted as  $P_r$ , (iii) Ratio of hydraulic radius of main channel ( $R_{mc}$ ) to flood plain ( $R_{fp}$ ) denoted as  $R_r$ , which normally varies with symmetry, (iv) channel longitudinal slope ( $S_0$ ), and (v) relative depth ( $D_r$ ) i.e. Ratio of depth of flood plain ( $H-h$ ) to total depth ( $H$ ) where  $H$  = main channel depth,  $h$  = flood plain depth. These dimensionless variables are considered to be the most influencing parameter for estimation of composite friction factor in compounds channel as suggested by Yang et al. (2007). Hence, in this study, these five flow variables are chosen as input parameters and composite friction factor as output parameter for the proposed ANFIS model.

#### 4.3.4 FUZZY LOGIC AND FUZZY INFERENCE SYSTEMS

The building of fuzzy logic systems initiate with the derivation of a set of IF-THEN fuzzy rules bearing the expertise and knowledge of modeling field (Dezfoli 2003). The modeling of suitable rule is cumbersome and hence a predefined method or tool to achieve the fuzzy rules from numerical and statistical analysis is most adaptive for this context. Fuzzy conditional statements (e.g. *if hydraulic depth( $D_r$ ) is small then friction factor is high*) are the levels of fuzzy sets, those are characterized by membership functions. Hence, these concise forms of fuzzy rules are often employed to make decisions in the situations of uncertainty which plays an essential role in the human ability to make decisions.

The fuzzy inference system and fuzzy decision making procedure comprised of five functional building blocks (Figure 4.15) such as (i) rule base, (ii) database, (iii) decision making unit, (iv) fuzzification interface and (v) defuzzification interface. The rule base and database are referred as knowledge base. The inference system is based on the logical rules which images input variables space to output variable spaces using IF-THEN statements and fuzzy decision making procedure (Jang and Gulley 1996; Dezfoli 2003). Due to the uncertainty of real and field values to fuzzy data, a

fuzzification transition is used to transform deterministic values to fuzzy values and defuzzification transition is used to transform fuzzy values to deterministic values (Dezfoli 2003).

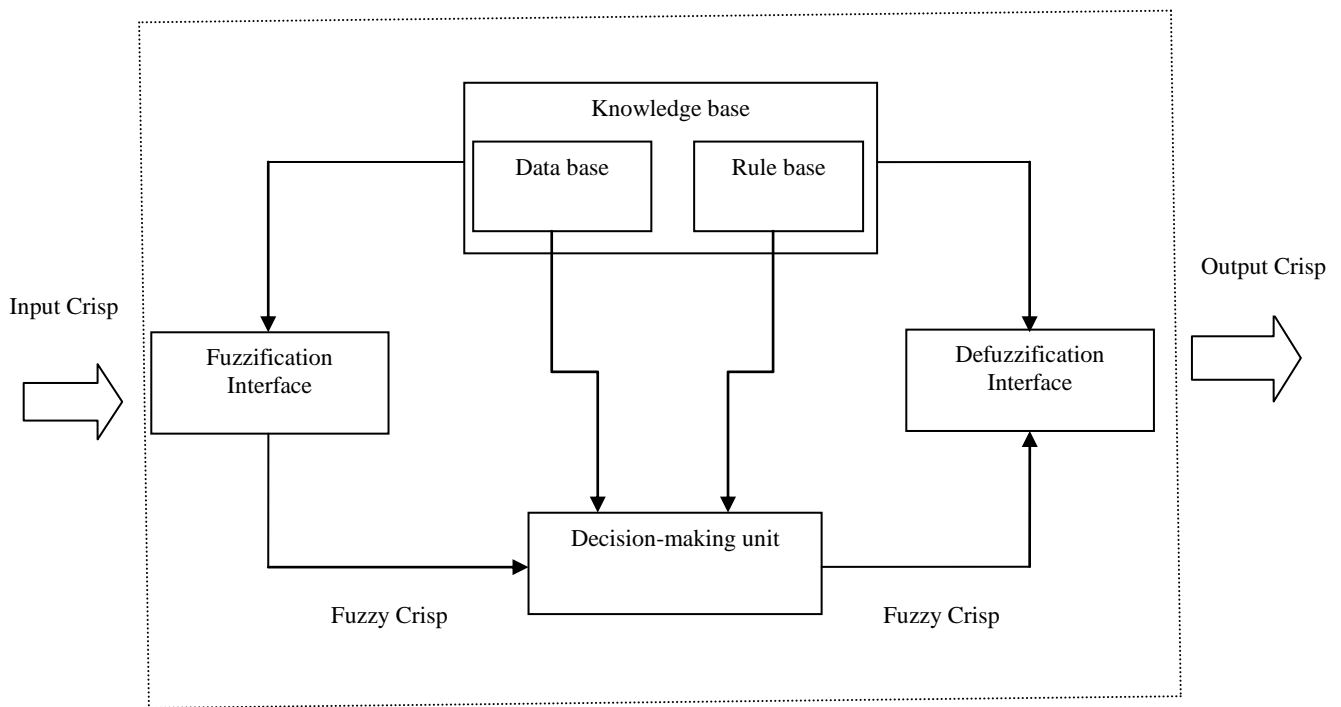


Figure.4.15. Schematic diagram of fuzzy based inference system

#### 4.3.5 ARCHITECTURE AND BASIC LEARNING RULES

A typical adaptive network shown in Figure. 4.16 is a network structure consisting of a number of nodes connected through directional links. Each node is characterized by a node function with fixed or adjustable parameters. Learning or training phase of a neural network is a process to determine parameter values to sufficiently fit the training data. The basic learning rule method is the back propagation method, which seeks to minimize some error, usually sum of squared differences between network's outputs and desired outputs. Generally, the model performance is checked by the means of distinct test data, and relatively good fitting is expected in the testing phase. Considering a first order Takagi, Sugeno and Kang (TSK) fuzzy interface system, a fuzzy model consists of two rules (Sugeno and Kang, 1988).

Rule 1 : If x is  $A_1$  and y is  $B_1$  then  $f_1=p_1x+q_1y+r_1$

Rule 2 : If x is  $A_2$  and y is  $B_2$  then  $f_2=p_2x+q_2y+r_2$ .

If  $f_1$  and  $f_2$  are constants instead of linear equations, we have zero order TSK fuzzy-model. Node functions in the same layer are of the same function family as described below. It is to be noted that  $O_i^j$  denotes the output of the  $i^{th}$  node in layer  $j$ .

Layer 1: Each node in this layer generates a membership grade of a linguistic label. For instance, the node function of the  $i^{th}$  node might be

$$O_i^1 = \mu A_i(x) = \frac{1}{1 + \left[ \left( \frac{x - c_i}{a_i} \right)^2 \right]^{b_i}} \quad (4.22)$$

Where  $x$  is the input to the node  $i$ , and  $A_i$  is the linguistic label (small, large) associated with this node; and  $\{a_i, b_i, c_i\}$  is the parameter set that changes the shapes of the membership function. Parameters in this layer are referred to as the "Premise Parameters".

Layer 2: Each node in this layer calculates the firing strength of each rule via multiplication:

$$O_i^2 = w_i = \mu A_i(x) \times \mu B_i(y), \quad i = 1, 2 \quad (4.23)$$

Layer 3: The  $i^{th}$  node of this layer calculates the ratio of the  $i^{th}$  rule's firing strength to the sum of all rule's firing strengths:

$$O_i^3 = \bar{w}_i = \frac{w_i}{w_1 + w_2}, \quad i = 1, 2 \quad (4.24)$$

For convenience outputs of this layer will be called normalized firing strengths.

Layer 4: Every node  $i$  in this layer is a squared node with a node function

$$O_i^4 = \bar{w}_i f_i = \bar{w}_i (p_i + q_i y + r_i) \quad (4.25)$$

where  $\bar{w}_i$  is the output of layer 3, and  $\{p_i, q_i, r_i\}$  is the parameter set. Parameters in this layer will be referred as "Consequent Parameters".

Layer 5: The single circle node computes the overall output as the summation of all incoming signals i.e.

$$O_i^5 = \text{Overall output} = \frac{\sum_i \bar{w}_i f_i}{\sum_i \bar{w}_i} \quad (4.26)$$

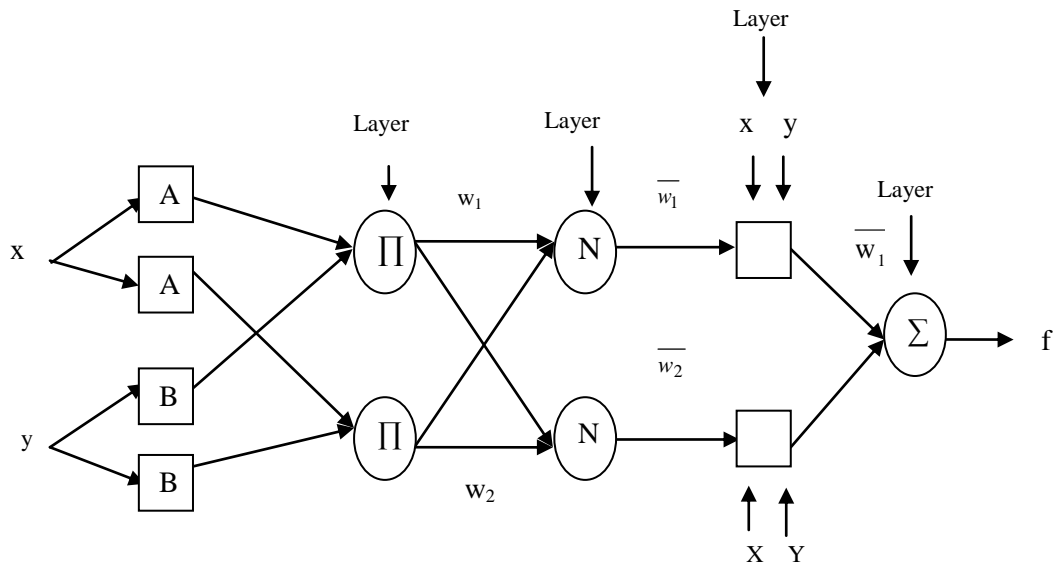


Figure.4.16. A typical architecture of ANFIS system.

Thus, an adaptive network is presented in Figure 4.16 is functionally equivalent to a fuzzy interface system shown in Figure 4.15. The basic learning rule of ANFIS is the back propagation gradient decent which calculates error signals (defined as the derivative of the squared error with respect to each nodes output) recursively from the output layer backward to the input nodes (Werbose 1974). This learning rule is exactly the same as the back-propagation learning rule used in the common feed-forward neural networks (Rumelhart et al. 1986). From ANFIS architecture (Figure 4.16), it is observed that the given values of the of premise parameters, the overall output can be expressed as a linear combination of the consequent parameters. Based on this observation, a hybrid learning rule is employed here, which combines a gradient decent and the least squares method to find a feasible of antecedent and consequent parameters (Jang 1991<sup>a</sup>, 1993). The details of the hybrid rule are given by Jang et al. (1997) where it is also claimed to be significantly faster than the classical back propagation method.

#### 4.3.6 HYBRID LEARNING ALGORITHM

From the ANFIS architecture shown in Figure 4.16, we observe that when the values of the premise parameters are fixed and the overall output can be expressed as a linear combination. The output f can be rewritten as:

$$f = \frac{w_1}{w_1 + w_2} f_1 + \frac{w_2}{w_1 + w_2} f_2$$

$$\begin{aligned}
&= \overline{w}f_1 + \overline{w}f_2 \\
&= (\overline{w}x)p_1 + (\overline{w}y)q_1 + (\overline{w}_1)r_1 + (\overline{w}_2x)p_2 + (\overline{w}_2y)q_2 + (\overline{w}_2)r_2
\end{aligned} \tag{4.27}$$

which is linear in the consequent parameters  $p_1, q_1, r_1, p_2, q_2, r_2$ . Therefore, the hybrid learning algorithm developed can be applied directly. More specifically, in the forward pass of the hybrid learning algorithm, node outputs go forward until layer 4 and the consequent parameters are identified by the least squares method. In the backward pass, the error signal propagates backward and the premise parameters are updated by gradient descent.

**Table.4.7. Summarizes the activities in each pass.**

	Forward Pass	Backward Pass
Premises Parameters	Fixed	Gradient Descent
Consequent Parameters	Least-Square Estimate	Fixed
Signals	Node Outputs	Error Signals

As mentioned, the consequent parameters thus identified are optimal under the condition that the premise parameters are fixed. Accordingly, the hybrid approach converges much faster since it reduces the dimension of the search space of the original back-propagation method. For this, the network fixes the membership functions and adapt only the consequent part; then ANFIS can be viewed as a functional-linked network (Klassen and Pao 1988; Pao 1989) where the enhanced representation, which take advantage of human knowledge and express more insight. By fine-tuning the membership functions, we actually make this enhanced representation.

#### 4.3.7 TRAINING AND TESTING OF ANFIS NETWORK

For the purpose of analysis, entire experimental data sets collected are divided into two sets (a) training set and (b) testing set data set. Out of total 228 data, 206 are considered as training data and 22 as testing data respectively. The testing data is collected by taking 2-3 numbers of data from each of different type of experimental data mentioned in Figure 4.6. Figure 4.17 shows the procedure adopted for the development of present ANFIS model. During the training, a five layered ANFIS architecture is constructed (Figure 4.18). During training, the number of nodes in the 2<sup>nd</sup> layer is gradually increased starting from two nodes. It is observed that the error is converged (decreasing) by increasing the nodes and it converged by adopting five nodes. These five layers are the input layer, three hidden layer and the output layer. The network was run on MATLAB platform using Pentium IV desktop computer. Gaussian type membership function (gauss2mf) is chosen for input layer and

linear type membership function is used for output layer during generating FIS (Figure4.19). During the learning process this function becomes steady after 10 iterations due to faster hybrid learning rule. This concludes that the model parameters are now well learned. After training process, the 22 testing data sets are finally used for verifying the accuracy of the proposed ANFIS model.

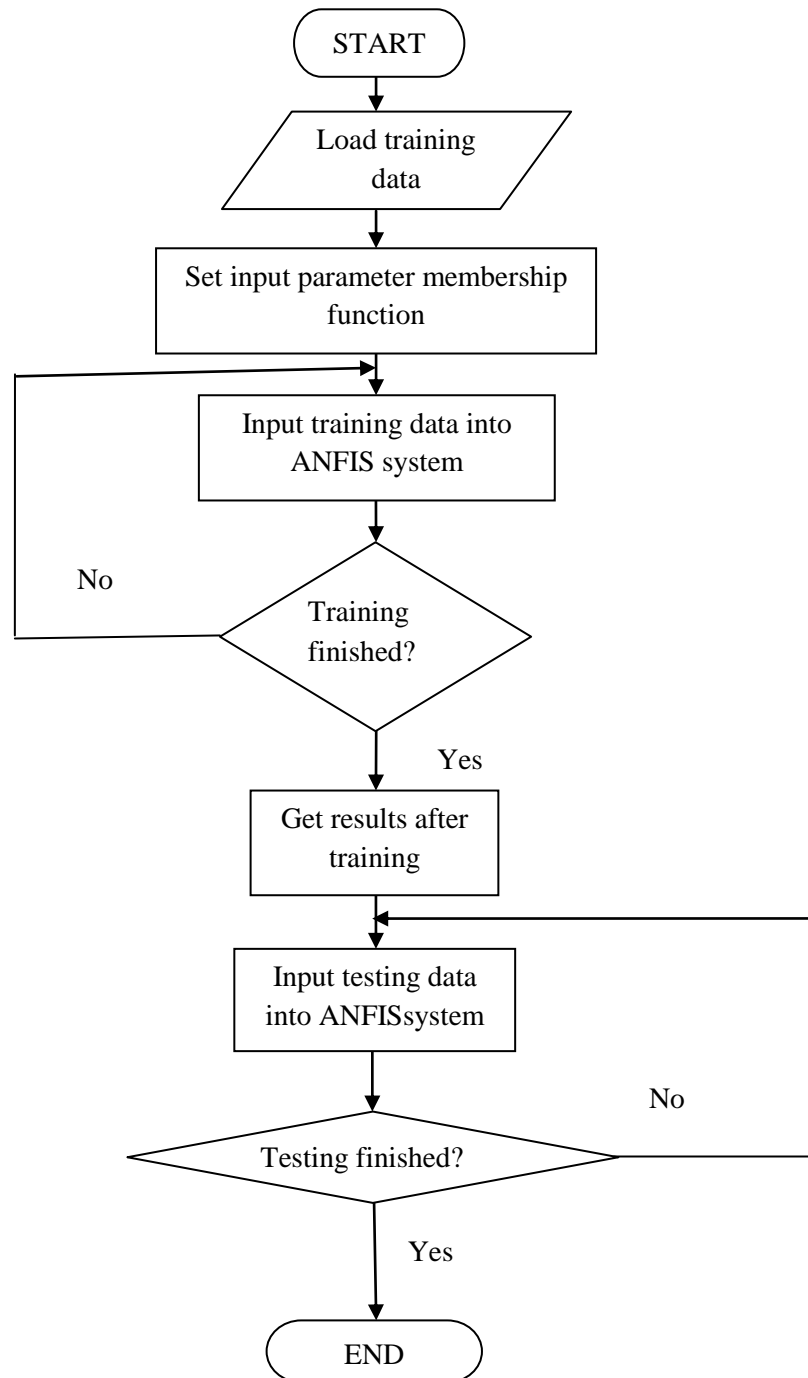


Figure.4.17. Procedure for developing the ANFIS model

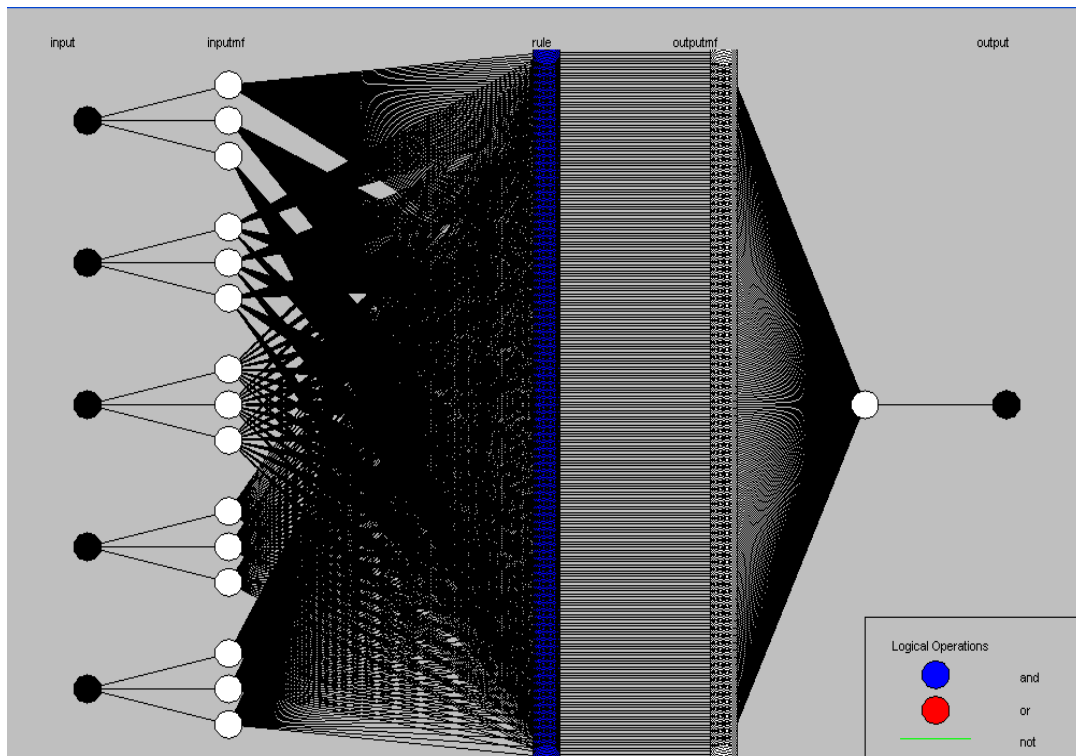


Figure.4.18. Architecture of five layered ANFIS model

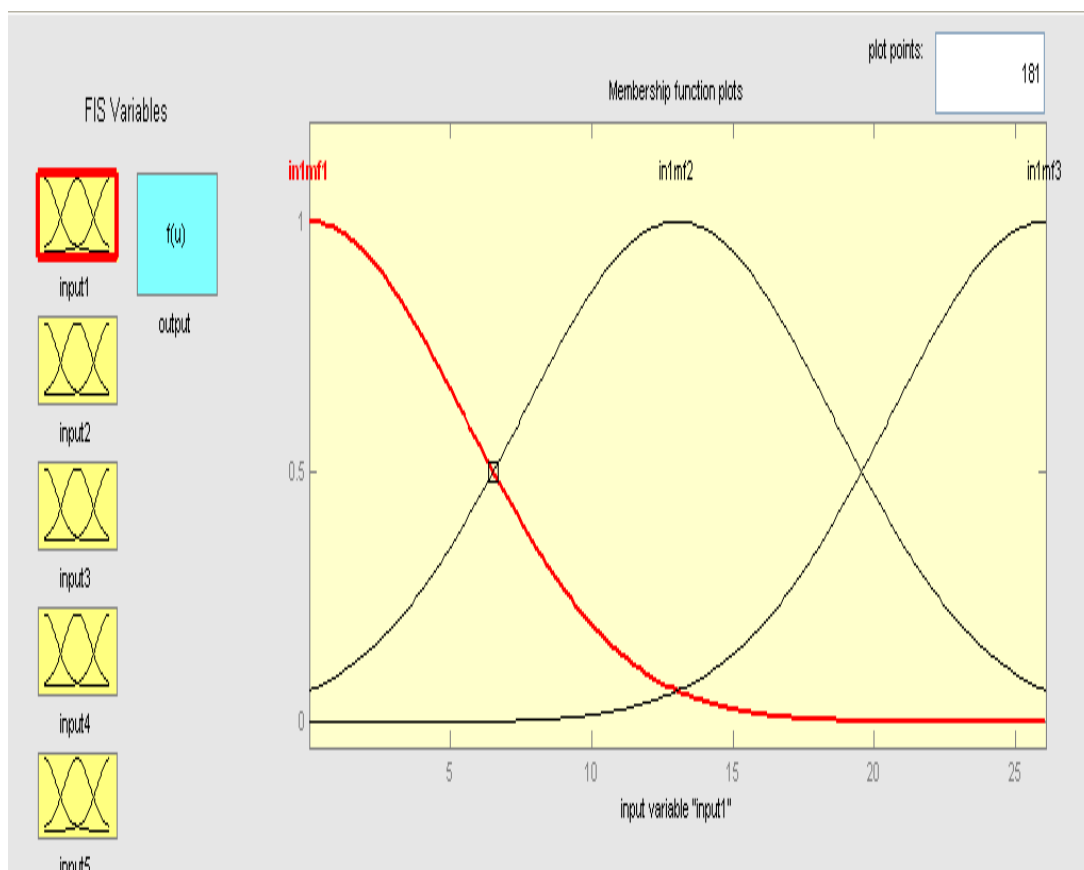


Figure.4.19. Membership-function is used for output during generating FIS

#### 4.3.8 COMPARISON OF DIFFERENT METHODS WITH TRUE VALUE FOR PREDICTION OF COMPOSITE FRICTION FACTOR.

To the study of efficacy of different standard models for prediction of composite friction factor, six sets of experimental data are used i.e. experimental data of Atabay (2004), Soong and DePue (1996), Tang and Knight (2001), Tang and Knight (2004) for mobile channel, Tominag and Nezu (1991), and FCF Series A, Khatua et al. (2011). The data collected are from different compound channels with different geometry and hydraulic conditions. Here "True Manning's factor" is calculated from total discharge of the compound channel by using Manning's equation as described by Yang et al.(2007). By keeping this as the true value other developed models such as KCM, LM, EBM, COX and D&H are compared below. The strength and weakness of these methods are applied to varieties of compound channels are presented below.

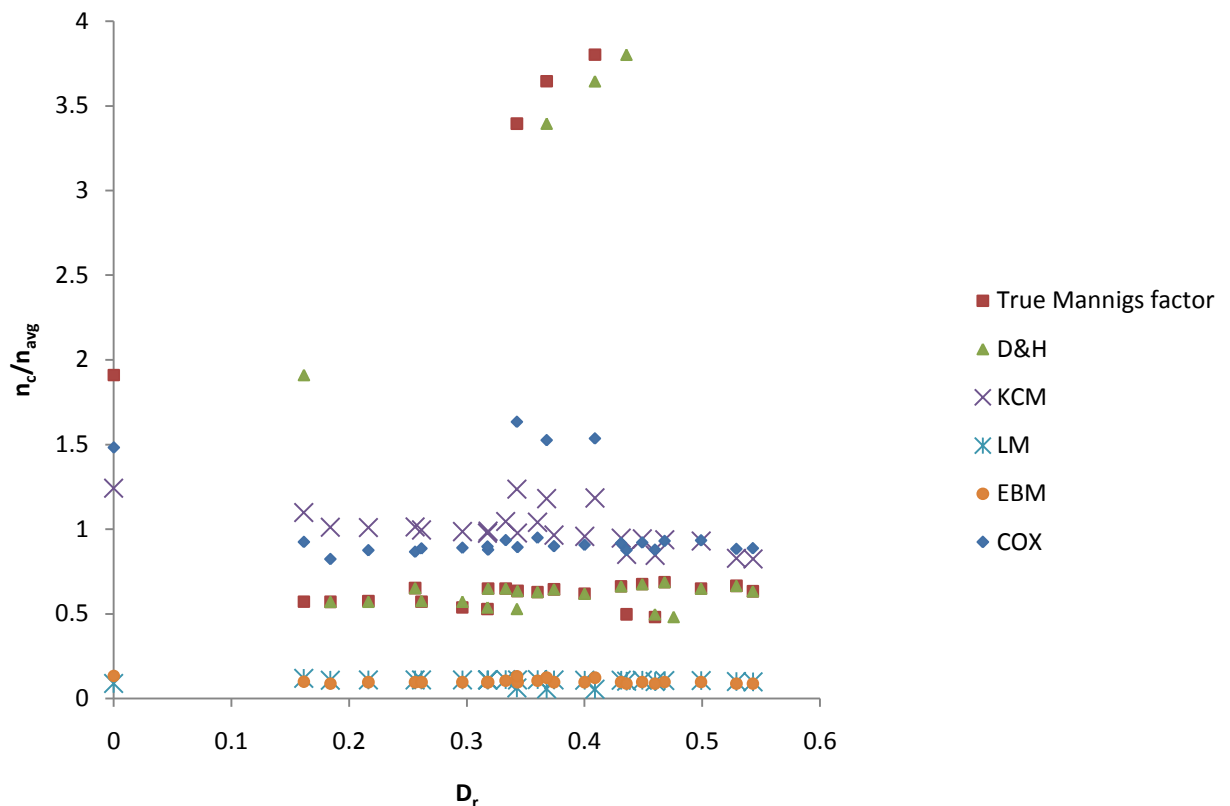


Figure.4.20. Application of methods in Atabay et al. (2004) experimental flow conditions.

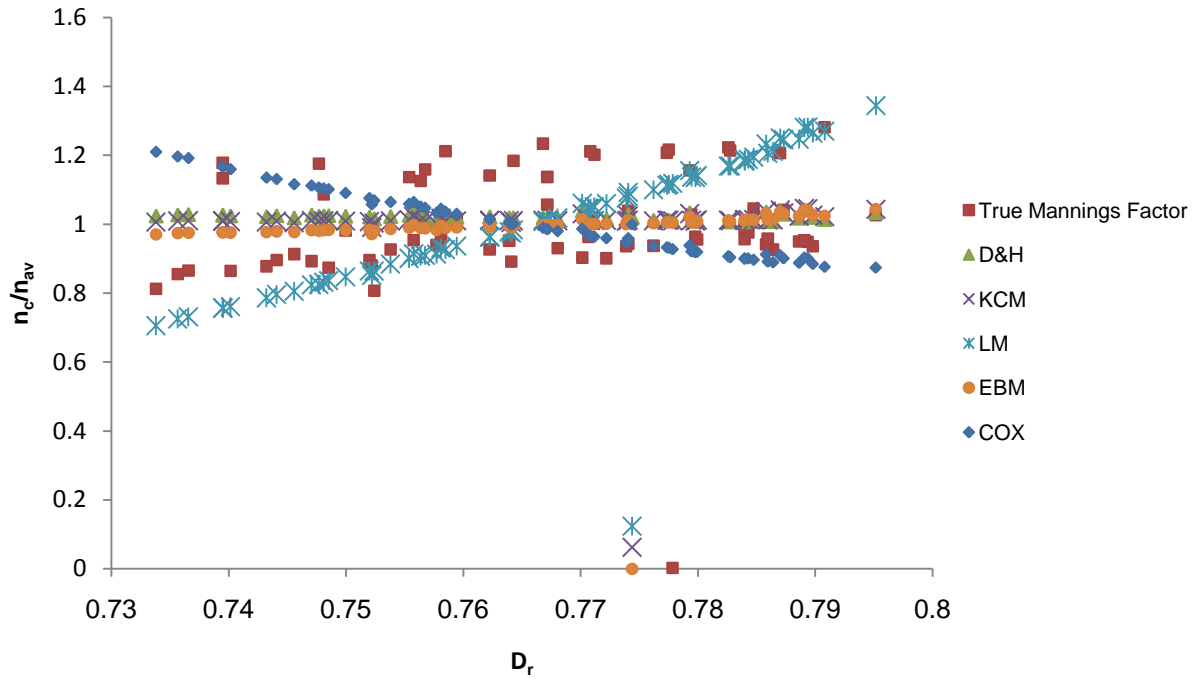


Figure.4.21. Application of methods in Soong and DePue (1996) experimental flow conditions.

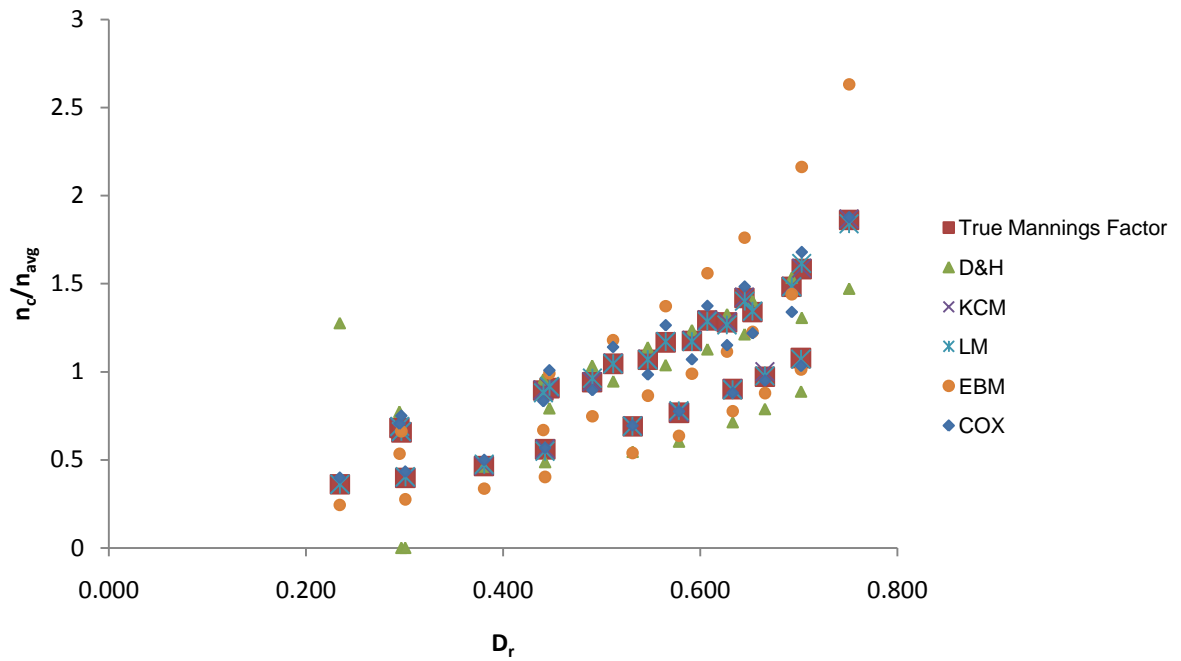


Figure.4.22. Application of methods in Tang and Knight (2001) experimental flow conditions.

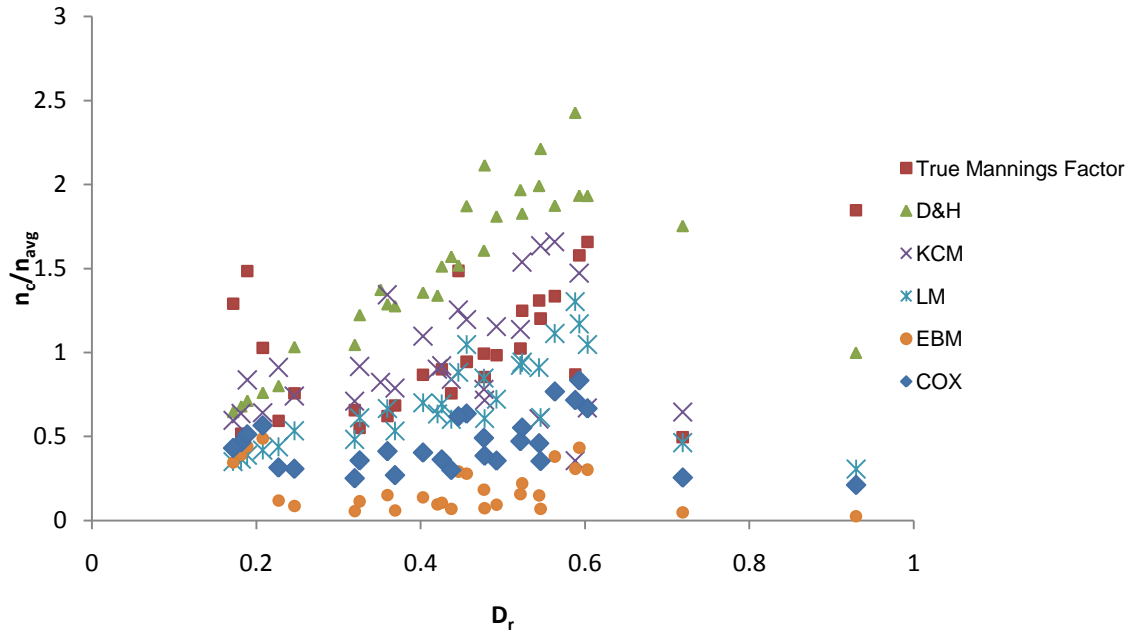


Figure.4.23. Application of methods for composite friction factor prediction in Tang and Knight (2001) mobile experimental flow conditions.

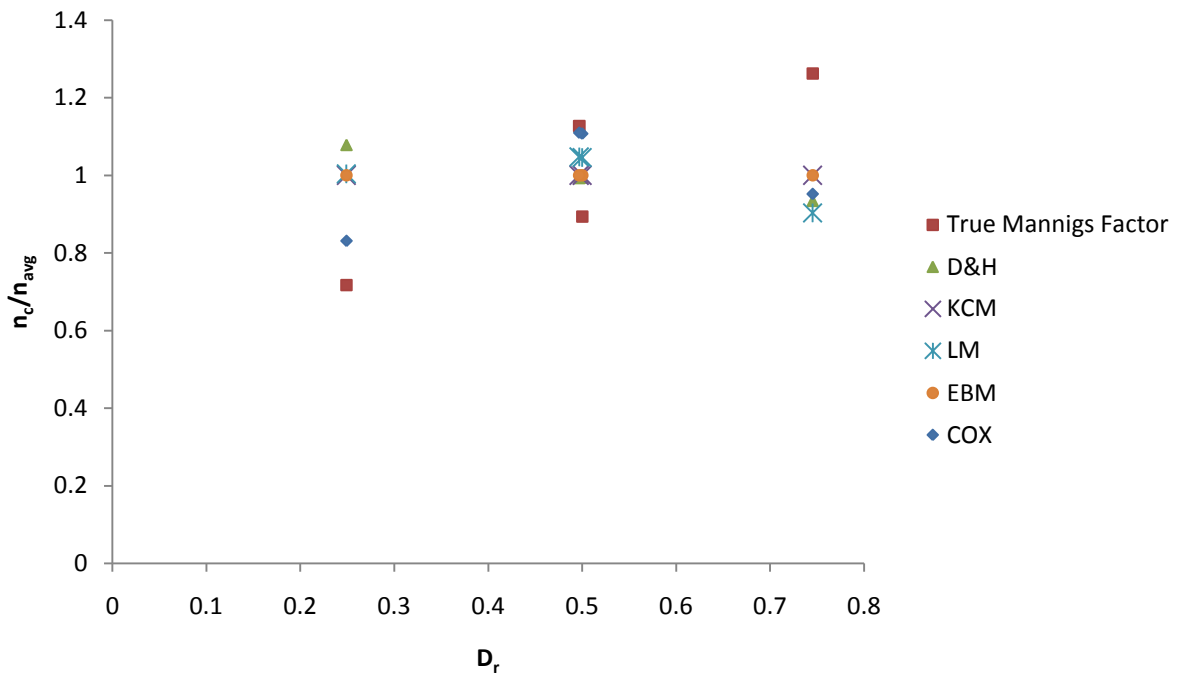


Figure.4.24. Application of methods in Tominaga and Nezu (1991) experimental flow conditions.

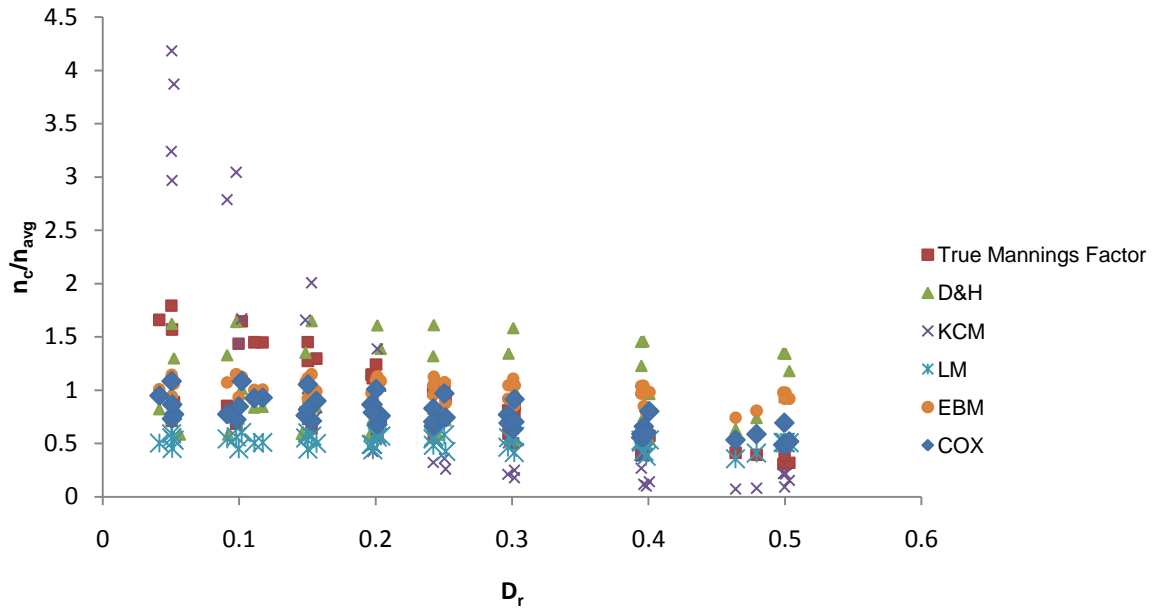


Figure.4.25. Application of methods in FCF- Series A experimental flow conditions.

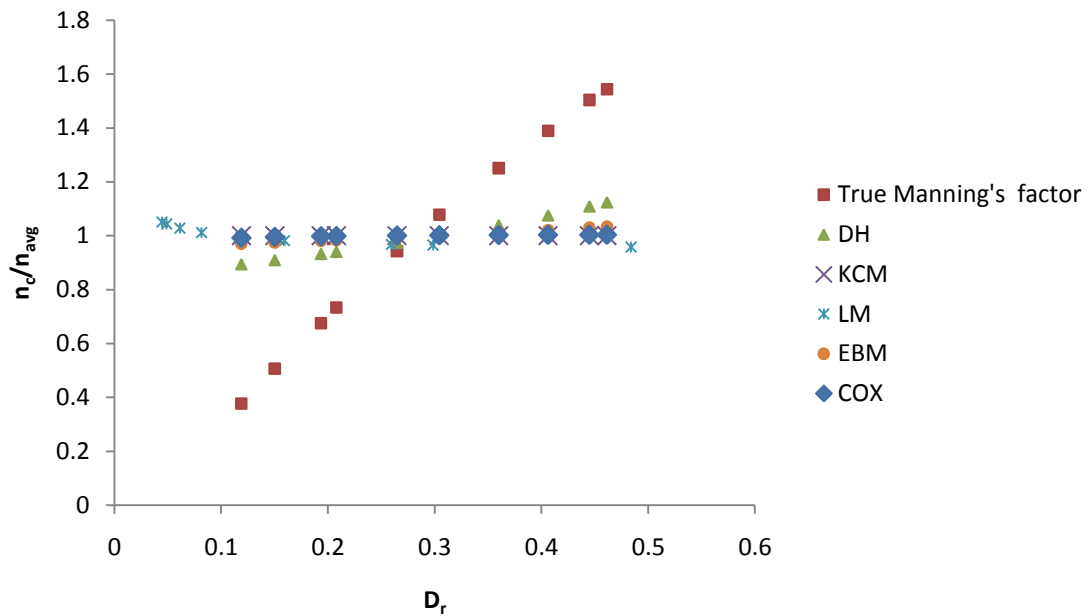


Figure.4.26. Application of methods in Khatua et al. (2011) experimental flow conditions.

Absolute relative errors of the above described methods are calculated for different data sets as in eqn. (4.28):

$$S = \frac{|n_{actual}| - |n_{predicted}|}{|n_{actual}|} \tag{4.28}$$

Where S = Absolute relative error,  $n_{actual}$  = composite friction factor,  $n_{predicted}$  = mean composite friction factor.

The standard errors are tabulated in Table 4.8.

**Table.4.8. Absolute relative error of different methods for different hydraulic conditions.**

Data set	Cox (1973)	Krishnamurthy and Christensen (1972)	Lotter (1993)	Einstein and Banks (1950)	Draccos and Haddger (1987)
FCF- Series A	28.33	49.47	24.16	32.6	15.73
Atabay et al.(2004)	17.28	18.10	35.75	33.43	14.98
Soong and DePue (1991)	13.12	15.28	33.21	7.42	34.38
Tominaga and Nezu (1991)	32.21	34.72	8.28	33.68	25.22
Tang (2001)	28.81	9.37	13.52	57.58	13.74
Tang (2001) mobile	28.24	46.14	27.61	33.721	26.14
Khatua et al. (2011)	26.44	24.38	25.12	26.07	21.23

#### 4.3.9 RESULTS OF ARTIFICIAL NEURO-FUZZY INFERENCE SYSTEM

After the computation using ANFIS analysis, the post processing is carried out. It can be observed from Figure 4.26 to Figure 4.29 that the proposed ANFIS network is well trained.

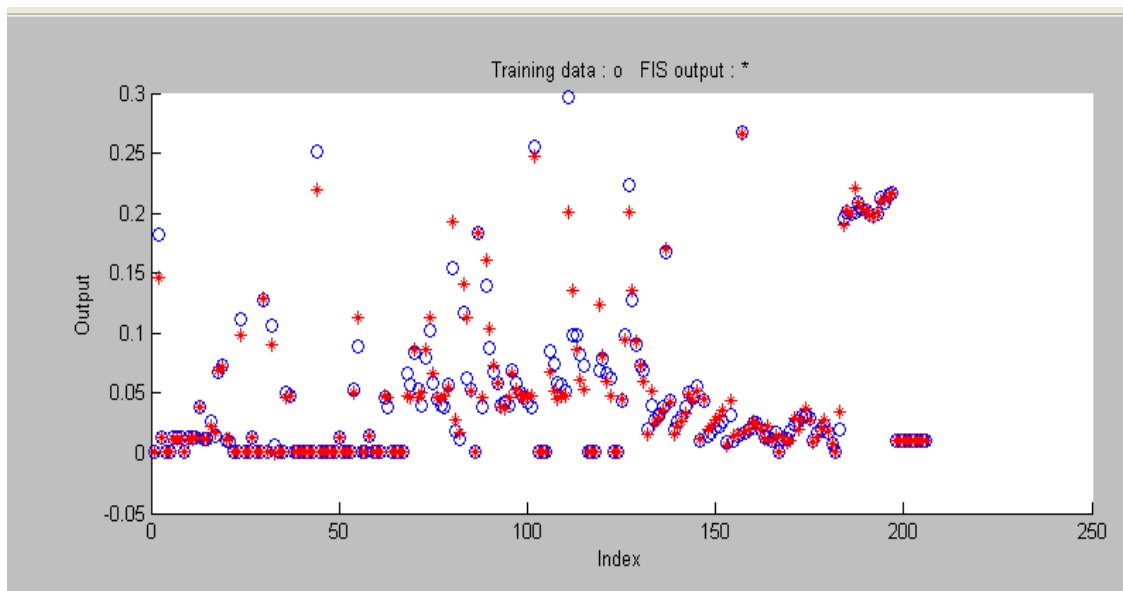


**Figure.4.27. Predicted data points through ANFIS model (training).**

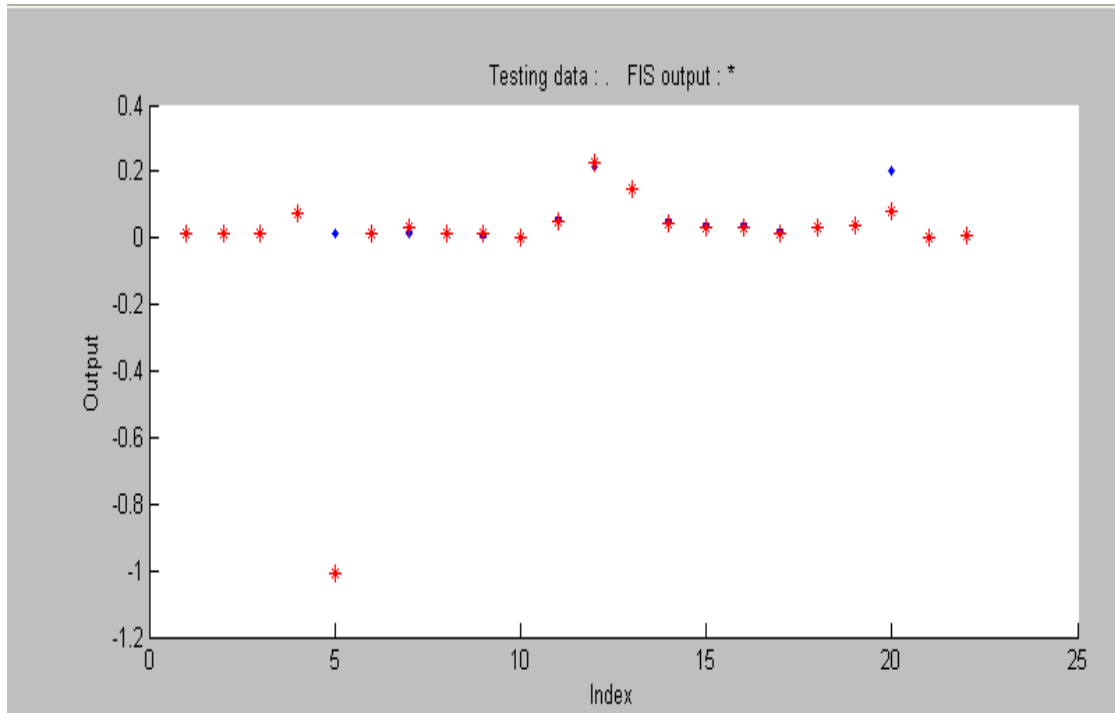


Figure.4.28. Predicted data points through ANFIS model (testing).

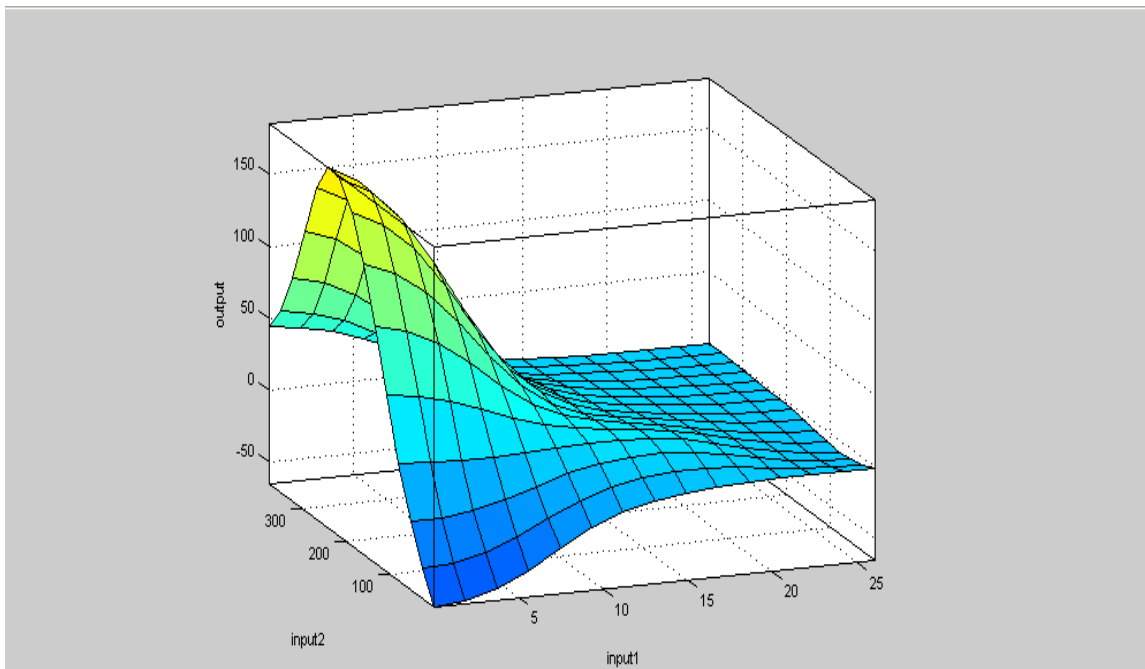


Figure.4.29. Surface plot of decision space.

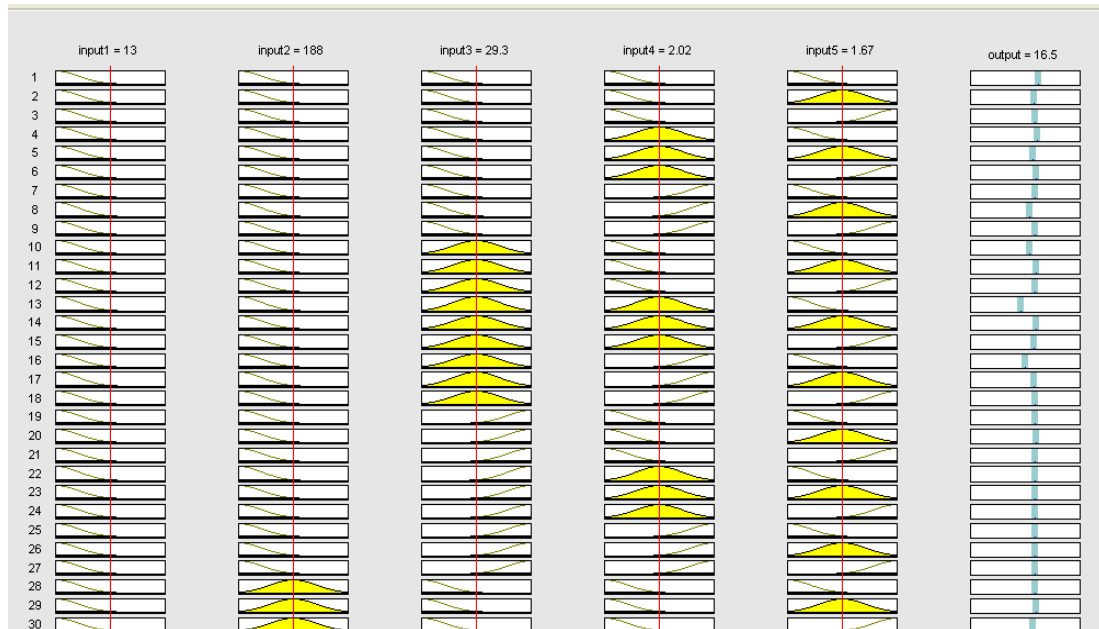


Figure.4.30. Rule base generated for prediction of Composite Friction Factor

The distribution of predicted values of composite friction factor over all training data set and testing data set are shown in Figure 4.27 and Figure 4.28 respectively. Similarly, the patterns of variations of actual and predicted composite friction factors are shown in Figure 4.27 and Figure 4.28 respectively. The blue dots indicate actual output and red dots represents predicted data. The surface plot (Figure 4.29) shows the coherence nature of the data distribution. It can be observed that the surface covers the total landscape of the decision space. A sample set of rule generation for prediction of composite friction factor is shown in Figure 4.30.

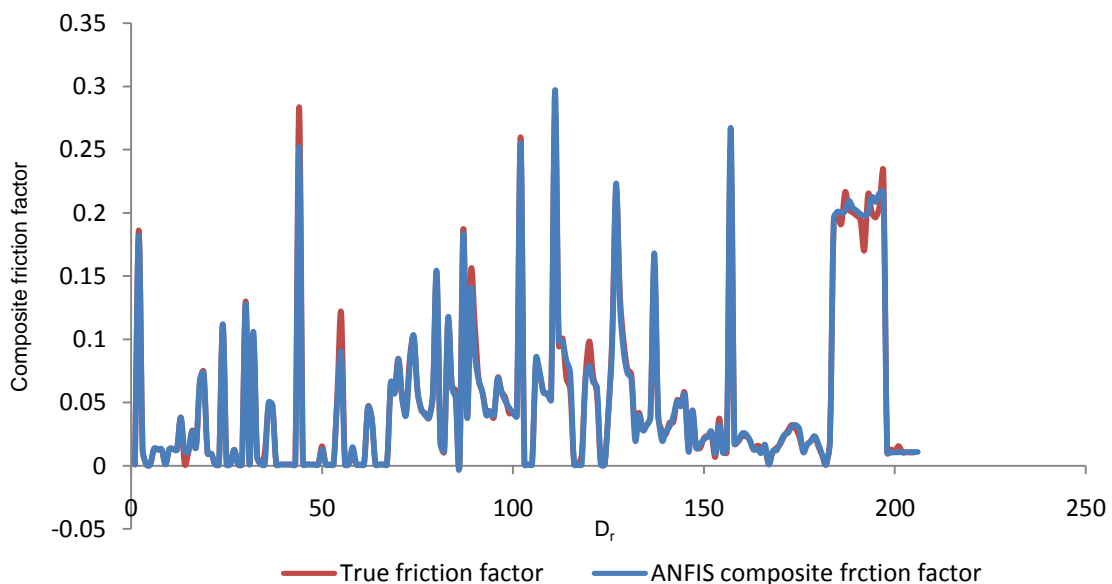
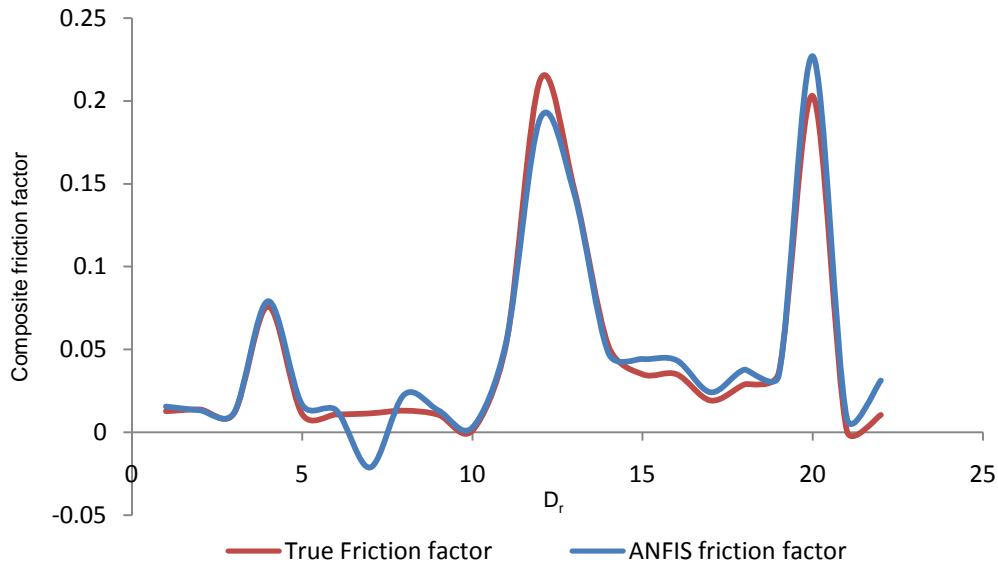
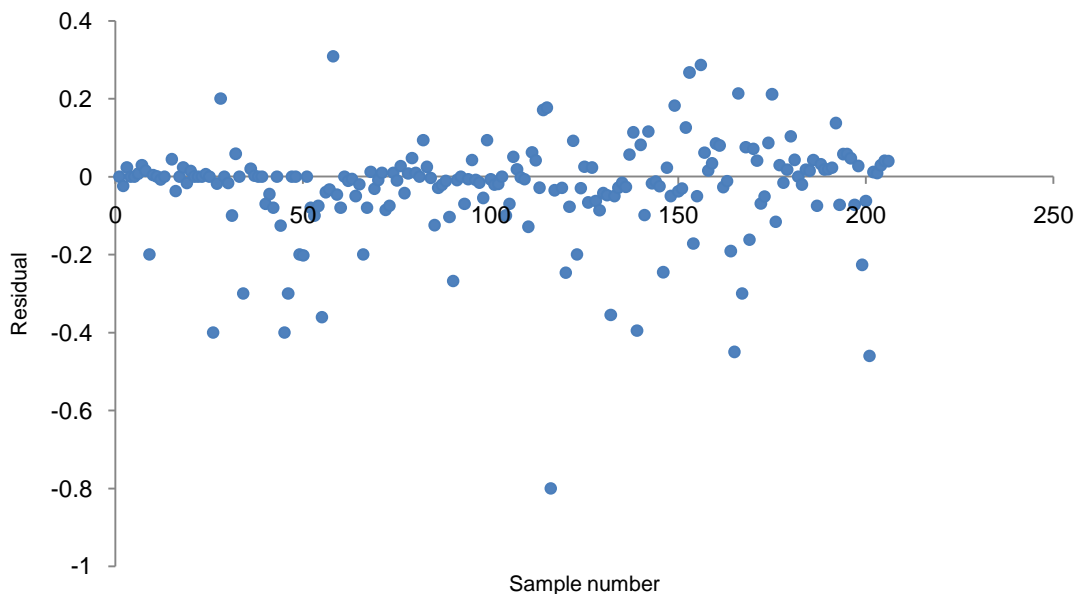


Figure.4.31. Distribution of Composite Friction Factor over all collected data for training data set data set.



**Figure.4.32. Distribution of Composite Friction Factor over all collected data for training data set data set.**

The distribution of training and testing data with sample number is shown in Figure 4.31 and Figure 4.32, which shows the pattern of distribution of the predicted versus actual data. The residual analysis is also carried out by calculating the residuals from the actual and predicted composite friction factor for training data set and shown in Figure 4.33. It also shows that the residuals are distributed evenly along the centerline of the plots. From the above illustrations, it can be said that the data are well trained and the ANFIS network properly incorporates the variation of patterns and non-linearity exists between the dependable parameters to predict the actual value of composite friction factor.



**Figure.4.33. Residual distribution of training data set**

#### 4.3.10 COEFFICIENT OF DETERMINATION ( $R^2$ )

To verify the accuracy of the results obtained by different methods, a regression analysis is also carried out. Regression curves are plotted in Figure 4.34 and Figure 4.35 between true composite friction factor and the predicted composite friction factor through ANFIS model both for training data and testing data respectively. It can be observed that the present model gives a high degree of coefficient of determination ( $R^2$ ) as 0.991 for training and as 0.962 for testing data respectively. The coefficients of determination obtained through other methods are shown in Figures (4.36- 4.40). From these figures, it can be observed that Eienstein and Banks Method shows the maximum variation from actual value of composite friction factor, that can be verified from co-efficient of determination of 0.687.

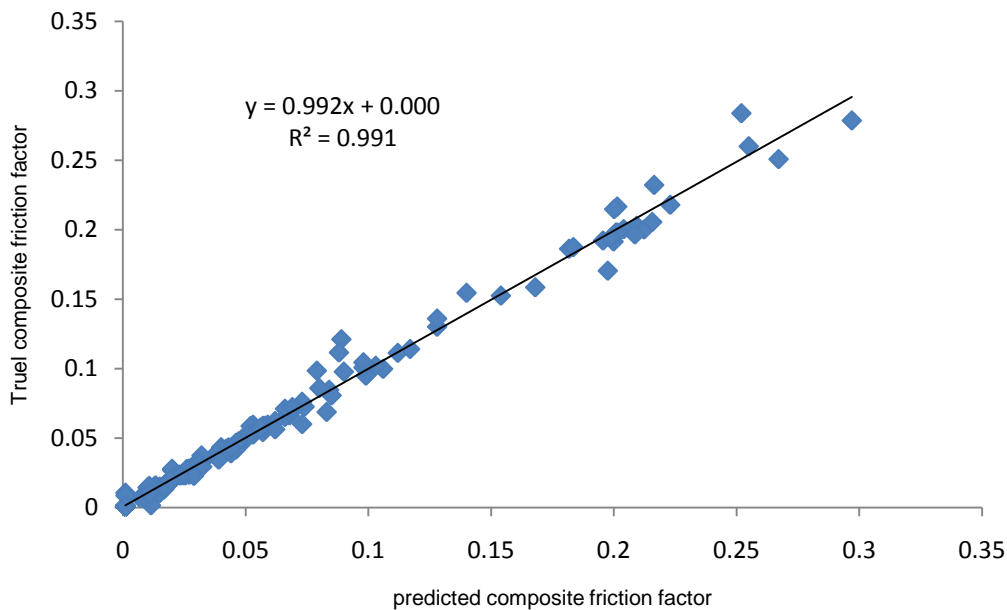


Figure.4.34. Correlation plot for training set of data points.

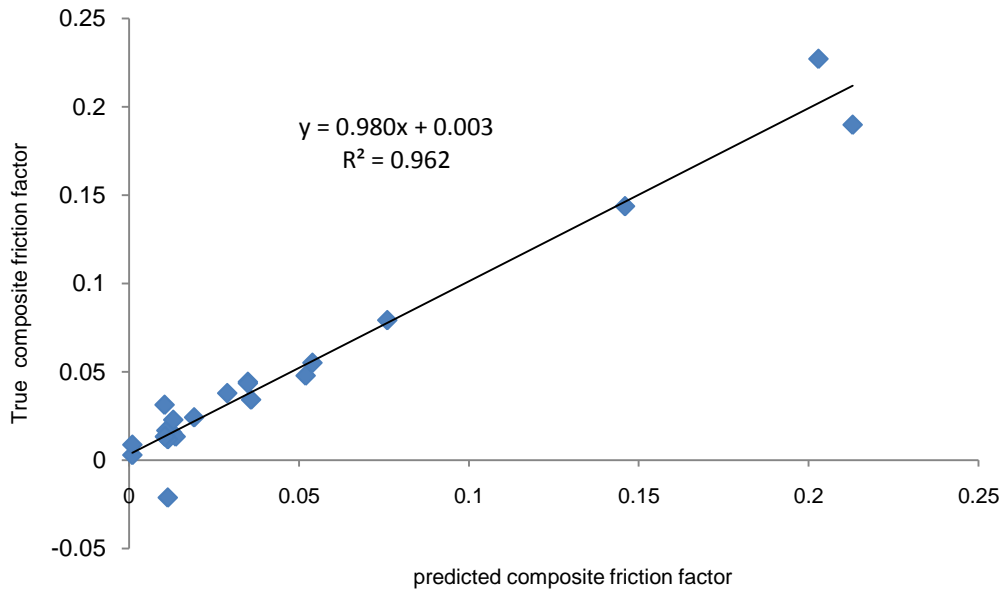


Figure.4.35. Correlation plot for testing set of data points.

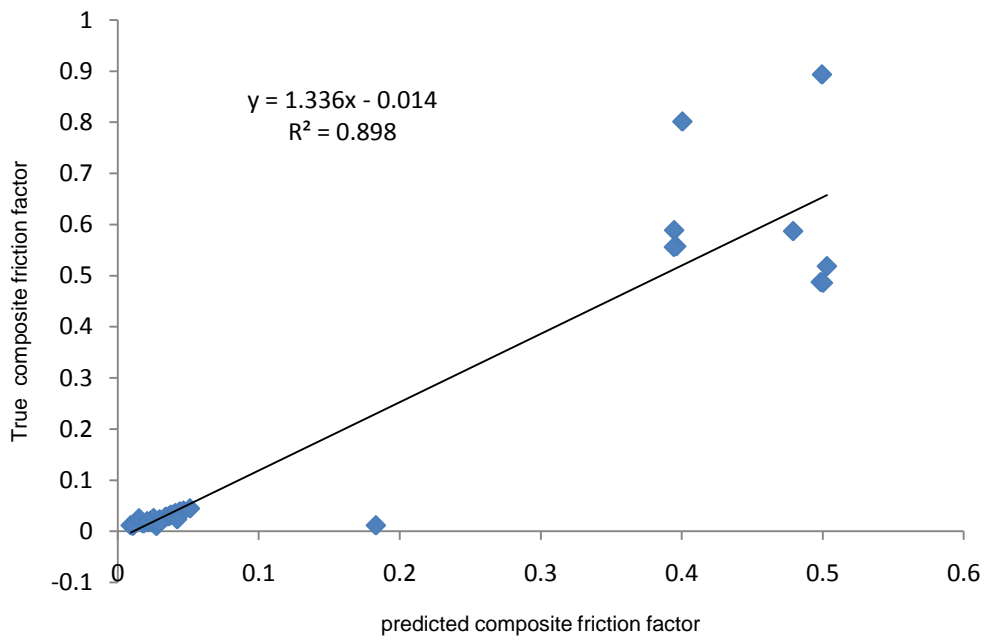


Figure.4.36. Correlation plot for Cox Method for data points.

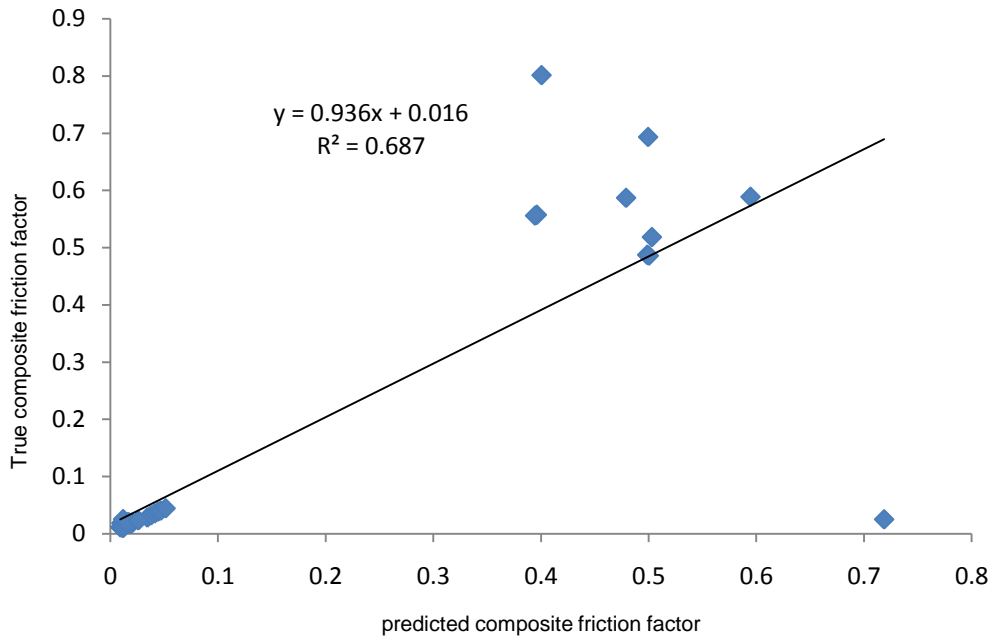


Figure.4.37. Correlation plot for Eienstein and Banks Method for data points.

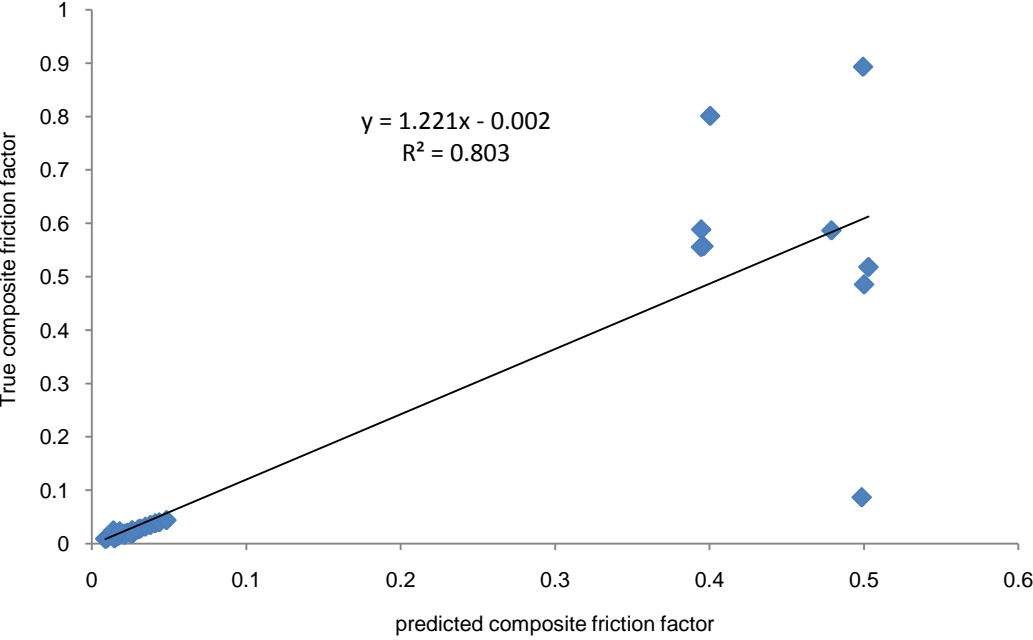


Figure.4.38. Correlation plot for Krishnamurthy and Christensen Method for data points.

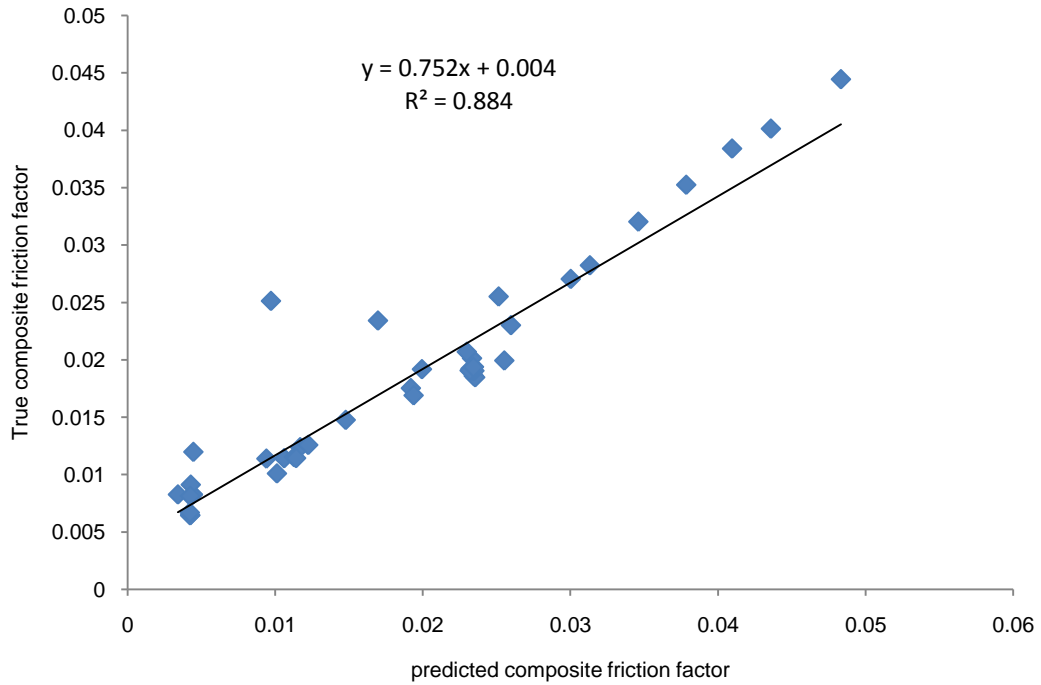


Figure.4.39. Correlation plot for Lotter Method for data points.

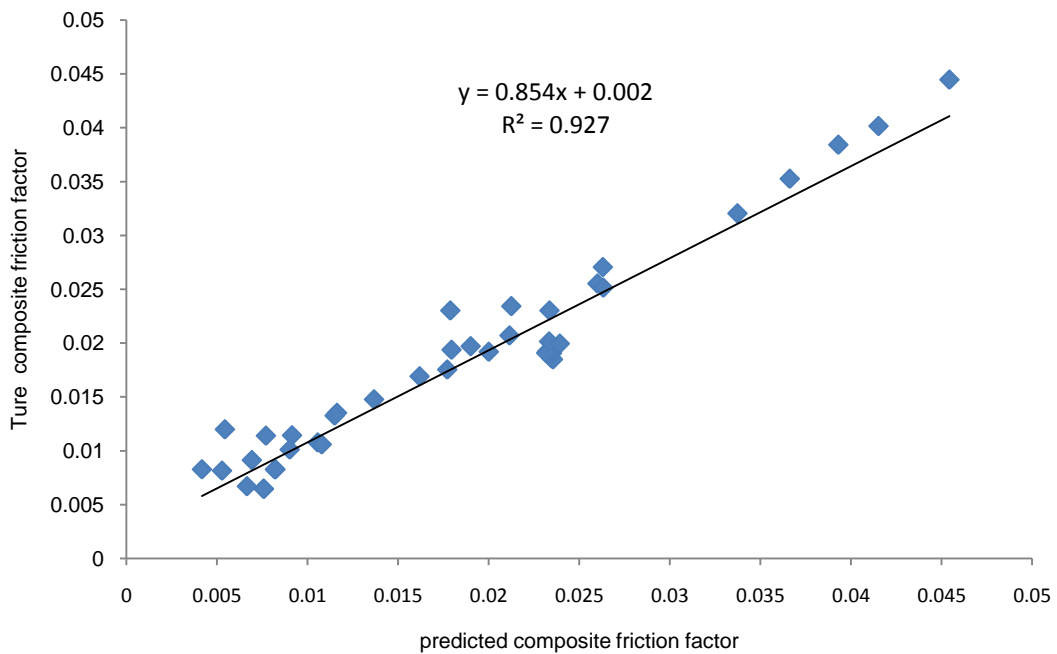


Figure.4.40. Correlation plot for Dracos and Haddger Method for data points

#### 4.3.11 DISCUSSION

- ✓ It can be inferred from the Figure 4.20, that D&H, KCM, COX are incorporating variation pattern of actual friction factor in experimental data of Atabay (2004). The experimentation is performed in both asymmetric and symmetric channel. Here the relative depth ( $D_r$ ) of compound channel varies from 0-0.6 and  $\frac{n_c}{n_{avg}}$  varies from 0.5-4 for True Manning's factor.

The methods are also showing variation of maximum 18.10% of error. While EBM and LM are not following the pattern and are showing error up to 35.76% as mentioned in Table 4.8. It is also observed from above analysis that model proposed by Dracos and Hardegger (1987) is showing the pattern of distribution with actual values because the model has been developed by taking momentum transfer into account.

- ✓ Figure 4.21 shows the comparison of empirical models with True Manning's factor. The comparison is carried out on the experimental data of asymmetric channel by Soong and DePue (1996) at University of Illinois Urbana Champaign, Here it can be observed that relative depth ( $D_r$ ) of compound channel varies from 0.73-0.8 and  $\frac{n_c}{n_{avg}}$  varies from 0.8-1.2

for True Manning's factor. The True Manning's factor is symmetrically distributed across the line  $Y=1$ . But this pattern of distribution is not followed by empirical models.

- ✓ From Figure 4.22 and Figure 4.24, the empirical models are showing the variation in both symmetrical and asymmetrical experimental data of Tang and Knight (2001) and Tominaga and Nezu (1991). Also the experimentation is carried out in smooth symmetric channel for Tang and Knight (2001) and both rough and smooth for Tominaga and Nezu (1991).

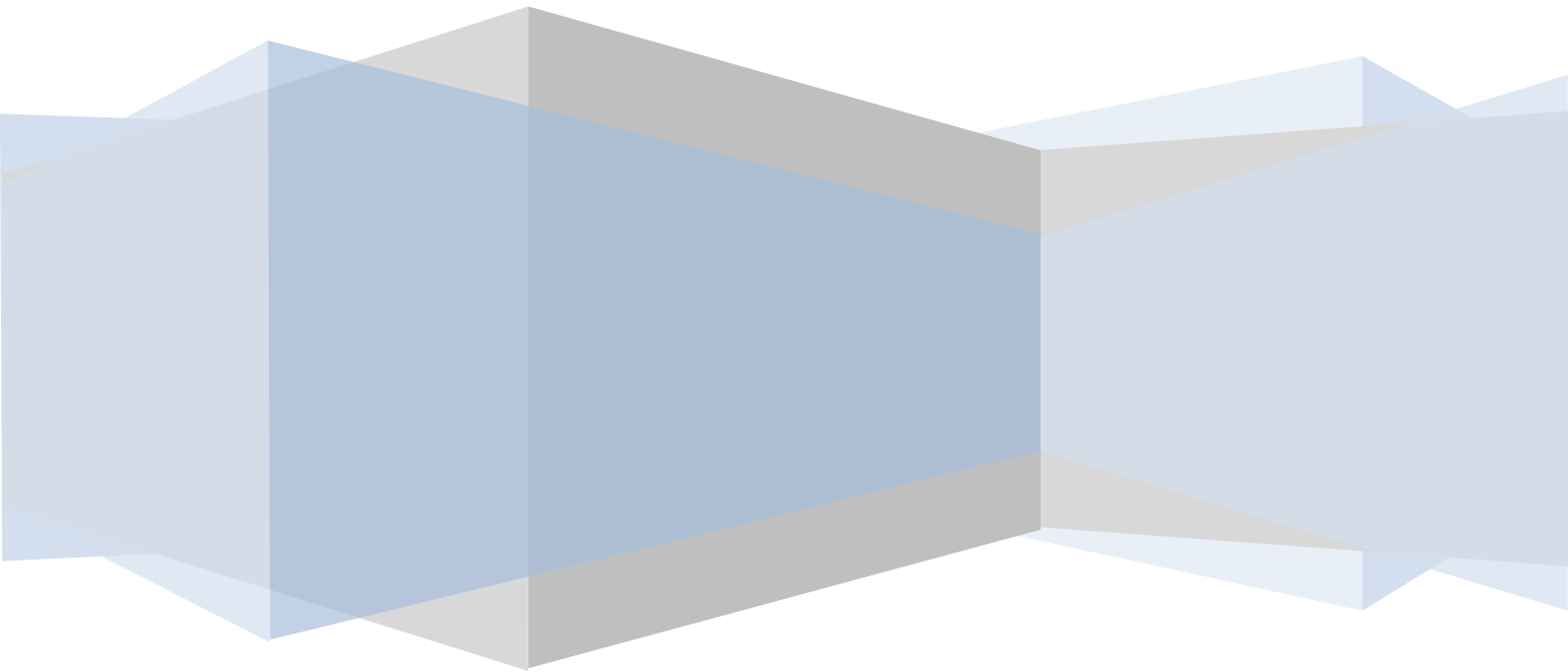
- ✓ Figure 4.23 shows the comparison of empirical models with True Manning's factor. Here, the methods are showing large variations on the experimental data of Tang and Knight (2001) mobile channel. Here, it can be observed that relative depth ( $D_r$ ) of compound channel varies from 0.2-1 and  $\frac{n_c}{n_{avg}}$  varies from 0-2.5 for True Manning's factor. Although methods show

variations, but Lotter and KCM are predicting the friction factor with reasonable accuracy. The empirical models, Cox, EBM, D&H are not following the distribution pattern of actual friction factor as shown in Figure 4.23.

- ✓ From Figure 4.25, it shows the comparison of empirical models with True Manning's factor. Here, the methods are showing large variations on the experimental data of FCF-Series A (both Symmetric and asymmetric smooth channel). Here it can be observed that relative depth ( $D_r$ ) of compound channel varies from 0.05-0.5 and  $\frac{n_c}{n_{avg}}$  varies from 0.5-2 for True Manning's factor. In this comparison only D&H is showing the accuracy. Other models although fitting well with the pattern of distribution but fails to predict the friction factor accurately.
- ✓ It can be further observed from Figure (4.22 - 4.25) that, D&H method is predicting the friction factor with maximum accuracy. The reason is that this method is developed by taking momentum transfer in to account. But this method is showing erroneous result in asymmetric channel.
- ✓ Figure 4.27 shows the variations of models in NIT (2008) experimental conditions. It can be inferred that, none of the models are following the variation patterns of True Manning's friction factor.
- ✓ From above comparison it can be inferred that, no empirical model can able to predict the composite friction factor in all hydraulic condition. Hence to counter the non-linearity on prediction of composite friction factor adaptive method i.e. Artificial Neuro-Fuzzy Inference System is adopted for subsequent analysis.
- ✓ From the plots, Figure (4.34 - 4.40) show the co-efficient of determination between True Manning's ' $n$ ' and predicted manning's ' $n$ ' by Dracos and harddager (1987) method are predicting the friction factor with coefficient of determination 0.9279.
- ✓ The developed ANFIS model is predicting the friction factor astoundingly with coefficient of determination 0.962. The method also is fitting the variation pattern as shown in Figure 4.35. Hence this model can be considered to predict friction factor in compound open channel for different hydraulic conditions as mentioned in Table 4.6.

# CHAPTER 5

## CONCLUSION



## 5. CONCLUSION

---

Based on analysis and discussions of this study certain conclusions can be drawn. The conclusions from the present work are as follows :

- ✓ LES simulation results are presented to show the velocity distribution and secondary current, momentum transfer from main channel to flood plain and vis-versa in an asymmetric compound channel. The discharge and composite friction factor found from the LES simulations are also in good agreement with experimental results.
- ✓ Different discharge and composite friction factor prediction methods are studied. These methods are applied to the published data of compound channels with different hydraulic conditions. The methods are found to give good results to some compound channels where as fail to give good results for compound channels of other geometry and hydraulic conditions.
- ✓ Simulation by LES is done for a compound channel of single flow depth. Simulating LES for different hydraulic condition for different compound channels are arduous and computationally expensive. Therefore, two adaptive numerical approaches such as BPNN and ANFIS have been applied to a numbers of global data systems to predict discharge and composite friction factor successfully to compound channels of different hydraulic conditions.
- ✓ Both BPNN and ANFIS predicted the flow and its resistance fairly as compared to the other models. ANFIS model is logically adaptive and incorporative for the variation within crisp data where as BPNN cannot. It is further seen that ANFIS model is computationally in-expensive and predicting the composite friction factor with lesser time than that with BPNN method.

### **Scope for the future study**

- ✓ The impact of sinuosity on discharge and composite friction factor prediction in compound open channel flows for different roughness condition and mobile bed condition can be extended.
- ✓ The study can further be extended for prediction of boundary shear stress, discharge distribution etc. for compound channels of different geometry and hydraulic conditions.
- ✓ LES modeling for other hydraulic and geometrical conditions can be carried out.

## Relevant Publications

- ❖ Sahu, M., Mahapatra, S.S., Khatua K.K. “***A Neural Network Approach for Prediction of Discharge in Straight Compound Open Channel Flow***”. Journal of Flow Measurement and Instrumentation (Elsevier).In Press..

# REFERNCES

1. Ackers P.(1992).Hydraulic design of two-stage channels. In: Proceedings of the institution of civil engineers, water, maritime and energy, London: Thomas Telford,4.pp.247–57.
2. Ackers P.(1993). Stage–discharge functions for two-stage channels: the impact of new researches. *Inst Water Environ Manage*, 7,pp.52–61.
3. Atabay S, Knight DW, Seckin G.(2004).Influence of a mobile bed on the boundary shear in a compound channel. In: *Proc. 2nd Int. Conf. Fluvial Hydraulics River Flow*, Napoli, Italy, 1,pp.337-45.
4. ANSYS, Inc. (2011). *Ansys-CFX*, version 13.0 Southpointe,Canonsburg PA, USA.
5. Beaman F.(2010).Large Eddy Simulation of open channel flows for conveyance estimation. Ph.D thesis, University of Nottingham.
6. Bigil A, and Altun H.(2008). Investigation of flow resistance in smooth open channels using artificial neural network. *Flow Measurement and Instrumentation*, 19,pp.404-8.
7. Bousmar D, Zech Y.(1999). Momentum transfer for practical flow computation in compound channels .*J Hydraul. Eng, ASCE*, 125(7),pp.696–706.
8. Cao Z, Meng J,Pender G, and Wallis S,(2006).Flow Resistance and Momentum Flux in Compound Open Channels. *J. Hydraul. Engg.*.132(12), pp.1272-1283.
9. Chow VT.(1959).Open-channel hydraulics. New York: Mc. Graw-Hill Book Co,.
10. Christodoulou GC ,Myers WRC.(1999).Apparent friction factor on the flood plain-main channel interface of compound channel sections.*Proc.28th IAHR Congress*, Graz, Austria.
11. Cox RG.(1973).Effective hydraulic roughness for channel shaving bed roughness different from bank roughness. *Misc. Paper H-73-2,U.S.Army Corps of Engineers Waterways Experiment Station*, Vicksburg, Miss.
12. Cokljat D.(1993).Turbulence models for non-circular ducts and channels. PhD Thesis. City University, London.
13. Colebatch GT.(1941). Model tests on the Lawrence Canal roughness coefficients. *J. Inst. Civil Eng.(Australia)*, 13(2),27–32.
14. Das KM and Kishor N.(2009).Adaptive fuzzy model identification to predict the heat transfer coefficient in pool boiling of distilled water. *J. Expert Sys. App.*, 36(2), pp.1142-1154.
15. Dezfoli KA.(2003).Principles of fuzzy theory and its application on water engineering problems. Tehran, Iran Jihad Press, 227.

16. Dracos T, and Hardegger P.(1987). Steady uniform flow in prismatic Channels with flood plains. J. Hydraul. Res. IAHR 25(2),pp.169–185.
17. Einstein HA. (1934).Der Hydraulische Profil-Radius. Schweiz-erische Bauzeitung, Zurich,103(8),89–91.
18. Einstein HA, and Bank RB.(1950). Fluid resistance of composite roughness. Transactions of American Geophysical Union, 31(4),pp. 603–610.
19. Engelund F. (1964).Flow resistance and hydraulic radius. Basic Re-search Progress Rep. No.6,ISVA,Technical Univ.of Denmark,pp.3–4.
20. Felkel K. (1960).Gemessene Abflüsse in Gerinnen mit Weidenbewuchs.' Mitteilung der BAW,Heft15,Karlsruhe,Germany.
21. Esen H, Inalli M, Sengur A, and Esen M.(2008).Modeling a ground-coupled heat pump system using adaptive neuro-fuzzy inference systems, J. of Refrigeration,31(1).pp.64-74.
22. Fadare DA, and Ofidhe IU.(2009). Artificial neural network model for prediction of friction factor in pipe flow, J applied science research, 5(6), pp.662-70.
23. <http://www.flowdata.bham.ac.uk/fcfa.shtml>.
24. <http://www.flowdata.bham.ac.uk/atabay/index.shtml>.
25. <http://www.flowdata.bham.ac.uk/tang/data.shtml>
26. Hin LS, Bessaih N, Ling LP, Ghani A, Zakaria NA, and Seng MY.(2008). Discharge estimation for equatorial natural rivers with over bank flow, Intl. J. River Basin Management ,6,(1),pp.13–21.
27. Hodges BR. and Street RL.(1999).On simulation of turbulent nonlinear free-surface flows. Journal of Computational Physics. 151, pp. 425-457.
28. Hodkinson A. and Ferguson RI.(1998). Numerical modeling of separated flow in river bends: model testing and experimental investigation of geometric controls on the extent of flow separation at the concave bank. Hydraulic Processes. 12, pp.1323-1338.
29. Horton RE.(1933).Separate roughness coefficients for channel bottoms and sides. Eng. News-Rec., pp.652–653.
30. Huthoff F, Roos PC, Augustijn DCM, and Hulscher SJMH. (2008).Interacting Divided Channel Method for Compound Channel Flow. J. Hydraul. Eng. 134, 1158.

31. Ida Y. (1960). Steady flow in wide channel—on the effect of shape of its cross section. In. Japanese Trans .Jpn. Soc. Civ. Eng., 69(3-2).1–18.
32. Jang RJ.(1991a).Fuzzy modeling using generalize d neural networks and Kalmman filter algorithm. Int. Proc. the ninth National Conference on Artificial Intelligence, 762-767.
33. Jang RJ.(1991b).Rule Extraction using generalized neural networks. Int. Proc. of the forth IFSA World congress,pp.82-86.
34. Jang RJ.(1993a). ANFIS: Adaptive-network-based fuzzy inference system. IEEE Transaction on Systems of Max and Cybernetics, 23(03), pp.665-685.
35. Jang RJ.(1994).Structure determination in fuzzy modeling: a fuzzy CART approach. In Proc. of IEEE International conference on Fuzzy Systems, Orlando, Florida.
36. Jang JSR, and Gulley N.(1996).Fuzzy Logic Toolbox: Reference Manual. The Math works Inc.
37. Jang JSR, Sun CT, and Mizutani E. (1997). Neuro-fuzzy and soft computing: a computational approach to learning and machine intelligence. Prentice-Hall International, London.
38. Kawahara Y and Tamai N.(1988). Numerical calculation of turbulent flows in compound channels with an algebraic stress turbulence model. Proceeding of the 3rdInternational Symposium on Refined Flow Modeling and Turbulence Measurements, Tokyo, Japan, pp. 9-17.
39. Khatua KK, Patra KC, and Mohanty P. (2011). Stage-Discharge Prediction for Straight and Smooth Compound Channels with Wide Floodplains J. Hydr. Engg., ASCE,
40. Klassen MS, and Pao YH.(1988).Characteristics of the functional link net: A higher order delta rule net. In IEEE Proceedings of the International Conference on Neural Networks. San Diego.
41. Krishnappan BG. and Lau YL.(1986).Turbulence modeling of floodplain flows. Journal of Hydraulic Engineering, ASCE. 112(4), pp. 251-266.
42. Krishnamurthy M, and Christensen BA.(1972). Equivalent roughness for Shallow channels. J. Hydraulics Div., 98(12),pp. 2257–2263.
43. Knight DW, and Demetriou JD. (1983).Floodplain and Main Channel Flow Interaction. J. Hydr. Eng., ASCE 109(8), pp. 1073-1092.

44. Knight DW, and Hamed ME.(1984), Boundary Shear in Symmetrical Compound Channels. J. Hydraul. Eng., ASCE, 110, pp.1412-1430.
45. Lambert MF, and Myers WRC.(1998). Estimating the discharge capacity in compound channels. International Proceedings Institute of Civil Engineering, Water, Maritime, and energy, 130.London, pp.84–94.
46. Larson R.(1988).Numerical simulation of flow in compound channels. Proceeding of the 3rd International Symposium on Refined Flow Modeling and Turbulence Measurements, Tokyo, Japan, pp. 527-536.
47. Lane SN, Bradbrook KF, Richards KS, Biron PA and Roy AG. (1999).The application of computational fluid dynamics to natural river channels: Three-dimensional versus two-dimensional approaches. Geomorphology. 29, pp.1-20.
48. Lotter GK.(1933).Considerations on hydraulic design of channel with Different roughness of walls. Transactions of All-Union Scientific Research Institution of Hydraulic Engineering, 9,pp.238–241.
49. Meneveau C. and Katz J.(2000). Scale-invariance and turbulence models for large-eddy simulation. Annual Review of Fluid Mechanics. 32, pp. 1-32.
50. Morvan HP.(2001).Three-dimensional simulation of river flood flows. PhD Thesis, Glasgow.
51. Myers WRC, and Elsayy (1975). Boundary Shear in Channel with Floodplain. Jr. Hydr. Engg, ASCE, 101(7), pp. 933-946.
52. Myers WRC,(1987). Velocity and Discharge in Compound Channels, Jr. Hydr. Engg., ASCE, Vol.113, No.6, pp.753-766.
53. Nakayama A, and Yokojima S.(2002).LES of open-channel flow with free-surface fluctuations. Proc. of Hydr. Eng., JSCE. 46, pp. 373-378.
54. Pan Y, and Banerjee S.(1995).A numerical study of free-surface turbulence in channel flow. Physics of Fluids, 7, pp. 1649.
55. Pao YH.(1989).Adaptive pattern Recognition and Neural Network. Adission-Willey Publishing Company, Inc, pp.197-222.
56. Pang B.(1998). River Flood Flow and its Energy Loss.J. Hydraul. Eng., ASCE, 124(2), pp. 228-231.

57. Pavlovskij NN.(1931). On a design formula for uniform movement in channels with non homogeneous walls. Transactions of All-Union Scientific Research Institution of Hydr. Eng, 3,pp.157–64.
58. Posey CJ.(1967). Computation of discharge including over-bank flow. Civil Engineering , ASCE, 37(4),pp.62–63.
59. Prinos P, and Townsend RD.(1984). Comparison of methods for predicting discharge in compound open channels. Adv Water Resour; 7(12): pp.180–7.
60. Rajaratnam N, and Ahmadi RM.(1979). Interaction between Main Channel and Flood Plain Flows. J. of Hydr. Div., ASCE, 105(5), pp. 573-588.
61. Riahi-Madvar H, Ayyoubzadeh AS, Khadangi E, and Ebadzadeh MM.(2009).An expert system for predicting longitudinal dispersion coefficient in natural streams by using ANFIS. J. Exp. Sys. App., 36(2), pp.1142-1154.
62. Rumelhart DE, Hinton GE, and William DE.(1986).Learning internal representations by error propagation. In: Rumelhart DE, McClelland JL (eds) Parallel distributed processing: explorations in the microstructure of cognition, The MIT Press, 1–8,pp. 318–362.
63. Salvetti MV, Zang Y, Street RL and Banerjee S. (1997). Large-eddy simulation of free surface decaying turbulence with dynamic subgrid-scale models. Physics of Fluids. 9, pp. 2405.
64. Sellin RJH.(1964). A laboratory investigation into the interaction between flow in the channel of a river and that of its floodplains. Le Houille Blanche,7, pp. 793-801
65. Sinha SK, Sotiropoulos F, and Odgaard AJ. (1998).Three-dimensional numerical model for flow through natural rivers. Journal of Hydraulic Engineering. 124(1), pp. 13-24.
66. Shi J, Thomas TG. and Williams JJR.(1999).Large eddy simulation of flow in a rectangular open channel. Journal of Hydraulic Research. 37(3), pp. 345-361.
67. Shiono K, Al-Romaih JS, and Knight DW. (1999) Stage-Discharge Assessment in Compound Meandering Channels. J. Hydraul. Eng, ASCE, 125(1),pp.66-77.
68. Soong TW. and DePue II PM.Variation of Manning's coefficient with channel stage. Unpublished MS thesis, University of Illinois Urbana-Champaign;1996.
69. Stephenson D, and Kolovopoulos P.(1990). Effects of momentum transfers in compound channels. J. Hydraul. Eng. ASCE, 116(12): pp.1512–22.

70. Sugeno M, and Kang GT.(1988).Structure identification of fuzzy model. Fuzzy Sets System, 28, pp.15–33.
71. Tang X, and Knight DW.(2001). Analysis of bed form dimensions in a compound channel. In: Proceedings of 2nd IAHR Symposium on River, Coastal and Estuarine Morph dynamics, Obihiro, Japan, pp.555-63.
72. Tang X, and Knight DW.(2001).Experimental study of stage-discharge relationships and sediment transport rates in a compound channel. In: Proceedings of 29th IAHR Congress, Hydraulics of Rivers, , Beijing, China, Tsinghai, 2, pp. 69-76.
73. Thomas TG. and Williams J.(1995a).Large eddy simulation of a symmetric trapezoidal channel at Reynolds number of 430,000. J. Hydraul. Res.. 33(6), pp. 825-842.
74. Thomas TG. and Williams J.(1995b).Large eddy simulation of turbulent flow in an asymmetric compound open channel. J. Hydraul. Res. 33(1), pp. 27-41.
75. Thomas TG. and Williams J.(1999). Large eddy simulation of flow in a rectangular open channel. J. Hydraul Res. 37(3), pp. 345-361.
76. ToebesGH, and Sooky AA.(1967). Hydraulics of Meandering Rivers with Floodplains. J waterways and Harbor Div, Proc. ASCE,93,pp. 213-36.
77. Tominaga A and Nezu I. (1991). Turbulent structure in compound open channel flows. J. Hydraul. Eng, ASCE, 117(1).
78. Van Prooijen BC, Battjes JA, and Uijttewaai WSJ.(2005).Momentum exchange in straight uniform compound channel flow .J. Hydraul. Eng, ASCE, 131(3),pp.175–83.
79. Walid HS, and Shyam SS.(1998). An artificial neural network for non-iterative calculation of the friction factor in pipeline flow. Comput Electron Agriculture, 21,pp.219–28.
80. Werbos P.(1974).Beyond regression: new tools for prediction and analysis in the behavioral sciences. Dissertation, Harvard University.
81. Wormleaton PR, Allen J, and Hadjipanous P. (1982), Discharge Assessment in Compound Channel Flow, J. Hydraul. Div., ASCE, 108(9), pp.975-994.
82. Yang K, Cao S, Liu X.(2005). Study on resistance coefficient in compound channels. Acta Mechanic Sinica; 21:pp.353-61.

83. Yang K, Cao S, and Liu X. (2007).Flow resistance and its prediction methods in compound channels, *Acta Mechanic Sinica*; 21, pp.353-61Yen BC. (2002). Open flow resistance. *J. Hydr. Eng*, 1(20), pp.20-39.
84. Yen BC. (2002). Open flow resistance. *J. Hydr. Eng*, 1(20), pp.20-39.
85. Yen BC.(1991).Hydraulic resistance in open channels in *Channel Flow Resistance :Centennial of Manning's Formula*, Water Resource Publications, Highlands Ranch, Colo.,pp.1–135.
86. Yuhong Z, and Wenxin H.(2009),Application of artificial neural network to predict the friction factor of open channel. *Commun Nonlinear sci Numer Simulat*. 14,pp.2373-8.
87. Zeng YH, Guymer I, Spence KJ,Huai WX. (2010) Application of analytical solutions in trapezoidal compound channel flow . *River Research and Applications*, doi: 10.1002/rra.1433.
88. Zheleznyakov GV.(1965).Interaction of Channel and Floodplain Streams. *Proc. 14th Congress of IAHR*, 5, Paris, France, pp. 144-148.

# REBUTTAL AND ERRATA

## Rebuttal

### # Examiner 1

1. **Query:** In Chapter -3: The numerical modeling for a compound open channel was conducted and compared with the published literature. The same model would have been simulated with different discharge, channel geometry and turbulent parameters. Due to the flow rate variation, it would be interesting to know the degree of variation in turbulent structures and secondary momentum flux. Otherwise, the present numerical modeling seems to be a case study.

**For better presentation, the chapter summary should be included.**

**Answer:** Simulation by LES has been done for a single flow depth of compound channel as explained in Chapter 3. This helps in predicting the flow variables such as discharge, composite friction factor for a given flow depth with particular flow condition and for extracting point to point information from the whole domain of computational space. In this study one-sided flood plain channel is taken into consideration because it is reducing computational domain by almost half. However, for carrying out LES and its validation for other hydraulic and geometric conditions, requires experimental information on turbulent structures. The information of experimentations on turbulent flow structures for different hydraulic and geometric conditions were not available. Therefore numerical simulations for variable conditions could not be performed. Further, for performing numerical simulation using LES of different flow depths have many limitations such as it is computationally expensive, time consuming and needs parallel computing system etc. For this reason many investigators such as: Larson R.(1988), Stoesser et al (2004) etc have also analyzed for a particular hydraulic and geometric condition of flow.

Introducing chapter summary only on chapter 3 creates heterogeneity in topography of thesis as other two chapters are devoid of it. Therefore, to maintain the homogeneity in the topography of the thesis, the overall summary has been explained in the conclusion chapter.

2. **Query:** In Chapter-4: more detailed information about the flume experiments need to be documented. At least, statistical summary of the controlling factors used in the modeling should be tabulated. As mentioned by the researcher, hydraulic data includes both rigid

**and mobile bed conditions. How can a single data-based model represent two distinct flow conditions? For each bed condition, a separate ANN model can be tested. From 129 dataset, 110 dataset were used for training the model. Is it an over-parameterised model?**

**Answer:** Details of the flume experiments with controlling factors are now documented in Errata.

It has been seen from the literature that application of ANNs is less done for simple open channel flow and very less for the compound channels. In the present study an effort has been made to predict discharge and resistance factor by applying Artificial intelligence models. To analyze this, 129 data sets from different experimental conditioned from different standard laboratories have been collected across the globe. It is a general practice by researcher to account around 75-80% of total data as training and 20-25% as testing. Following the same 110 data (85%of data) for training and 19 (15% of data) for testing were taken and has been published, for instance Garbrecht (2006). Hydraulic data were also taken judicially from each to cover all sorts of hydraulic conditions i.e. both rigid and mobile bed conditions. The statistical summary of the controlling factors used for modeling are given as Table 2.

- 3. Can we learn the dominated relations between the controlling factors and discharge from the ANN set-up? Therefore, sensitive analysis of the model results with the chosen variables should be carried out. The most dominated controlling factor(s) need to be identified. It is good that the ANN model has been developed by the researcher for estimating the discharge. How can any other researcher/field engineer use this model? Besides the discharge prediction, a detail about the weightage factors and dominated controlling factors is to be addressed.**

**Answer:** Yes. The dominated relation between controlling factors and discharge has been identified by performing the sensitivity analysis. The detailed sensitivity analysis is attached at the end of this report. From the analysis, it is found that  $H_r$  (hydraulic depth) and  $S_0$  (Longitudinal channel slope) are two sensitive parameters. The dominating controlling factors are taken as input to predict the discharge. The parameters are selected following the work of Yang et al. (2007) and other researchers. Yang et al. (2007) has given a description of these factors by systematically analyzing each factor in different hydraulic conditioned data.

The ANN model is developed in MATLAB platform (MATLAB 2009). The procedure to model the network is very systematically mentioned in MATLAB manual. Further, as this model is of single hidden layer one can use Neural Network toolbox of MATLAB to model and get the results. From this, other engineer and researchers can be easily find out these information and carry out the process to predict the required variables.

4. **Query: In Chapter-4: for estimating the composite friction factor, Adaptive – Neuro Fuzzy interference system approach (ANFIS) was used. Why did the researcher use the approach, not ANN approach? The ANFIS has performed well as compared with other analytical approaches.**

**Answer:** The objective of this research to predict the discharge in compound open channel flow. In this study two approaches are taken to predict the discharge. Firstly, the influential variables as described by Yang et al. (2005) are taken as input of BPNN to predict the discharge. Secondly, Manning's equation is considered to predict the discharge. However for predicting discharge through Manning's equation, accurate prediction of composite friction factor is required. As in compound channel of different hydraulic conditions due to secondary current and momentum transfer it is highly unpredictable to predict composite friction factor accurately through empirical relations. Hence ANFIS approach is adopted for this analysis. Basically both the approaches are predicting discharge but in different way. By this, we have studied two approaches instead of a single approach. By comparing the two approaches, it has been noticed that, ANFIS model is logically adaptive and incorporative for the variation within crisp data whereas BPNN cannot. It is further seen that ANFIS model is computationally in-expensive and predicting the composite friction factor with lesser time than that with BPNN method.

5. **It is a well known fact that the ANFIS has very sensitivity to the input data and model parameter settings. How can any other researcher/field engineer use this model? Why not the second best model be identified from this study? Sensitivity analysis of the model output needs to be carried out.**

**Answer:** Sensitivity analysis is used to study the influence of changes in discharge with the changes of inputs. The inputs in the test samples are varied one at a time systematically by  $\pm 10\%$  from its base value holding other items at their original values. By doing so, the average effect of

input under consideration on the output can be estimated. The analysis is included at the end of this report.

As mentioned for BPNN, in question no 4 the ANFIS toolbox of MATLAB platform is used for the analysis. The detailed description of its applicability is quiet simple and user-friendly. Further, it doesn't require high-level mathematical understanding to run the model. From this, other engineer and researchers can easily find out this information and carry out the process to predict the required variables.

- 6. Query: There are topographical and grammatical mistakes in the thesis. For example, present continuous tense is used in pages 90-91. Use past/present continuous tense instead of that in the thesis, wherever needed. The others are highlighted in the attached pdf file.**

**Answer:** The topographical and grammatical mistakes have been incorporated in ERRATA.

#### # Examiner 2

- 1. Query: The ANN is used as a black box. It would have been better if some insight into the problem were shown by carrying out input sensitivity analysis, parametric variation on the trained network.**

**Answer: Yes.** Sensitivity analysis of the input parameter has been done to verify the sensitive parameter. It has been noticed that input 3 and input 4 are more sensitive parameter. A separate section is included after errata section to convey the analysis.

- 2. Query: Drawing inference on the basis of % may not be adequate. Error statistics such as RMSE, Bias and many more would have explained the errors more completely.**

**Answer:** The error of the trained network is analyzed with help of residual analysis. The distribution pattern of the residuals follows normal distribution and hence justifies the degree of accuracy. Further, RMSE of the BPNN model has now been done and included at Table.1 in Errata. It has been noticed that RMSE is less for the proposed BPNN model.

- 3. Query: The ANN model could have been further improved by adopting alternative architectures such as RBF, ANFIS, GRNN and optional training algorithm.**

**Answer:** It has been noticed that application of ANNs in the study of open channel flow is less documented. Hence in this study an effort has been taken to predict discharge and resistance factor to flow with Artificial intelligence models. The ANN network is trained with other training algorithm. It has been observed that, gradient decent training algorithm fit well with the given set of data. The objective of this study is to predict the discharge of compound open channel with accuracy which was done efficiently. Improvement by adopting alternative architectures such as RBF, ANFIS, GRNN and optional training algorithm could not be done in future as a scope for further research to evaluate most efficient model.

**4. Query: Before applying ANN insufficiency of traditional linear and nonlinear regression methods could have been ascertained.**

**Answer:** It is a well-established fact that ANNs can predict more accurately than linear and non-linear regression models. Further, ANNs are adaptable to data variation and further reduces the number of variable required to predict as described by Kashani et al (2007). From literature it has observed that Researchers such as Kashani et al (2007) Rezapour et al. (2010), Shu and Burn (2004) have already applied both regression and ANN to predict flood and observed that ANN is dominating nonlinear regression models as per the accuracy is concern.

**5. Query: The use of ANFIS to estimate the friction factor is not convincing. First of all, why use ANFIS and not ANN and others? Also, why in the first place do you want to estimate 'n', when its 'true' value can be calculated in a straight forward manner as stated on page 61 by using Mannings' equation as per Yang et al. (2007)?**

**Answer:** Neural network and fuzzy logic are two complementary technologies. Neural network can learn from data, however the knowledge or pattern developed by it are although robust but not implemental. Fuzzy logic on the other hand is easy to implement due to its linguistic rules in the form of IF-THEN. Hence, the integration of ANN with learning capability and fuzzy logic with decision-making capability can be made to build a versatile intelligence system. The combination of both ANN and FIS thus improves system performance without intervene of operators. For this reason, the logical pattern of the prediction is possible.

The value of manning's roughness co-efficient ( $n$ ) can be calculated unless the true value of discharge is known. In our case, we have firstly through experiments calculated discharge and from that we have obtained manning's roughness co-efficient ( $n$ ). Therefore by knowing

manning's roughness co-efficient ( $n$ ) and the geometry discharge of a compound channel is predicted. For this reason an ANFIS has been developed' to predict manning's roughness co-efficient ( $n$ ), so that the discharge can be predicted using Manning's equation.

#### References:

1. Tang X, and Knight DW.(2001). Analysis of bed form dimensions in a compound channel. In: Proceedings of 2nd IAHR Symposium on River, Coastal and Estuarine Morph dynamics, Obihiro, Japan, pp.555-63.
2. Tang X, and Knight DW.(2001).Experimental study of stage-discharge relationships and sediment transport rates in a compound channel. In: Proceedings of 29th IAHR Congress, Hydraulics of Rivers, Beijing, China, Tsinghai, 2, pp. 69-76.
3. Yang K, Cao S, and Liu X. (2007).Flow resistance and its prediction methods in compound channels, Acta Mechanic Sinica; 21, pp.353-61Yen BC. (2002). Open flow resistance. J. Hydr. Eng, 1(20), pp.20-39
4. Kashani MH, Montaseri M,Yaghin MAL, (2007). Flood estimation at an ungauged sites using a nonlinear regression model and artificial neural network. J. Agric & Environ. Sci. 2(6), 784-791.
5. Rezapour OM, Shui LT and Ahmad DB, (2010). Review of Artificial Neural Network Model for Suspended Sediment Estimation, Australian J. Basic and App. Sci., 4(8): 3347-3353.
6. Shu C and Burn DH, (2004). Artificial neural network ensembles and their application in pooled flood frequency analysis, Water Resources Research, 40.
7. Naot D, and Rodi W, (1982).Calculation of Secondary Currents in Channel Flow. J. Hydraul Div., ASCE, 108(8), pp. 948-968.
8. Yang K, Cao S, Liu X.(2005). Study on resistance coefficient in compound channels. Acta Mechanic Sinica; 21:pp.353-61.
9. Yang K, Cao S, and Liu X. (2007).Flow resistance and its prediction methods in compound channels, Acta Mechanic Sinica; 21, pp.353-61Yen BC. (2002). Open flow resistance. J. Hydr. Eng, 1(20), pp.20-39.
10. Larson R.(1988).Numerical simulation of flow in compound channels. Proceeding of the 3rd International Symposium on Refined Flow Modeling and Turbulence Measurements, Tokyo, Japan, pp. 527-536.

11. Stoesser T, Rodi W. (2004). Large Eddy Simulation of Flow over Rough Channel Beds. BAW Workshop Soil and Bed Stability - Interaction Effects between Geotechnics and Hydraulic Engineering. Sept. 17th. Karlsruhe.
12. Garbrecht J D. (2001). Comparison of Three Alternative ANN Designs for Monthly Rainfall-Runoff Simulation. J. Hydrol. Eng. 11, 502.

## ERRATA

Sl.no	Page no.	Mentioned in the thesis/Reviewers comment	modification/correction/response to the reviewers comment
1	29	give proper citation for the Equation	Citation for the Equation 3.1. is provided in page no 29.
2	40	Rewrite the sentence: The simulation result has also attained the same pattern and which show high degree of accuracy of simulation.	The sentence is rewritten in Page 40.
3	40	Why difference is too large in this region?(Figure 3.8)	The reason behind the difference is mentioned in page no 41.
4	52	Modification of sentence	The sentence is modified in page no 52.
5	57	give more statistical information about the experiments	Statitistical information about the experiments can be referred in Table 2 of Errata.
6	60	This seems to be MATLAB generated graph. This can be re-plotted with other plotting software	The Figure 4.8 is replaced with a re-plotted figure.
7	64	In Figure 4.14, (a) How can it be zero?  (b) mention the unit above the graph.	(a) The equation in Figure 4.14 is modified.  (b) The unit of the actual and predicted discharge are cm <sup>3</sup> /sec in Figure 4.14..
8	66	This should be included in a separate chapter.	Keeping in view the thesis title, the prediction of discharge and its resistance factors by BPNN and ANFIS has been kept in a separate section. Thus, by separating it in to a separate chapter, there may be misalignment in the topography of the thesis.
9	88	The data are too much variation in this region. Why?	The variation in prediction of composite friction factor in EBM in mobile channel condition. The method is not incorporating these changes properly.

Table. 1 RMSE and average analysis of the BPNN network and earlier developed models

Source of Data	Actual Discharge cm <sup>3</sup> /sec	ANN cm <sup>3</sup> /sec	Error In %	VDCM cm <sup>3</sup> /sec	Error in %	COHM cm <sup>3</sup> /sec	Error	EDM cm <sup>3</sup> /sec	Error In %
<b>Atabay (2001)</b>	0.018	0.018	3.8	0.021	1.23	0.018	2.1	0.015	13.7
	0.021	0.022	7.2	0.023	4.26	0.201	3.0	0.018	15.08
	0.24	0.258	15.8	0.234	13.47	0.230	4.5	0.022	9.14
	0.027	0.029	8.1	0.015	51.72	0.026	3.8	0.03	9.5
	0.05	0.050	1.2	0.055	9.56	0.048	3.3	0.042	15.85
<b>FCF phase-A</b>	0.208	0.226	8.1	0.073	64.8	0.195	6.25	0.203	2.6
	0.234	0.205		0.091	60.9	0.233	0.25	0.222	4.8
	0.605	0.636	5.2	0.702	13.8	0.675	11.67	0.585	3.2
	0.212	0.204	3.39	0.167	21.2	0.240	13.36	0.205	3.6
	0.480	0.475	1	0.360	25.0	0.527	9.96	0.476	8.2
<b>Illinois</b>	0.034	0.037	9.4	0.052	51.22	0.027	21.0	0.031	9.8
	0.042	0.047	9.31	0.027	34.50	0.037	9.9	0.038	8.5
	0.047	0.045	3.8	0.017	62.65	0.038	17.18	0.042	10.2
	0.036	0.037	3.6	0.003	91.44	0.036	1.94	0.032	12.3
	0.046	0.045	1.73	0.078	68.2	0.039	15.13	0.064	10.6
<b>Tang et al. (2001) Rigid channel</b>	0.015	0.016	6.67	0.014	0.2	0.016	7.9	0.014	5.7
	0.018	0.0167	7.2	0.017	3.2	0.019	2.7	0.017	5.2
	0.034	0.0305	11.07	0.033	3.11	0.027	20.37	0.032	6.0
	0.015	0.0143	4.67	0.014	3.11	0.017	15.75	0.015	3.9
	0.024	0.0257	5.76	0.024	0.8	0.027	15.4	0.023	4.4
<b>Tang et al. (2001) Mobile Channel</b>	0.0143	0.01390	2.80	0.017	20	0.011	25.85	0.017	17.65
	0.0306	0.0284	7.1	0.007	77.8	0.024	22.44	0.042	38.4
	0.01023	0.011	7.0	0.011	7.0	0.009	12.47	0.104	2.1
	0.0172	0.0152	11.62	0.019	13.3	0.011	35.08	0.022	28.52
	0.01971	0.0214	8.5	0.003	82.14	0.013	31.71	0.023	18.56
<b>NIT Rourkela (Type-I)</b>	0.019861	0.0205	3.2	0.019	30.9	0.016	20.95	0.015	24.75
	0.0253	0.0248	2.1	0.09	26.67	0.022	10.64	0.023	7.11
<b>Average Absolute error</b>		6.26		31.2		12.76		10.8	
<b>RMSE</b>		0.150127		0.150791		0.150152		0.150251	

**Sensitivity analysis:**

In order to find the robustness of the proposed model, sensitivity analysis is carried out. The procedure for the sensitivity analysis is adopted following the work of Mahapatra and Khan (2007). The method, Sensitivity analysis is used to study the influence on output with the change of inputs. The inputs in the test samples are varied one at a time systematically by ±10% from its base value holding other items at their original values. By doing so, the average impact of inputs under consideration on the output can be estimated. Once the network is well trained, the relationship among inputs and outputs are established and network provides the scope for assessment of impact of each input on output. The scaled change in output is calculated with the current input increased by 10% and the current input decreased by 10%. The scaled change on output is given by:

$$\begin{aligned} & \text{Scaled change in output} \\ & = \frac{\text{Scaled output for 10\% increase in input} - \text{Scaled output for 10\% decrease in input}}{2} \end{aligned} \tag{1}$$

Thus, the results obtained are the scaled output change per 10% change on input. The calculation is repeated for every input and every flow condition and then averaged across all the facts, yielding a single-mean scaled change in output for each input criterion. Increase/decrease of an input from its base value results in increase/decrease in performance level. Logically, the net effect of change in input results in a positive score for average scaled change on output.

**Sensitivity analysis of BPNN network:**

The input parameters for the BPNN network are: (i) influence of flood plain and main channel roughness (  $f_r$  ); (ii) Ratio of area of flood plain to main channel ( $A_r$ );(iii) relative depth ( $H_r$ ) i.e. depth of flood plain to total depth; (iv) channel longitudinal slope ( $S_0$ ); and (v) ratio of hydraulic radius of flood plain and main channel ( $R_r$ ) . The sensitivity of network is verified after changing each input by 10% one by one sequentially, while by keeping other parameters constant, which is summarized in Table1.

Table 1. The errors of the BPNN network by increasing inputs sequentially by 10%.

Output	Input 1	Input 2	Input 3	Input 4	Input 5
Actual Output	Output after changing $f_r$ only	Output after changing $A_r$ only	Output after changing $H_r$ only	Output after changing $S_0$ only	Output after changing $R_r$ only
0.0102	0.0914	0.4718	0.0167	0.4427	0.3912
0.0037	0.1112	0.503	0.0106	0.4496	0.4472
0.0047	0.1099	0.5015	0.0116	0.4503	0.4451
0.0008	0.1311	0.5384	0.0082	0.4631	0.511
0.0048	0.1528	0.5846	0.0127	0.4902	0.5924
0.0414	0.1819	0.6805	0.0512	0.581	0.7365
0.0518	0.2545	0.8326	0.0639	0.6531	0.8642
0.0022	0.0123	0.1201	0.0008	0.0698	0.0728
0.022	0.0135	0.145	0.0203	0.0606	0.0966
0.025	0.0207	0.156	0.0232	0.0619	0.1369
0.0208	0.0212	0.1628	0.0189	0.0702	0.1775
0.0233	0.0287	0.1793	0.0212	0.0717	0.2315
0.0193	0.034	0.207	0.0167	0.0823	0.3305
0.0003	0.0415	0.3036	0.0036	0.116	0.6077
0.0032	0.0373	0.297	0.007	0.1191	0.5974
0.1003	0.2101	0.7434	0.0925	0.0447	1.2528
0.1108	0.2222	0.7614	0.1029	0.0348	1.2716
0.0074	0.0095	0.1718	0.0053	0.1219	0.0945
0.0038	0.0122	0.1733	0.0016	0.125	0.1246
0.0101	0.0005	0.1907	0.0078	0.1248	0.1735

Table 2. Statistical summary of controlling factors.

Source of data	Main channel side slope	Flood plain type	Roughness type	Main channel Cross-sectional geometry	Longitudinal Slope	Main Channel Width (m)	Ratio of main channel to flood plain depth	Discharge (m <sup>3</sup> /s)
<b>FCF-Series A</b>								
Series 1	1:1	Symmetric	Smooth	Trapezoidal	1.027×10 <sup>-3</sup>	3000	0.057-0.4	0.208-1.015
Series 2	1:1	Symmetric	Smooth	Trapezoidal	1.027×10 <sup>-3</sup>	3000	0.041-0.47	0.212-1.114
Series 3	0:1	Symmetric	Smooth	Trapezoidal	1.027×10 <sup>-3</sup>	3000	0.051-0.5	0.225-0.835
Series 6	1:1	Asymmetric	Smooth	Trapezoidal	1.027×10 <sup>-3</sup>	3000	0.052-0.503	0.224-0.929
Series 8	0:1	Symmetric	Smooth	Rectangular	1.027×10 <sup>-3</sup>	3000	0.05-0.5	0.186-1.109
Series10	2:1	Symmetric	Smooth	Trapezoidal	1.027×10 <sup>-3</sup>	3000	0.051-0.464	0.237-1.094
<b>Tominaga and Nezu (1991)</b>								
S(1-3)	0:1	Asymmetric	Smooth	Rectangular	6.72×10 <sup>-4</sup>	0.2	0.49	0.738
<b>Tang and Knight (2001)</b>								
ROA	0:1	Symmetric	Smooth	Rectangular	1.027×10 <sup>-3</sup>	1.213	0.295-0.702	0.0101-0.05
ROS	0:1	Symmetric	Smooth	Rectangular	1.027×10 <sup>-3</sup>	1.213	0.295-0.702	0.0101-0.05
<b>Tang and Knight (2001) Mobile</b>								
LOSR	0:1	Symmetric	Rough	Rectangular	1.027×10 <sup>-3</sup>	1.213	0.1817-0.92	0.108-0.155
ALL	0:1	Symmetric	Rough	Rectangular	1.027×10 <sup>-3</sup>	1.213	0.1817-0.92	0.108-0.155
<b>Atabay et al.(2004)</b>								
ROA	0:1	Asymmetric	Smooth	Rectangular	1.027×10 <sup>-3</sup>	1.213	0.18-0.476	0.015-0.55
ROS	0:1	Symmetric	Smooth	Rectangular	1.027×10 <sup>-3</sup>	1.213	0.18-0.476	0.0155-0.553
<b>Soong and Depue (1996)</b>								
	1:1	Asymmetric	Rough	Trapezoidal	0.001	0.02	0.737-0.734	1.212-2.237
<b>Khatua et al. (2011)</b>								
Type I	0:1	Symmetric	Smooth	Rectangular	0.0019	0.12	0.11-0.46	0.039-0.087

Table 2. The absolute scaled change of output in the BPNN network with the change of inputs.

Output	Input 1	Input 2	Input 3	Input 4	Input 5
Actual Output	Output after changing $f_r$ only	Output after changing $A_r$ only	Output after changing $H_r$ only	Output after changing $S_0$ only	Output after changing $R_r$ only
0.0102	0.0482	0.0039	0.0016	0.0154	0.0040
0.0037	0.0385	0.0000	0.0130	0.0144	0.0005
0.0047	0.0390	0.0001	0.0124	0.0146	0.0006
0.0008	0.0294	0.0034	0.0397	0.0145	0.0006
0.0048	0.0205	0.0196	0.0966	0.0168	0.0068
0.0414	0.0102	0.0811	0.2714	0.0332	0.0342
0.0518	0.0011	0.1695	0.5144	0.0466	0.0846
0.0022	0.0078	0.1538	0.2988	0.0175	0.0948
0.022	0.0088	0.1352	0.2639	0.0121	0.0840
0.025	0.0125	0.1067	0.2096	0.0117	0.0665
0.0208	0.0154	0.0814	0.1618	0.0128	0.0514
0.0233	0.0210	0.0531	0.1118	0.0125	0.0336
0.0193	0.0309	0.0169	0.0456	0.0142	0.0108
0.0003	0.0435	0.0229	0.0112	0.0223	0.0152
0.0032	0.0459	0.0198	0.0090	0.0232	0.0130
0.1003	0.0113	0.6390	0.6381	0.0076	0.5006
0.1108	0.0146	0.6694	0.6696	0.0060	0.5270
0.0074	0.0006	0.1359	0.2533	0.0147	0.0826
0.0038	0.0017	0.1145	0.2138	0.0161	0.0691
0.0101	0.0039	0.0833	0.1578	0.0148	0.0505

Table 3. The error of the BPNN network by decreasing inputs sequentially by 10%.

Output after changing $f_r$ only	Output after changing $A_r$ only	Output after changing $H_r$ only	Output after changing $S_0$ only	Output after changing $R_r$ only
0.11455	0.4618	0.21135	0.5273	0.18695
0.1252	0.4657	0.2365	0.56785	0.2129
0.12495	0.46565	0.236	0.56695	0.21235
0.13835	0.4711	0.26745	0.61735	0.245
0.15665	0.47995	0.3107	0.68665	0.29035
0.1932	0.50695	0.40225	0.8371	0.38865
0.20995	0.5488	0.47205	0.9713	0.46935
0.04395	0.13195	0.0378	0.04775	0.03185
0.04005	0.14175	0.0403	0.0596	0.03275
0.05245	0.1383	0.05935	0.0882	0.0518
0.06775	0.13545	0.0822	0.1201	0.07465
0.08575	0.13335	0.10845	0.1548	0.10105
0.1227	0.13175	0.161	0.22055	0.1541
0.2326	0.13995	0.3117	0.39715	0.3078
0.23	0.13955	0.30815	0.39315	0.30425
0.44045	0.20245	0.5877	0.7079	0.59935
0.4436	0.2042	0.5919	0.7127	0.604
0.05275	0.19025	0.0473	0.09545	0.0373
0.06635	0.182	0.0643	0.11745	0.0551
0.0796	0.18005	0.08605	0.14995	0.07685

The BPNN network is trained by achieving 116944 epochs. The momentum and learning parameter are set to 0.07 and 0.5 respectively. After this analysis, mean and variance of the outputs of each experiment are calculated. These values are tabulated in Table 3.

Table 4. The mean of the BPNN network by varying inputs sequentially by 10%.

Changing parameter	Mean of outputs by increasing 10%	Mean of outputs by decreasing 10%
$f_r$	0.084825	0.38346
$H_r$	0.38619	0.232215
$A_r$	0.024835	0.468535
$S_0$	0.23164	0.572285
$R_r$	0.457775	0.014135

It can be observed from Figure 1. and Figure 2 that by increasing and decreasing of input1 by 10% the error shows an uneven trend; rather, the error increases by increasing the input value. However, the scaled mean values of outputs are lowest for this case. The trend is same for input 3 and input 5. But for hydraulic depth (input 3 ( $A_r$ )) and Slope (input 4 ( $S_0$ )) the trend is at the increasing manner. Hence the input 3 and input 4 are more sensitive to changes and burgeons the impact with the changes.

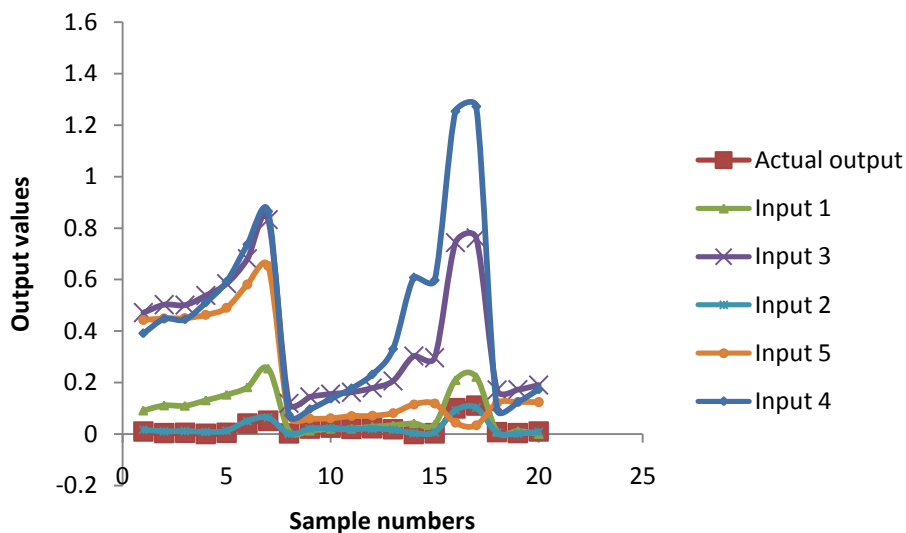


Figure 1. Mean values of outputs by changing the inputs

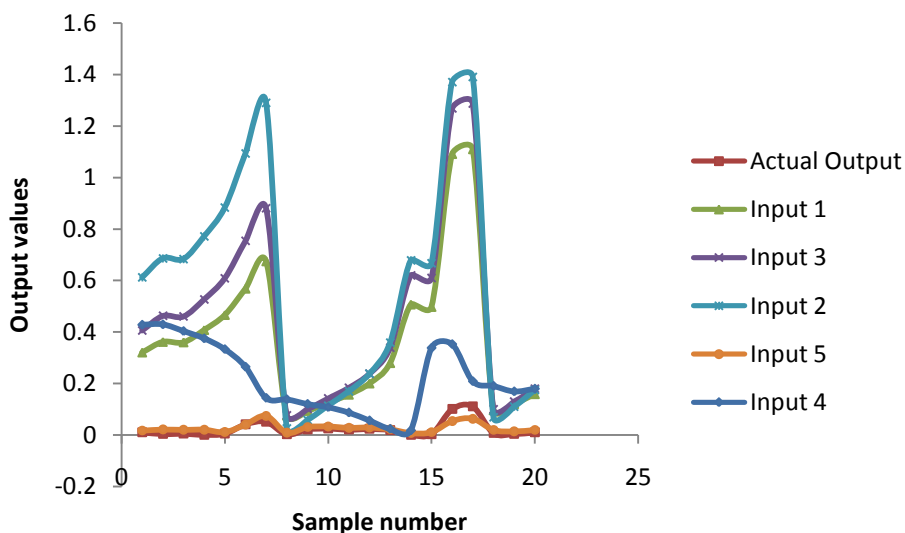


Figure 2. Mean values of outputs by changing the inputs

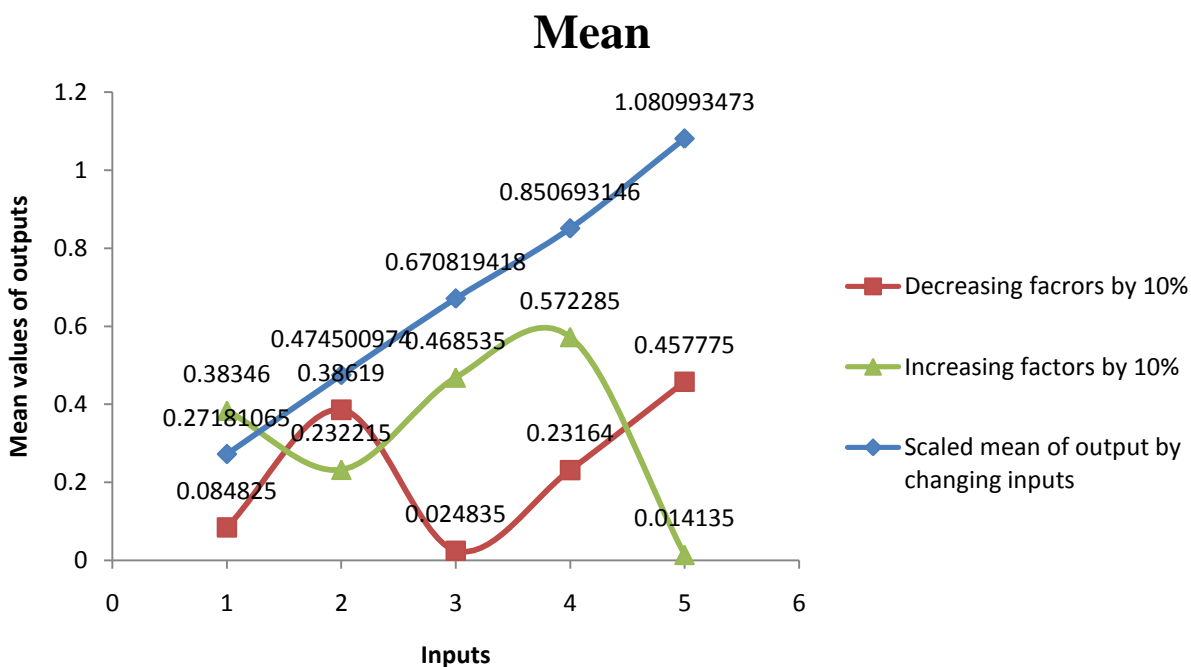


Figure 3. Mean values of outputs by changing the inputs

**Sensitivity analysis of ANFIS network:**

Sensitivity analysis is inevitable to verify the performance of the proposed ANFIS model, as well as to testify its performance. Therefore, for this case also same procedure as discussed above for BPNN model is adopted.

The input parameters for ANFIS network are: (i) relative Width (B<sub>r</sub>), Ratio of width of flood plain (B-b) to total width (B) where B = main channel width, b = flood plain width; (ii) The ratio of perimeter of

main channel ( $P_{mc}$ ) to flood plain perimeter ( $P_{fp}$ ) denoted as  $P_r$ ; (iii) Ratio of hydraulic radius of main channel ( $R_{mc}$ ) to flood plain ( $R_{fp}$ ) denoted as  $R_r$ , which normally varies with symmetry; (iv) channel longitudinal slope ( $S_0$ ); and (v) relative depth ( $D_r$ ) i.e. Ratio of depth of flood plain ( $H-h$ ) to total depth ( $H$ ) where  $H$  = main channel depth,  $h$  = flood plain depth. The sensitivity of parameters after changing inputs by 10% is summarized in Table 1.

The ANFIS network is trained by achieving 10 epochs. After this analysis, mean of the outputs by changing each inputs sequentially for the model are calculated. These values are tabulated in Table 5. It can be observed from Figure 6 and Figure 7 that, by increasing and decreasing of inputs 1 by 10% the error shows an uneven trend, rather the error increases by increasing the input value. However, the scaled mean value of outputs is lowest for this case. The trend is same for input 2 and input 5. But for input 5 ( $H_r$ ) the trend is at the increasing manner. Hence the input 5 ( $D_r$ ) and input 2 ( $P_r$ ) are more sensitive to changes and burgeons the impact with the changes.

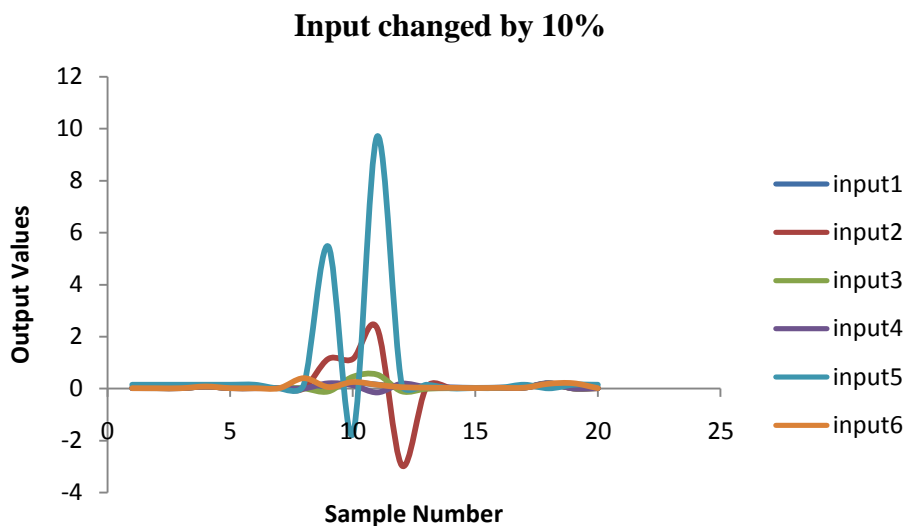


Figure 4. Mean values of outputs by changing the inputs

Table 5. The errors of the BPNN network by increasing inputs sequentially by 10%.

Output	Input 1	Input 2	Input 3	Input 4	Input 5
Actual Output	Output after changing $f_r$ only	Output after changing $A_r$ only	Output after changing $H_r$ only	Output after changing $S_0$ only	Output after changing $R_r$ only
0.012698	0.0115	0.014	0.0132	0.149	0.0132
0.01374	0.013	0.0106	0.0103	0.149	0.0102
0.011429	0.0122	0.0128	0.0122	0.149	0.0122
0.076027	0.0734	0.0762	0.0781	0.149	0.0762
0.010751	0.0118	0.0144	0.0136	0.149	0.0136
0.013034	0.011	0.0115	0.0108	0.149	0.0108

0.010574	0.013	0.0136	0.0129	0.0103	0.0129
0.001	0.001	0.0011	0.0011	0.149	0.3958
0.054	1.1361	-0.1166	0.1973	5.4722	0.0552
0.213	1.1338	0.449	0.1242	-1.7551	0.248
0.146	2.3045	0.5327	-0.1528	9.7092	0.143
0.052	-2.959	-0.1111	0.1816	0.149	0.0489
0.035	0.0331	-0.0113	0.0509	0.149	0.0336
0.035	0.0217	0.0091	0.0304	0.0108	0.0238
0.019176	0.0173	0.0178	0.0183	0.0204	0.0173
0.028921	0.0241	0.0244	0.0254	0.0288	0.0239
0.035941	0.032	0.0329	0.0346	0.149	0.0324
0.20293	0.1898	0.1869	0.184	0.0098	0.1821
0.001	0.0008	0.0008	0.0008	0.149	0.2012
0.010483	0.0093	0.0117	0.0114	0.149	0.0114

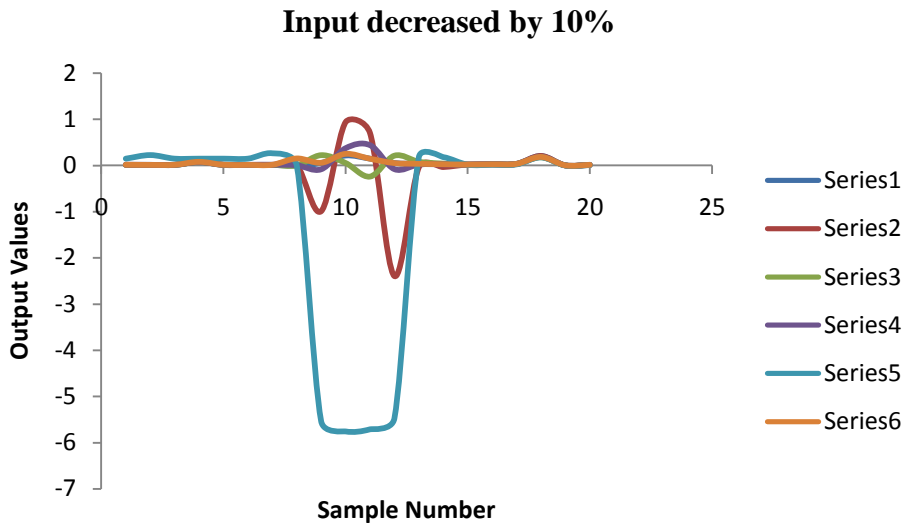


Figure 5. Mean values of outputs by changing the inputs

Table 6. The absolute scaled change of output in the ANFIS network with the change of inputs.

Output	Input 1	Input 2	Input 3	Input 4	Input 5
Actual Output	Output after changing $f_r$ only	Output after changing $A_r$ only	Output after changing $H_r$ only	Output after changing $S_0$ only	Output after changing $R_r$ only
0.012698	0.0135	0.0125	0.0132	0.149	0.0132
0.01374	0.0132	0.0098	0.0101	0.2266	0.0102
0.011429	0.0138	0.0118	0.0122	0.149	0.0122
0.076027	0.0788	0.0761	0.0741	0.149	0.0762
0.010751	0.0136	0.0128	0.0136	0.149	0.0136
0.013034	0.0124	0.0101	0.0108	0.149	0.0108
0.010574	0.0132	0.0122	0.0129	0.2652	0.0129
0.001	0.001	0.001	0.001	0.001	0.149
0.054	-0.9927	0.2242	-0.0868	-5.5383	0.0552

0.213	0.9377	0.053	0.3718	-5.7603	0.248
0.146	0.7035	-0.2445	0.4388	-5.7138	0.143
0.052	-2.3986	0.2137	-0.0839	-5.4754	0.0489
0.035	-0.0416	0.0799	0.0167	0.1808	0.0336
0.035	-0.0347	0.0394	0.0209	0.182	0.0238
0.019176	0.0184	0.0169	0.0163	0.0185	0.0173
0.028921	0.0236	0.0234	0.0224	0.0176	0.0239
0.035941	0.0323	0.0318	0.0301	0.0245	0.0324
0.20293	0.2053	0.1772	0.1816	0.1779	0.1821
0.001	0.0008	0.0008	0.0008	0.0008	0.001
0.010483	0.0113	0.0112	0.0114	0.01	0.0114

Table 7. The errors of the ANFIS network by decreasing inputs sequentially by 10%.

Output after changing $f_r$ only	Output after changing $A_r$ only	Output after changing $H_r$ only	Output after changing $S_0$ only	Output after changing $R_r$ only
0.001	-0.00075	-1.6263E-19	0	-3.3E-19
0.0001	-0.0004	-1E-04	0.0388	1.3E-18
0.0008	-0.0005	3.25261E-19	0	6.5E-19
0.0027	-5E-05	-0.002	0	8.6E-18
0.0009	-0.0008	-4.3368E-19	0	-8.7E-19
0.0007	-0.0007	6.50521E-19	0	1.3E-18
0.0001	-0.0007	0	0.12745	0.0E+00
0	-0.00005	-0.00005	-0.074	-2.5E-01
-1.0644	0.1704	-0.14205	-5.50525	-2.2E-19
-0.09805	-0.198	0.1238	-2.0026	0.0E+00
-0.8005	-0.3886	0.2958	-7.7115	-2.6E-18
0.2802	0.1624	-0.13275	-2.8122	1.3E-18
-0.03735	0.0456	-0.0171	0.0159	-5.4E-18
-0.0282	0.01515	-0.00475	0.0856	-1.7E-18
0.00055	-0.00045	-0.001	-0.00095	-4.3E-19
-0.00025	-0.0005	-0.0015	-0.0056	1.7E-18
0.00015	-0.00055	-0.00225	-0.06225	1.3E-18
0.00775	-0.00485	-0.0012	0.08405	1.7E-17
1.36E-20	1.36E-20	1.35525E-20	-0.0741	-2.0E-01
0.001	-0.00025	1.0842E-19	-0.0695	2.2E-19

Table 8. The mean of the ANFIS network by varying inputs sequentially by 10%.

Changing parameter	Mean of outputs by increasing 10%	Mean of outputs by decreasing 10%
$B_r$	0.10452	-0.06876
$P_r$	0.059025	0.038665
$R_r$	0.042915	0.0544
$S_0$	0.76472	-1.0319
$D_r$	0.078285	0.055935

References:

1. Mahapatra S.S., and Khan M.S.(2007). A neural network approach for assessing quality in technical education: an empirical study. International Journal of productivity and quality management. 2(3); 287-306.

## BRIEF BIODATA OF THE AUTHOR

---

**NAME** : Mrutyunjaya Sahu

**FATHER'S NAME** :Mr. Bana Bihari Sahu

**MOTHER'S NAME** :Mrs. Chandrakala Sahu

**DATE OF BIRTH** :31<sup>st</sup> July 1985

**NATIONALITY** :Indian

**PRESENT ADDRESS** :Dhirubhai Ambani Hall of Residence,  
National Institute of Technology  
Rourkela - 769008

**EDUCATIONAL QUALIFICATIONS:** B.TECH, Civil Engineering, 2009  
National Institute of Technology,  
Rourkela 769008.

**RESEARCH EXPERIENCE:** Author has published 5 international journal Articles and 3 international conferences Articles.

**PROFESSIONAL MEMBERSHIP:** Author is student member of American Society of Civil Engineering (ASCE), American Society of Mechanical Engineering (ASME), International Society of Hydrological Research (IAHS).



Department of Civil Engineering  
National Institute of Technology  
Rourkela - 769008, Orissa, India

---